The Role of Inhibitory Mechanisms and Memory in Influenza Associated Bacterial Super-infections

by

Ellyse Margaret Cipolla

BS, Michigan State University, 2013

Submitted to the Graduate Faculty of the

School of Medicine in partial fulfillment

of the requirements for the degree of

Doctor of Philosophy

University of Pittsburgh

2022

UNIVERSITY OF PITTSBURGH

SCHOOL OF MEDICINE

This thesis was presented

by

Ellyse Margaret Cipolla

It was defended on

August 23, 2022

and approved by

Kong Chen, PhD.
Assistant Professor, Department of Medicine

Rachel A. Gottschalk, PhD.
Assistant Professor, Department of Immunology

Lawrence P. Kane, PhD.
Professor and Vice Chair for Education, Department of Immunology

Janet S. Lee, MD.
Professor and Director of the Acute Lung Injury Center of Excellence, Department of Medicine

Dissertation Director: John F. Alcorn, PhD.
Professor, Department of Pediatrics

The Role of Inhibitory Mechanisms and Memory in Influenza Associated Bacterial Super-infections

Ellyse Margaret Cipolla, PhD.

University of Pittsburgh, 2022

Influenza associated secondary bacterial super-infections have devastating impacts on health and result in an increased risk of morbidity and mortality. The current field suggests that immunological mechanisms directed against primary influenza infection act to suppress anti-bacterial mechanisms resulting in a beneficial lung environment for colonization by opportunistic pathogens such as methicillin-resistant *Staphylococcus aureus* (MRSA). Understanding these aberrant immune mechanisms can provide insight into immunological pathways which can be targeted for prevention of bacterial super-infections. With this in mind I investigated the role that immune inhibitory-receptors play in bacterial super-infection. Previous studies on chronic and acute viral infections suggested that programmed death-1 (PD-1), a well-known inhibitory receptor, may play a role in weakening the adaptive immune response, in particular the T cell response, to viral infection by suppressing proliferation and production of key cytokines related to viral clearance. To study PD-1, I performed mouse studies using wild type (WT) and PD-1 global knock-out mice infected with influenza followed by a secondary bacterial infection with MRSA. I also performed antibody blockade studies in WT mice targeting PD-1 and its ligand Pd-l1. We observed a change in expression of other inhibitory markers, suggesting that they may work in conjunction with each other and the loss of one may alter the expression of the others. In conjunction with the PD-1 studies, I also developed a project looking at the role of immune memory in susceptibility to secondary infections. I found that immune memory to heterotypic

influenza strains resulted in a significant decrease in MRSA colonization. Following this observation, I studied multiple pathways commonly associated with bacterial super-infections. Results from these studies highlighted changes in both the innate and adaptive immune systems suggesting a more effective viral response leading to less hindrance of the innate immune system and a more effective anti-bacterial response. These studies presented herein highlight two novel areas in the field of super-infection. The first being the role that inhibitory pathways play in secondary infections, and the second being the importance of understanding how pre-existing immunity to pathogens can shape our immune response to secondary infections.

Table of Contents

List of Tables

List of Figures

Preface

Throughout my time at the University of Pittsburgh I have met various people that have helped me through my PhD journey. Firstly, I would like to thank my mentor, Dr. John Alcorn, who has supported me through my time at graduate school, and has provided an environment that strives to foster independent thinkers. I would also like to thank my committee: Drs. Larry Kane, Kong Chen, Rachel Gottschalk, and Janet Lee. They have always been supportive and helpful in my graduate school career. I am forever thankful for their guidance throughout the years.

I joined the laboratory in the spring of 2018, and since then I have watched as the laboratory has gone through substantial growth. When I first joined, I was welcomed by the older graduate students, Drs. Helen Rich and Jen Grousd, who were always available when I needed help with understanding immunology concepts. At this time, I was also welcomed by two technicians in the laboratory, Dharti Ukani and Marianna Ortiz, who were instrumental in helping to train me when I first started. Both of them were always there to talk with, and help me become a more confident scientist and person. As the landscape of the laboratory changed throughout my tenure there were numerous other individuals who were instrumental to my success including our laboratory manager, Saran Kupul, who acted as a motherly figure to all of the graduate students encouraging me with kind words and making me feel like an important scientific researcher. One other individual that was instrumental in my success was Kara Nickolich, another technician in the laboratory, who helped me extensively throughout my PhD with large cutups and early morning experiments trying to develop multiple flow cytometry panels. Without Marianna, Dharti, Saran, or Kara, I am sure that I would not have had as much fun in the laboratory or been the scientist that I am today. I would also like to thank the other scientists, Drs. Bo Zhai and Radha Gopal, as

well as Post-doc, Dr. Flavia Rago, as well as the graduate students that came after me: Brydie Huckestein, Dani Antos, Leigh Miller, Ally Duray, and Brooke Dresden. Specifically, I would like to single my wonderful bay mates in the lab, Brydie and Dani, who I have spent countless hours with talking about science, helping me with large cut-ups, and listening to loud music with while working.

Lastly, I would like to thank my friends and family. My parents and sisters have always been supportive and encouraging in my decision to become a scientist. The friends that I have made along the way have proven to be invaluable for the challenges that have occurred throughout the years. I am extremely grateful that I was part of a cohort that was friendly and supportive of each other. Three people in particular have been with me throughout the best and most turbulent moments of graduate school: Stephanie Grebinoski, Kristin DePeaux, and Jessica Filderman. I have built countless memories with each of them and I am forever grateful for their friendship.

Graduate school has been a very long journey with many ups and downs, but I have developed so many meaningful relationships without which I would not be the person or scientist that I am today.

1.0 Introduction

1.1 The immune system, Influenza, and Bacterial Super-infections

Throughout the years there have been multiple influenza pandemics, with the most famous being the 1918-1919 H1N1 outbreak. The 1918 pandemic is one of the most well-known infectious disease pandemics because it resulted in the deaths of more than 50 million people. An interesting pattern emerged whereby a majority of those who succumbed to influenza infection also had secondary bacterial infections, otherwise known as bacterial super-infections[1]. This synergy between virus and bacteria was subsequently seen in the pandemics that followed, including the most recent 2009 H1N1 influenza pandemic[2]. Individuals who are at most risk for influenza-associated bacterial super-infections are the young, elderly, and immunocompromised, although previously healthy adults were also at risk during the 1918 pandemic. Today secondary bacterial infections have been associated with several other viral pathogens, including SARS-CoV-2, which is responsible for the ongoing Covid-19 pandemic[3].

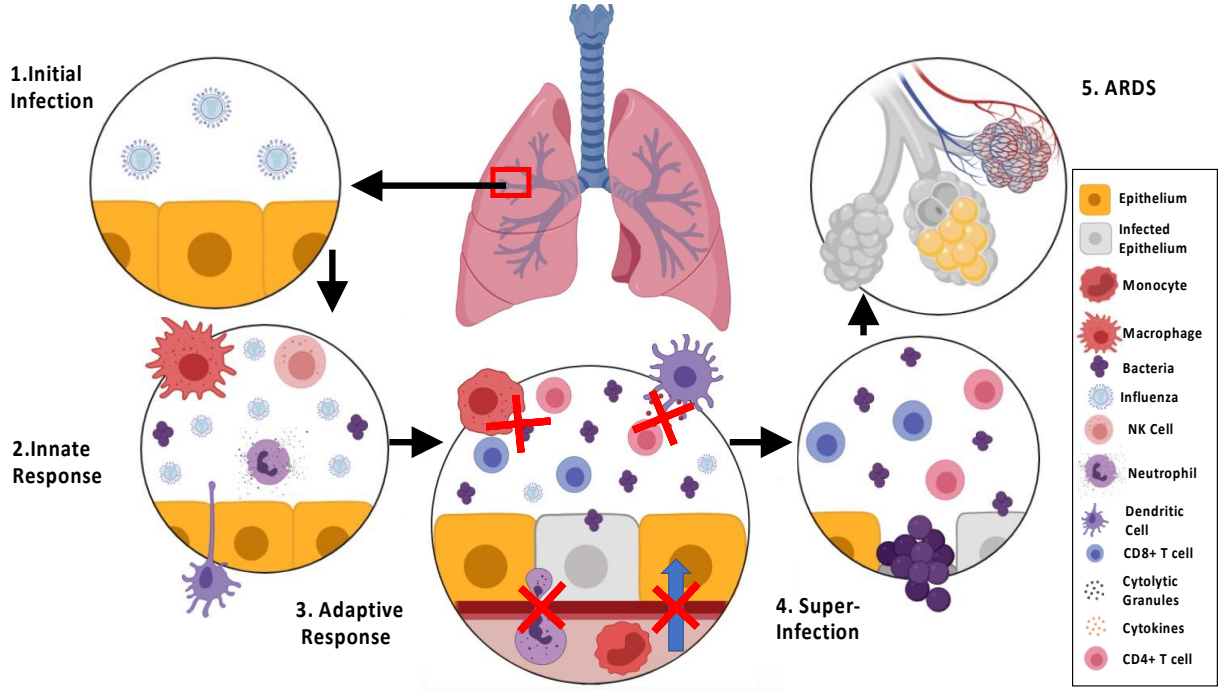

Figure 1.1 The immune response during an Influenza associated secondary bacterial super-infection. A bacterial super-infection begins with the initial infection by influenza virus of target epithelial cells (1). Once the epithelium is infected, it signals the innate immune system which is characterized by monocytes, macrophages, neutrophils, NK cells, and dendritic cells (2). This innate immune response is important not only to control the infection at the early stages but, through antigen presenting cells of the innate immune system, for stimulating and activating the adaptive immune response (3). The adaptive immune response is characterized by $CD4^+$ and $CD8^+$ T cells as well as B cells. As the adaptive immune system is activated in this context, it will be heavily skewed toward an anti-viral response, which in turn will hinder the anti-bacterial response through various mechanisms. This results in an environment for opportunistic pathogens to thrive and the eventual development of a super-infection (4). In the event of a particularly severe infection, an acute respiratory distress syndrome (ARDS) can occur (5). Developed with BioRender.

1.1.1 Influenza Infection and Pulmonary Immune Response

Influenza virus is spread via the aerosolization of liquid droplets from an infected individual and is primarily acquired via the naso-oropharyngeal route. After initial infection, influenza virus disseminates into the airways and lung space where it primarily targets the epithelium for sites of replication and life-cycle completion. The epithelium represents the first line of defense against the infection and, once targeted, sets off a cascade of immunological events. This is marked by the production of signaling molecules, cytokines, that go on to stimulate the innate arm of the immune system. This initial cytokine wave is of a pro-inflammatory nature, which stimulates defense mechanisms against invading pathogens. Some of the cytokines of particular importance during this initial pro-inflammatory response are Cxcl10, IL-6, IL-1 family cytokines, IL-12 family cytokines, and the interferon family which includes Type I, II, and III[4]. These signaling molecules recruit and stimulate the innate immune system, which includes dendritic cells, neutrophils, NK cells, monocytes, and macrophages[5, 6]. Following stimulation of the innate immune system, antigen presenting cells, such as dendritic cells, traffic to lymph nodes where they stimulate cells of the adaptive immune system which include $CD4^+$ and $CD8^+$ T cells, and B cells [6]. Once the adaptive cells traffic to the infection site, they are the major players in clearance of the viral infection[6]. Following clearance, the immune system then moves towards a recovery phase where long-term protection mechanisms against influenza virus, i.e. antibody producing B cells and memory T cells, are formed.

1.1.2 Bacterial infection and Pulmonary Immune Response

The lung has several mechanisms to protect against pathogenic invaders, ranging from physical barriers to cellular mechanisms of defense. As pathogens, such as bacteria, travel through the respiratory system they first encounter a layer of mucus and ciliated cells that act to physically impede tissue invasion of foreign substances[7]. If foreign particles get through this first line of defense, the body has several other mechanisms to target foreign invaders. One of these mechanisms consist of antimicrobial peptides, which are part of the innate immune defense, and which act in several ways to limit pathogenic infection[8]. As part of the overall system of innate immune defense, there are several cell types that defend against bacterial infection. Alveolar macrophages play various roles in antimicrobial defense, including the sensing of pathogens via pattern recognition receptors, as well as bacterial phagocytosis[9, 10]. Neutrophils represent another layer of the innate immune defense against bacterial infection. Neutrophils are readily recruited to the sight of infection within the lung and their major role is the phagocytosis of invading pathogens[11]. The innate immune system represents only one layer of defense that the host has against invading pathogens. The adaptive immune system also plays a critical role in host defense in the lung during bacterial infections. In particular, Th17 cells and their respective signaling molecules have been implicated in this antibacterial defense due to their role in recruitment of phagocytic cells[12, 13]. All of these immune responses are key to protecting the lungs against microbial pathogens.

1.1.3 Synergy of Aberrant Immune Mechanisms: How Influenza-associated Bacterial Super-infections Form

When the influenza virus infects a host, the host immune response is focused on eliminating infected cells, which is primarily driven by phagocytes and their cytolytic products. During this time the host becomes susceptible to super-infection due to reduced accumulation of macrophages, impaired neutrophils, immune cell death, and tissue damage due to inflammation, all of which creates a favorable environment for bacterial colonization (Fig. 1.1) [2, 14, 15, 16]. Super-infection is established via a dysregulation in the immune system resulting from the synergy of bacterial factors (i.e. LPS and staphylococcal enterotoxin B) and viral infection[2, 17, 18]. During influenza infection both viral and host factors are associated with increased super-infection susceptibility[2]. One hypothesis focuses on the targeting and destruction of the main host sites of bacterial colonization, i.e. epithelial cells, by the influenza virus, leading to increased bacterial colonization[19, 20, 21, 22]. Other studies have looked at the role of viral neuraminidase, an enzyme on the surface of the virus required for replication that cleaves sialic acid, which disrupts the epithelium, allowing bacterial adherence[23, 24].

Susceptibility to influenza associated bacterial super-infections is driven by competing immune responses that nurture an environment suitable for opportunistic pathogens. The two most common opportunistic pathogens that have been found to be associated with influenza infections are *Staphylococcus aureus* including methicillin resistant strains, and *Streptococcus pneumoniae*. One of the prevailing hypotheses regarding susceptibility to bacterial super-infections is the idea that the anti-viral immune mechanisms hinder subsequent bacterial immune mechanisms.

Interferon pathways have been extensively studied for their role in bacterial super-infection. Infection with *S. pneumoniae* followed by an influenza infection has been shown to lead to an increase in Type I interferon production which subsequently leads to a reduction in CCL2 production and phagocytic cell recruitment, resulting in increased bacterial burden[25]. Another study on Type I interferons showed that knocking out the IFNα/β receptor (IFNAR1) in mice led to a better antibacterial response, which was also attributed to a reduction in phagocytic recruitment[26]. Type I interferons are not the only members of the interferon family that have been implicated in diseases pathogenesis. Type II interferon (IFN-γ) has also been implicated in increased susceptibility to bacterial super-infections due to its role in the downregulation of the scavenger receptor MARCO, which results in the inhibition of macrophage phagocytic function[27]. Lastly, levels of Type III interferon (IFN-λ) have been shown to be positively correlated with bacterial burden, potentially via inhibition of bacterial uptake by phagocytic cells[28, 29]. In addition to the interferon pathways acting in a deleterious way, there is also evidence that Toll-like receptor (TLR) pathways are altered following influenza exposure resulting in a reduction in phagocytic cell recruitment and subsequent bacterial clearance [30, 31]. Alterations in phagocytic cells during super-infection are likely not limited to what is discussed here and this remains an area of interest for researchers studying bacterial super-infections.

Phagocytic cells are not the only cell types that become impaired following influenza challenge. The impaired production of the cytokine TNF-α by natural killer (NK) cells following influenza virus challenge was shown to result in an impaired antibacterial defense[32]. Cells associated with the Type 17 pathway play a pivotal role in bacterial defense and promotion of bacterial clearance via their role in recruitment of phagocytic cells such as neutrophils. Studies in mice have shown that following an influenza virus challenge, the production of type 17 cytokines,

IL-23, IL-22, and IL-17, are suppressed via impairment of IFN signaling through the STAT1 transcription factor, leading to bacterial outgrowth and promotion of a bacterial superinfection in the lung[33, 34]. Several reviews have detailed the numerous other susceptibility mechanisms associated with bacterial super-infection[14, 31, 35, 36]. Each of these mechanisms aids in creating an environment that is beneficial for bacterial colonization (Fig. 1 2).

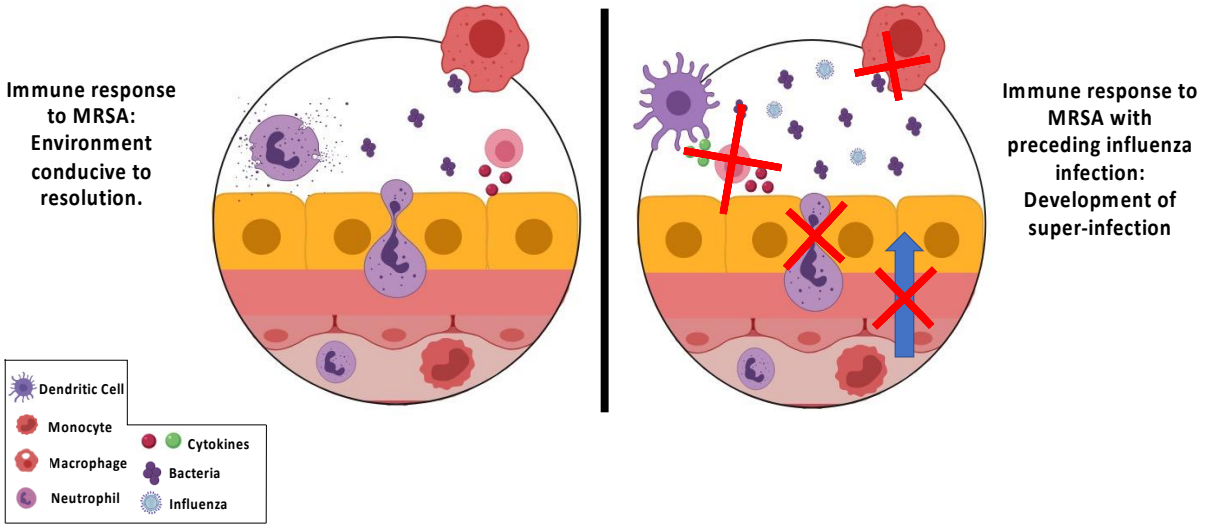

Figure 1.2. Dysregulation of anti-bacterial immune mechanisms by a preceeding influenza infection.

An ideal environment for MRSA resolution is characterized by phagocytic cells, such as neutrophils, monocytes, and macrophages, that engulf bacterial species leading to the resolution of the infection. Immune responses to preceding influenza infections result in dysregulation of the phagocytic component of the immune system and the eventual establishment of a super-infection. Developed with BioRender.

1.2 Inhibitory Mechanisms

Mounting an effective immune response is key to defending the host against external stimuli, such as pathogens. An effective immune response is characterized by a cascade of immunological events that target the area of infection. If left unchecked, this targeted response can cause detrimental off-target effects to the infected area in some cases results in immunopathology. Due to this the immune system has developed mechanisms that act as brakes on the immune response in order to weaken the response and eventually return the host to a state of homeostasis[37]. Several mechanisms are involved in immune regulation, including cellular mechanisms, most notably an immunosuppressive sub-population of $CD4^+$ T cells, the regulatory T cells (Tregs)[38]. In addition to cellular mechanisms of immunosuppression there are co-stimulatory and inhibitory receptors, which are expressed on various cell types and have diverse modes of action to shut down immune cell responses.

The most well-known inhibitory receptor (or checkpoint receptor) is the programmed death-1 (PD-1) receptor, which is found on both adaptive and innate immune cells[39, 40]. The checkpoint receptor PD-1 contains immunoreceptor tyrosine-inhibitory motifs and switch motifs within its cytoplasmic tail, which play a key role in its interaction with signaling molecules downstream of the T cell receptor (TCR)[39]. Signaling through PD-1 is diverse and context dependent meaning that in some cases it can have stimulatory effects, such as during initial T cell stimulation, and in others it can have inhibitory effects, such as during chronic stimulation[39]. Following the discovery of PD-1, several other inhibitory receptors were discovered including T-cell immunoglobulin and mucin-domain containing-3 (Tim-3), lymphocyte-activation protein 3 (Lag3), and natural killer cell receptor 2B4. Since the discovery of immune checkpoint receptors, researchers have sought to target these pathways for the development of novel immunotherapeutics

for the treatment of several diseases from cancers to chronic viral infections and autoimmune diseases[41, 42, 43]. Many of these therapeutics targeting inhibitory pathways are in clinical use today. Examples of antibody therapies targeting inhibitory pathways that are in clinical use today are pembrolizumab and nivolumab for Pd-1 and ipilimumab for CTLA-4. These therapies have been shown to be effective treatments for several cancers including melanoma[44, 45].

1.2.1 Inhibitory Mechanisms and Viral Infections

The roles of inhibitory mechanisms during both chronic and acute viral infections have been extensively studied. Studies in chronic viral infection models have shown that $CD8^+$ T cells become functionally impaired over time, which was found to be in part due to the PD-1 pathway[46, 47, 48, 49]. As PD-1 was being implicated in multiple chronic infections, researchers then became interested in studying its role during acute infections due to the observation that upon T cell activation, PD-1 is readily upregulated on the cell surface[39, 50]. This is of particular interest because during acute infections effector cells are extremely important in defense and clearance. Studies on the acute Armstrong strain of lymphocytic choriomeningitis virus (LCMV), found that targeting the PD-1 pathway early on led to enhanced $CD8^+$ T cell effector function, resulting in better clearance[50]. This pattern of inhibition of effector cell function and proliferation by the PD-1 pathway was subsequently found in numerous other acute viral infections[51, 52, 53]. Studies on the role of the PD-1/PD-L1 axis in influenza virus infections have corroborated previous findings that suggest PD-1 acts to limit the $CD8^+$ T cell response during the effector phase, which when targeted leads to a quicker immunological response following viral infection[54, 55, 56]. Another study looked further at impairment of $CD8^+$ T cells during influenza infection by researching the critical role that PD-1 plays in regulating the effector to memory cell transition[57]. The observations seen in this

study were found to be dependent on timing of PD-1 blockade relative to infection, where the memory compartment is hindered if PD-1 is knocked out from early effector stage and sustained through the recovery and memory formation stage[57]. The role of inhibitory effectors during acute viral infections continues to be studied, with the most recent evidence gained from Covid-19 pandemic patient samples[58, 59]. T cells were reportedly reduced in these studies and researchers observed an exhausted phenotype correlated with expression of PD-1, PD-L1, and Tim-3 on the surface of immune cells. Although several studies have determined that targeting PD-1 can enhance the immune response to disease, it is important to note that this can lead to a highly inflamed state and possible off-target immunopathological effects[60].

1.2.2 Inhibitory Mechanisms and Bacterial Infections

Inhibitory mechanisms have become an emerging area of interest for researchers studying how the immune system is weakened in response to persistent bacterial infections. Studies on *Helicobactor pylori* suggest that the PD-1 pathway plays a role in T cell dysfunction that is commonly seen in chronic infections[61, 62, 63]. Interestingly, targeting the PD-1 pathway during *Mycobacterium tuberculosis* infection resulted in a magnification of the bacterial infection and a reduction in infiltrating immune cells resulting in worse infectious outcomes which researchers linked to $CD4^+$ T cells[64, 65, 66]. Several studies on sepsis and another study on acute liver injury, showed that the PD-1 pathway plays a role in weakening the immune responses of several immune cell types including macrophages, monocytes, and Kupffer cells, making them less able to defend against bacteria[67, 68, 69, 70, 71]. Although several studies regarding the role of inhibitory mechanisms during bacterial infections were highlighted here there is still much that remains to be elucidated. The studies mentioned above regarding the effects of PD-1 effect on myeloid cell responses during

bacterial infections provides rationale for studying this pathway in the context of bacterial super-infections, which are characterized by a dampened bacterial response.

1.3 Immune Memory

Following a primary immune response targeted against a pathogen, the immune system enters a recovery phase that eventually leads to homeostasis within the previously infected space. In order to return to homeostasis, the immune system must shut down its inflammatory response, accomplished in part by a contraction in the majority of immune cells and the retention of a small amount that will go on to form the memory compartment. Memory lymphocytes are essential during re-infection from the original pathogen because of its ability to respond and mobilize quickly assisting in the efficient neutralization of the pathogen. Both the innate and adaptive immune systems can form a memory compartment.

1.3.1 Innate Immune Memory or Trained Immunity in Infection

Innate immune memory, or trained immunity, is the ability of the innate immune system to recognize and react against various pathogens without necessarily coming in contact with the pathogen previously[72, 73]. The innate cells that have been observed to gain memory characteristics are macrophages, monocytes, NK cells, and innate lymphoid cells. There have been several studies to date looking at the induction of trained immunity in mouse models. In these studies, it has been shown that both bacterial ligands as well as cytokines can induce trained immunity against bacterial species with no prior exposure[72, 74, 75, 76]. As researchers began to discover that the innate

immune compartment was able to form memory, several studies have looked further at innate immune memory at the level of individual innate immune cell subsets. Memory or memory-like NK cells have been found in numerous disease models. In murine cytomegalovirus (MCMV), it has been reported that a small subset of NK cells that express the receptor Ly49H act similarly to $CD8^+$ memory T cells, meaning that they are able to respond and proliferate more quickly upon re-challenge[77, 78]. Additional support for NK cell memory was found in several viral disease studies from Epstein-Barr Virus (EBV), as well as human and simian immunodeficiency viruses (HIV and SIV) which have been highlighted extensively in detail in review articles[79, 80]. Macrophages have also been shown to develop memory-like phenotypes upon re-exposure to a pathogen. In a mouse model of recurrent *S. aureus* infection, investigators determined that experienced macrophages at the site of infection are able to mobilize and respond more quickly against re-challenge[81]. Although there are several studies demonstrating innate memory, this area still remains much less understood than its adaptive counterpart.

1.3.2 Adaptive Immune Memory and its Role in Influenza Infection

The adaptive immune memory compartment is composed of long-lived, antigen-experienced, T and B cells that have undergone phenotypic and genotypic changes distinct from their naïve and effector counterparts that make them better able to defend against a pathogen upon re-challenge[72, 82, 83]. Both $CD4^+$ and $CD8^+$ T cells can form a memory compartment. The role of memory T cells in influenza has been extensively studied due to the role they play in protecting against heterotypic influenza strains, which makes them potential candidates for targeting and development of universal vaccines[84, 85]. Once the memory T cell compartment is formed it can be further segmented into either tissue-resident memory (Trm), central memory (Tcm), or effector

memory (Tem) which are classified based on location and, phenotypically, by surface marker expression[86]. Although each of the memory cell subsets plays essential protective functions, Trm cells are of particular importance because of their unique ability to thrive in mucosal tissues and act as first responders upon re-challenge. The importance of Trm cells is particularly evident in pulmonary diseases such as influenza. Research on influenza and heterotypic immunity in mouse models determined that Trm cells are essential for defense and protection against multiple influenza strains[87, 88]. In a mouse model of bacterial pneumonia, $CD4^+$ Trm have been shown to play a role in remodeling cells of the lung epithelium leading to a quicker and more robust innate immune response upon re-challenge[89]. Interestingly, lung Trm cells, in particular $CD8^+$ Trm, do not persist over long periods of time. This observation is believed to be due to several mechanisms ranging from changes in the environmental milieu of cytokines which could lead to the stimulation of apoptotic pathways[90, 91]. The role of immune memory in susceptibility to influenza-associated bacterial super-infections is a new frontier for understanding how acute respiratory infections can drive changes in the lungs that reinforce protective mechanisms which are stimulated upon re-challenge events and which can act to lessen the damage incurred by the lung during infection.

2.0 The role of the Inhibitory Receptor PD-1 in Susceptibility to Influenza Associated Secondary Bacterial Infections.

2.1 Summary

T cell inhibitory pathways have been carried out in many diseases, including cancer, chronic infections, and most recently acute infections. Most studies have focused on interfering with T cell inhibitory pathways to re-invigorate the immune response during immune challenge, which is called checkpoint blockade. The targeting of inhibitory T cell mechanisms during influenza infection represents a potentially new area of therapeutic treatment. A common complication of influenza infection is the development of a bacterial super-infection. Given the suppression of antibacterial immune responses during super-infection, targeting of inhibitory mechanisms is attractive. As of yet, there is no published research reporting the use of checkpoint inhibitor blockade in influenza associated bacterial super-infection. With the emergence of antibiotic resistant bacterial strains, such as methicillin-resistant *Staphylococcus aureus* (MRSA), treating super-infections remains an ongoing area of concern. In this study we show that influenza drives the expression of inhibitory molecules on both myeloid and adaptive immune cells in the lung of infected mice. Using PD-1 KO mice as well as antibody blockade of PD-1 we determined that blocking the PD-1 pathway resulted in no change in susceptibility to super-infection in terms of bacterial burden and weight loss. However, there were significant changes observed at the cellular level in our treatment groups. These findings provide more insight into the role of inhibitory molecules, in particular PD-1, during acute infections.

2.2 Introduction

One of the major scientific insights in the field of influenza-associated bacterial super-infections is that impaired immune cellular responses drive susceptibility. There have been many studies on the role of interferons (IFNs) in promoting susceptibility to secondary bacterial infections in mouse models[92, 93, 94]. Type I interferon production and suppression of type 17 immunity have been implicated in increased susceptibility to bacterial super-infection[33, 92, 95, 96]. When production of type 17 effector molecules by both $CD4^+$ T cells and γδ T cells is diminished, there is altered neutrophil recruitment to the site of infection, resulting in higher bacterial burdens in super-infected animals. Studies in other murine super-infection models have shown that influenza infection reduces the number of $CD8^+$ T cells that respond to bacterial lung infection, as well as rendering $CD4^+$ T cells ineffective, leading to impaired antibacterial immunity[31, 97, 98]. When IFN-γ production from T cells is ablated during influenza infection, bacterial clearance is improved in some mouse models, due to increased macrophage activity[27, 92, 93, 94].

There are currently two main strategies to alleviate bacterial super-infections; one is to directly target the virus through therapeutics and vaccines, and the second is to treat the bacterial infection with antibiotics. Prevention of influenza spread has been mainly attributed to implementation of vaccination strategies. However, due to its high mutation rate, new strains of influenza virus emerge yearly, resulting in the yearly development of new vaccine variants with varying efficacies against circulating strians[99, 100]. Antivirals have also been developed, however, unless administered early during infection and symptom onset they are considered ineffective[101]. Current treatments for super-infection rely on early administration of antibiotics. Even with the advent of new antibiotics and newly developed vaccines against pneumococci bacterial strains[19,

[102], the continued presence of influenza- associated bacterial super-infections highlights the need for better strategies and therapeutics to combat infection, especially with the emergence of new antibiotic-resistant strains of *Staphylococcus aureus* like MRSA[103].

Immune-checkpoint blockade is an emerging approach for the treatment of chronic and acute infections. During an immune response, co-stimulatory and co-inhibitory receptors are upregulated on T cells, collectively referred to as checkpoint receptors[104]. When T cells are chronically stimulated by antigen they are driven into a state of impairment to protect the organism against immunopathology[105]. This state is characterized by high and prolonged expression of multiple inhibitory receptors, and gradual loss of effector function in the form of decreased proliferation and effector molecule production[104, 105]. This results in the delay or failure to eliminate pathogen[105]. Studies have uncovered multiple inhibitory receptors that are upregulated on exhausted T cells, including but not limited to T-cell immunoglobulin and mucin-domain containing-3 (Tim-3), lymphocyte-activation gene 3 (Lag3), natural killer cell receptor 2B4 (2B4), and the well-studied PD-1[13]. Immune-checkpoint blockade, currently a therapeutic approach for cancer treatment, is the targeting of inhibitory pathways to reverse exhaustion. This is predominantly accomplished with *in vivo* administration of antibodies that block inhibitory receptor ligand pairs, leading to increased T cell proliferation and effector function[46, 105, 106].

T cell impairment has been demonstrated in chronic viral infection models where T cells failed to proliferate and produce effector molecules to control infection[46, 107, 108]. When exhaustion pathways like the PD- 1/PD-L1 axis are blocked, T cell functionality improves, leading to better viral clearance[46, 107]. T cell impairment has also been documented during acute infections. However, studies on checkpoint receptors in acute infections have been controversial, showing

both beneficial and detrimental effects, depending on the study. In one study on acute Friend retrovirus, it was shown that $CD8^+$ T cells upregulate PD-1 but retain functionality and aid in viral clearance[109]. Studies on human metapneumovirus (HMPV) and influenza virus, both common causes of acute respiratory infections, have shown that during infection, PD-1 and PD-L1 are upregulated on $CD8^+$ T cells at the site of infection[56]. Blockade of this axis during infection resulted in improved viral clearance by day five in an HMPV model[56]. This study also showed that when mice are challenged with influenza PR8 (H1N1), by day fourteen influenza specific cells are impaired[56]. When PD-1 was knocked out and mice are challenged with X31 (H3N2) there are more influenza specific cells and these cells produce more IFN-γ, and CD107a[56]. This study also characterized the expression of PD-1 by lymphocytes and PD-L1 by alveolar epithelial cells in human lung autopsy samples from the 2009 influenza pandemic, and found a role for this pathway during acute infection in humans[56]. Another study on the role of PD-L1 during influenza infection showed that blockade of PD-L1, which is expressed by the airway epithelium and regulated by type I interferon receptor signaling, improved $CD8^+$ T cell function, characterized by increased expression of IFN-γ, CD107a, and granzyme B by day three in a re-challenge model, resulting in increased viral clearance by day five[110]. During respiratory viral reinfection with HMPV, PD-1 was the dominant inhibitory receptor upregulated early during re-challenge[54]. After PD-1 was blocked, $CD8^+$ T cell functionality improved, resulting in restored function and improved viral clearance in this mouse model[54]. The authors recapitulated this finding during reinfection using influenza virus, showing that more functional influenza specific cells are found at day seven in PD-1 KO mice[54].

Cellular impairment of immune cells is a well-known factor that enhances susceptibility to bacterial super-infections. As mentioned above, the impairment of T cells during infection has

been associated with disease progression in various models of infection. Merging these two ideas provides rationale for studying impairment pathways, such as the PD-1 pathway, during acute bacterial super-infections. Currently, there has been little research conducted on the role of T cell impairment in influenza associated bacterial super-infections,

2.3 Materials and Methods

2.3.1 Mouse Model and Sample Collection

PD-1 global KO mice were a generous gift from Dr. John Williams, and Wild-type C57BL/6 mice were purchased from Taconic Biosciences (Germantown, NY). Mice were housed in the BSL2 facility at Rangos Research Center (Pittsburgh, PA). On day zero male mice were infected with 100 pfu of mouse adapted influenza A/PR/8/34 H1N1 or PBS vehicle. After 6 days the mice were challenged with $5x10^7$ colony forming units (cfu) of USA300 MRSA suspended in PBS. On day 7 mice were euthanized and harvested. All infections were given via oropharyngeal aspiration. Mice were euthanized via pentobarbital injection followed by exsanguination by severing the renal artery. No mice died prior to euthanasia. All studies were performed on sex-matched mice. All animal studies were conducted with approval from the University of Pittsburgh Institutional Animal Care and Use Committee.

2.3.2 Murine Infections and Pathogen Preparation

All mice were anesthetized using inhaled isoflurane and were infected via oropharyngeal aspiration (OA). Methicillin-resistant *Staphylococcus aureus* (MRSA) USA300 was grown overnight in a *S. aureus*-specific media using an orbital shaker set at 37• C until the next morning at which point stationary phase was reached. Media sterility was ensured with a blank broth control tube added at the same time as MRSA incubation. Following incubation, the optical density of MRSA was measured at 660 nm and multiplied by the previously calculated coefficient of extinction, $1.48x10^9$, to get colony forming units (CFU). Once this number was calculated it was divided by $5x10^7$ to get the dose information per mouse. The culture was then centrifuged at 10,000×g for five minutes, broth was aspirated, and the cell pellet was resuspended in PBS to ensure delivery of 50uLs per mouse. For influenza preparation, frozen stocks of Influenza H1N1 A/PR/8/34 were diluted in PBS to doses between 1:10 and 1:20, to deliver 50 μLs of virus per mouse resulting in a reduction of about 15-20% of body weight by harvest day 7.

2.3.3 Antibody blockade

Wild-type C57BL/6 mice were given either 200ug of Pd-l1(B7-H1) (clone: 10F.9G2) or its corresponding isotype rat IgG2b (clone: LTF-2) or they were given PD-1 (CD279) (clone: 29F.1A12) or is corresponding isotype rat IgG2a (clone: 2A3) antibodies from BioXCell (Lebanon, NH). Injections were given on days 1, 3 and 5 following initial influenza infection on day 0.

2.3.4 Bacterial Plating

Right upper lung lobes from mice were collected and homogenized in 1ml of PBS. After homogenization, 10-fold dilutions were dot plated on culture plates. Plates were then incubated at 37^{o} Celsius overnight, and cfu was assessed by bacterial colony counting.

2.3.5 Bronchoalveolar Lavage Fluid Collection and Differential Cell Counting

Upon harvest, mice were cannulated and lavaged with 1ml of PBS for bronchoalveolar lavage fluid (BALF) collection. BALF was spun down and pelleted and supernatant was collected and stored for downstream analysis. Pelleted cells were treated with ACK lysing buffer (Gibco Fisher Scientific, Hampton, NH) to remove red blood cells. The cell pellet was then resuspended in 500µl of PBS and total cell count was determined by hemocytometer. 200µLs of resuspended cells were then concentrated on a microscope slide using a cytocentrifuge (ThermoFisher Scientific, Waltham, MA) and stained with Diff-Quik staining solution (Fisher Scientific, Hampton, NH) to determine monocyte, neutrophil, eosinophil, and lymphocyte counts.

2.3.6 RNA Extraction and qPCR

Mouse lungs were isolated and snap-frozen in liquid nitrogen or suspended in Allprotect Tissue Reagent (Qiagen, Hilden, Germany). RNA was extracted as directed using the Qiagen Rneasy Mini Kit (Qiagen, Hilden, Germany). cDNA was synthesized using the iScript cDNA synthesis kit (Bio-Rad, Hercules, CA). qPCR was conducted using SsoAdvanced universal probes supermix (Bio-Rad, Hercules, CA) and target specific TaqMan real-time PCR assay primer probes

(ThermoFisher Scientific, Waltham, MA). Viral burden was determined by quantitative real-time RT-PCR on lung RNA for viral matrix protein (M1) as described previously [111, 112]. Forward Primer:5′-GGACTGCAGCGTAGACGCTT-3′, Reverse Primer:5′-CATCCTGTTGTATATGAGGCCCAT-3′,Probe:5′-/56-FAM/CTCAGTTAT/ZEN/TCTGCTGGTGCACTTGCCA/3IABkFQ/−3′.

2.3.7 Protein Assays and Lincoplex

The Pierce™ BCA protein assay kit (ThermoFisher Scientific, Waltham, MA) was used as directed to determine protein levels in BALF. Cytokine production was measured in lung homogenates via Bioplex using the Luminex™ Magpix™ multiplexing platform with the Bio-Plex Pro Mouse Cytokine 23-plex assay (Bio-Rad, Hercules, CA) as directed. Mouse lung homogenates were used to determine IgM protein using an IgM uncoated ELISA kit as directed (Invitrogen-ThermoFisher Scientific, Waltham, MA).

2.3.8 Flow Cytometry

Mouse lungs were aseptically dissected using sterile scissors. Lungs were then digested for an hour at 37^{o} Celsius in 1mg/ml collagenase media (DMEM Gibco Fisher Scientific, Hampton, NH). After an hour, lungs were mashed through 70 micron filters to obtain a single cell suspension. The single cell suspension was treated with ACK lysing buffer (Gibco Fisher Scientific, Hampton, NH) to remove red blood cells. After red blood cell lysis, cells were resuspended in PBS. Single cell suspensions were stained as follows for spectral flow cytometry analysis. For the T cell panel, cells were stained with anti-CD45 (30-F11, BD OptiBuild, Franklin Lakes, NJ), CD90.2 (30-H12,

BD OptiBuild, Franklin Lakes, NJ), FoxP3 (MF-14, BioLegend, San Diego, Ca), Cd4 (RM4-5, BD Biosciences, Franklin Lakes, NJ), Tbet (4B10, BioLegend, San Diego, Ca), Il-10 (JES5-16E3, BD Biosciences, Franklin Lakes, NJ), Gata3 (L50-823, BD Biosciences, Franklin Lakes, NJ), Lag3 (C9B7W, BioLegend, San Diego, Ca), Cd8a (53-6.7, BD Biosciences, Franklin Lakes, NJ),Il-17a (TC11-18H10.1, BioLegend, San Diego, Ca), Cd44(IM7, BioLegend, San Diego, Ca), Rorγt (Q31-378, BD Biosciences, Franklin Lakes, NJ), PD-1 (RMP1-30, BioLegend, San Diego, Ca), Cd244.2(m2B4(B6)458.1,BioLegend, San Diego, CA), Tim3 (B8.2C12,BioLegend, San Diego, CA), Cd11b (M1/70, Invitrogen-ThermoFisher Scientific, Waltham, MA), Cd11c (N418, BioLegend, San Diego, Ca), and IFNγ (XMG1.2, BD Biosciences, Franklin Lakes, NJ). NP366 tetramers were obtained from the NIH tetramer core facility (Bethesda, MD) and were stained at 37^{o} Celsius for 30 minutes prior to viability stain. For the myeloid panel, cells were stained with anti-CD45 (30-F11,Invitrogen-ThermoFisher Scientific, Waltham, MA), Pd-l2 (TY25,BioLegend,San Diego, CA), F4/80 (T45-2342,BD Biosciences, Franklin Lakes, NJ), Cd64a/b (X54-5/7.1,BD Biosciences, Franklin Lakes, NJ), Pd-l1 (10F.9G2,BioLegend, San Diego, CA), Cd103 (2E7,Invitrogen-ThermoFisher Scientific ,Waltham, MA), Ly6c (HK1.4,BioLegend, San Diego, CA), Cd11b (M1/70,BD Biosciences, Franklin Lakes, NJ), MHC-II (M5/114.15.2,BD Biosciences, Franklin Lakes, NJ), B220 (RA3-6B2,Invitrogen-ThermoFisher Scientific , Waltham, MA), Tcrb (H57-597,BioLegend, San Diego, CA), SiglecF (1RNM44N,Invitrogen-ThermoFisher Scientific, Waltham, MA), Cd24 (M1/69,BioLegend, San Diego, CA), PD-1 (RMP1-30,BioLegend, San Diego, CA), Cd244.2 (m2B4(B6)458.1,BioLegend, San Diego, CA), Nk1.1 (PK136,BioLegend, San Diego, CA), Cd11c (N418,Invitrogen-ThermoFisher Scientific. Waltham, MA), and Tim3 (B8.2C12,BioLegend, San Diego, CA). The viability dye, Zombie NIR (BioLegend, San Diego, CA), was used to exclude live cells from dead

cells in both panels. Our mastermix for cell staining contained Super Bright Complete Staining Buffer (ThermoFisher Scientific, Waltham, MA) as well as True-Stain Monocyte Blocker (BioLegend, San Diego, CA) for the myeloid panel. Intracellular staining was performed at room temperature using the eBioscience™ Foxp3/Transcription Factor Staining Buffer Set (ThermoFisher Scientific, Waltham, MA) as directed by the manufacturer. All samples were run on the Cytek Aurora (Cytek Biosciences, Fremont, CA). Flow cytometric analysis was performed using FlowJo (TreeSTAR) software.

2.3.9 Statistical Analysis

Data were analyzed using GraphPad Prism software (San Diego, CA). Experiments were repeated 3-6 times as indicated. All data are presented as mean ± SEM, unless otherwise noted. Mann-Whitney test or one-way ANOVA followed by multiple comparisons were used for statistical significance with a p value of equal or less than 0.05.

2.4 Results

2.4.1 WT super-infected mice display elevated levels of cells expressing PD-1.

To determine if the PD-1 pathway was being stimulated during super-infection, we used flow cytometry to probe for cells that expressed PD-1 from infected mouse lungs. First, we determined the percentage of T cells that expressed PD-1. We found that there was an increase in the number (?; proportion?) of PD-1 expressing $CD4^+$ and $CD8^+$ T cells in influenza and super-

infected mouse lungs, and a significant decrease in PD-1 expressing T cells in MRSA alone infected mouse lungs (Fig. 2.1a). Next, we assessed the presence of PD-1 expressing cells in the myeloid compartment. There was an increase in PD-1 expressing exudative macrophages in super-infected lungs which was similar in the influenza alone treatment (Fig. 2.1b). When we looked at inducible monocytes and neutrophils, we found that there was a decrease in cells that expressed PD-1 in the MRSA alone and super-infected groups, which was not the case for the group infected with influenza alone, which displayed an increase in these cells (Fig. 2.1b). These data suggest that PD-1 expression is stimulated in response to influenza and could potentially play a role during influenza associated bacterial super-infections.

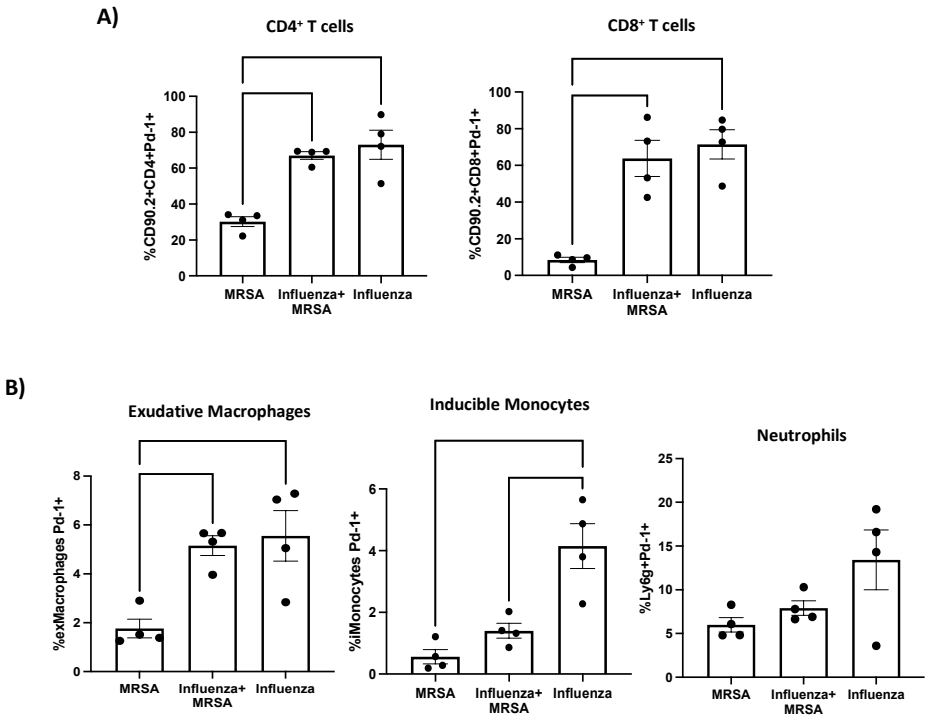

Figure 2.1 PD-1 is expressed on multiple cell types in influenza and super-infection and the percentage of PD-1$^+$ cells increases upon influenza infection.

Lungs from infected WT C57Bl/6 mice were collected and processed for multidimensional flow cytometric analysis. Dead cells were excluded from all analyses prior to downstream gating. A) T cells were gated via CD45$^+$CD90.2$^+$ and further broken down into percent of CD4$^+$ and CD8$^+$ (N=4). B) Myeloid cells were first gated using CD45 followed by CD11b and Cd11c and further gated into specific subsets based on major surface marker expression. Gating strategies can be found in Appendix fig. A.1.1 and A.2.3 which shows the T cell and myeloid strategy respectively. p values: *<0.05, **<0.01, ***<0.001, ****<0.0001.

2.4.2 Absence of PD-1 has a limited effect on super-infection susceptibility.

Due to the increase in immune cells that expressed PD-1 following super-infection, we used global PD-1 KO mice to determine if the pathway plays a role in secondary infection susceptibility (Appendix Fig. A.1.2). Super-infected PD-1 KO mice and their WT counterparts displayed similar reductions in weight loss following secondary MRSA challenge (Fig. 2.2a). MRSA burden as well as PR8 gene expression remained unchanged between the PD-1KO and WT MRSA alone and super-infected groups (Fig. 2.2b and c). We further confirmed these results with an antibody blockade against PD-1 in WT mice that were MRSA alone or super-infected (Appendix Fig. A.1.2b, Fig 2.2d and e). When we targeted one of the ligands, PD-L1, associated with PD-1 signaling we again saw no change in weight loss or MRSA burden, however, there was a significant increase in expression of PR8 in anti-PD-L1 treated super-infected mice (Appendix Fig A.1.3a). These results together suggest that PD-1 plays a limited role in susceptibility to super-infection, when taking only MRSA burden and weight loss into account.

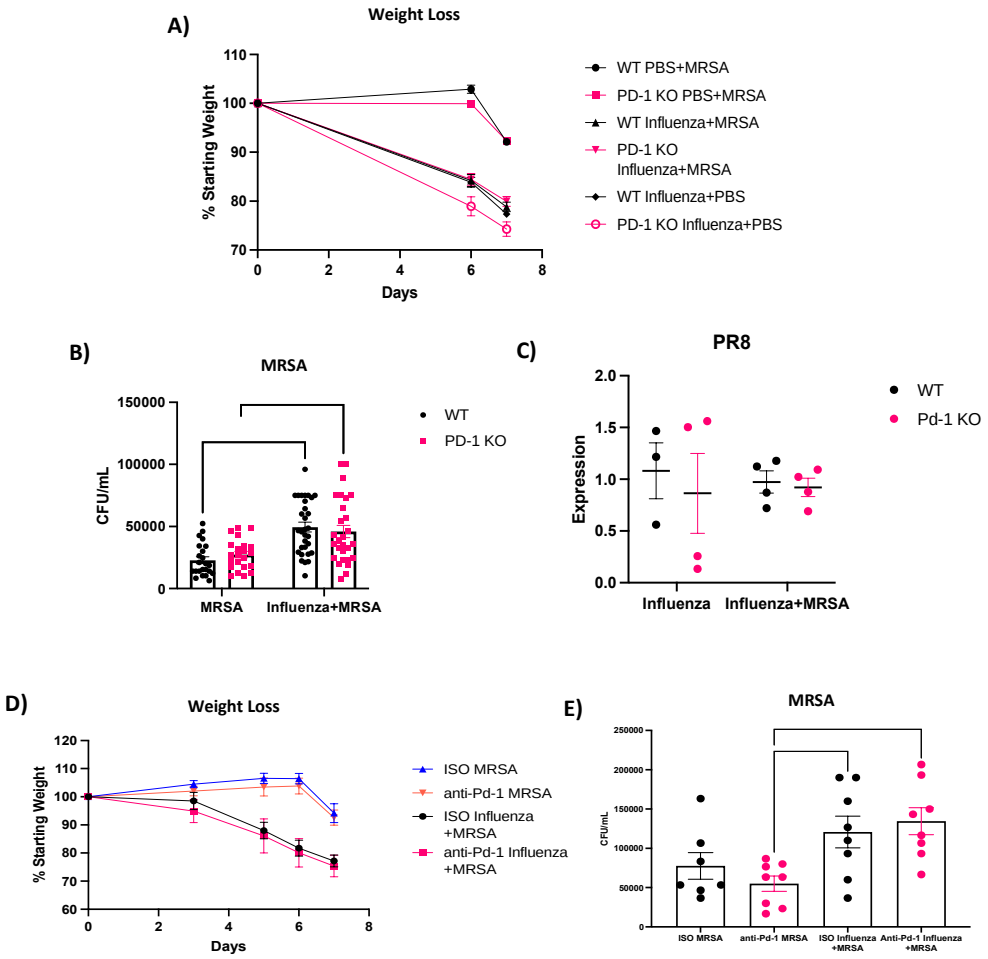

Figure 2.2 Global PD-1 KO mice and PD-1 antibody blockade has little effect on weight loss, MRSA burden, and relative gene expression of PR8 as compared to their WT or Isotype control counterparts during super-infection. A) WT and PD-1 KO treatment groups percent of weight loss was calculated starting from day zero, then again on day six when MRSA was given, and lastly on day seven the day of harvest (WT MRSA n= 19, PD-1 KO MRSA n=18, WT super-infected n=19, PD-1 KO super-infected n=18, WT influenza n=12, PD-1 KO Influenza n=12). B) Number of MRSA colonies plated from infected mouse lung homogenates (WT: MRSA n= 23, super-infected n=31; PD-1 KO: MRSA n=22, super-infected n=28). C) Relative gene expression of viral protein was assessed in cDNA from total mouse lung via relative gene expression analysis of PR8 (matrix protein) (WT influenza n=3, PD-1 KO influenza n=3, WT super-infection n=4, PD-1 KO super-infection n=4). D) Percent of weight loss was calculated starting from day zero, then sampled again on days three and five when antibody blockade was given, day six when MRSA was given, and lastly on day seven the

day of harvest (ISO MRSA n=7, anti-PD-1 MRSA n=8, ISO super-infected n=8, anti-PD-1 super-infected n=8). E) Number of MRSA colonies plated from infected mouse lung homogenates (ISO MRSA n=7, anti-PD-1 MRSA n=8, ISO super-infected n=8, anti-PD-1 super-infected n=8). P values: *<0.05, **<0.01, *<0.001, ****<0.0001.**

2.4.3 Lungs of global PD-1 KO super-infected mice have increased lung leak compared with WT mice.

We next sought to determine if targeting the PD-1 pathway during super-infection resulted in detrimental alterations to the lung environment. To test this, we checked protein levels in the bronchoalveolar lavage fluid (BALF), a measure of epithelial leak during injury. This resulted in the observation that PD-1 KO super-infected mice displayed a significant increase in protein concentration, suggesting that lung leak was more prevalent in this group as compared to their WT counterparts (Fig. 2.3a). However, the increase in BALF protein seen in global KOs was not recapitulated following antibody blockade of PD-1 or PD-L1 in WT mice (Fig. 2.3b, Appendix A.1 3b). To further determine if the lungs of super-infected KO mice were shifting towards a more damaged phenotype, we tested various molecular markers associated with lung integrity such as tight junction protein 1 (Tjp1), secretoglobin family 1A member 1 (scgb1a1), and surfactant protein-c (sftpc). Expression of all of these markers was decreased in PD-1 KO super-infected mice, compared to infection with MRSA alone; however, the levels were not significantly changed when they were compared to their WT super-infected counterparts (Fig. 2.3c). From histological analysis of the lungs of global PD-1 KO and WT mice, we determined that there is no significant difference in damage assessed in either the parenchyma, airways, or blood vessels beyond the elevated trend seen in super-infected mice compared to MRSA alone (Fig. 2.3d). These data

suggest that globally knocking out PD-1 potentially results in greater susceptibility to lung leak during super-infections.

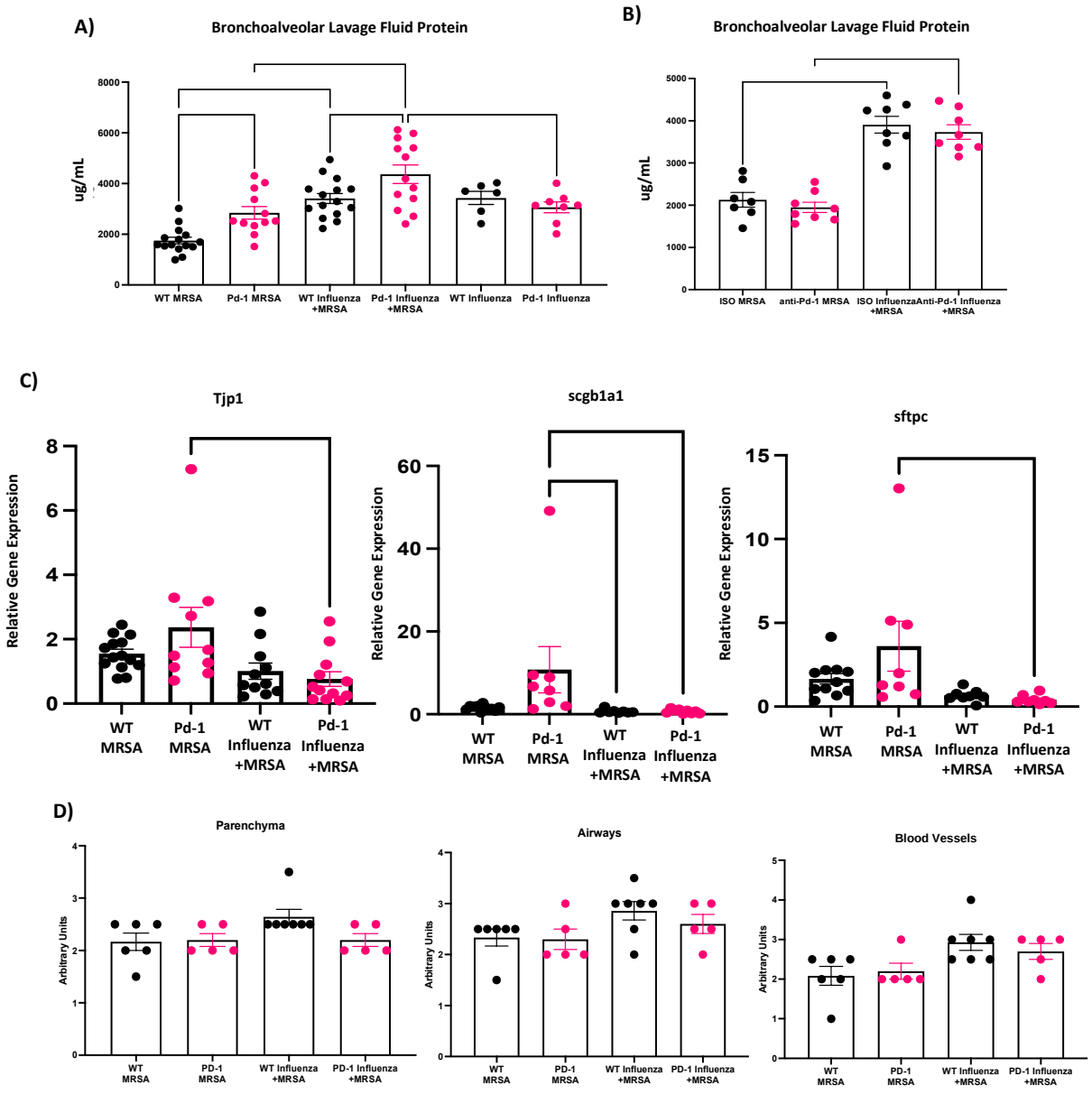

Figure 2.3 Global PD-1 KO mice have higher levels of protein in the BAL of MRSA alone and super-infected treated mice than WT mice or mice treated with an antibody against PD-1. A) BAL protein from PD-1 KO and WT infected mice was quantified from BAL collected at day of harvest (WT MRSA n= 15, PD-1 KO MRSA n=12, WT super-infected n=15, PD-1 KO super-infected n=13, WT Influenza n=6, PD-1 KO Influenza n=8). B) BAL protein from antibody PD-1 and isotype treated mice was quantified from BAL collected at day of harvest (ISO MRSA n=7, anti-PD-1 MRSA n=8, ISO super-infected n=8, anti-PD-1 super-infected n=8). C) RNA was extracted from mouse lungs and made into cDNA which we then used to probe for various genetic

targets (*Tjp1*: WT MRSA n= 14, PD-1 KO MRSA n=10, WT super-infected n=11, PD-1 KO super-infected n=12; *Scgb1a1*: WT MRSA n= 11, PD-1 KO MRSA n=8, WT super-infected n=8, PD-1 KO super-infected n=9; *Sftpc*: WT MRSA n= 11, PD-1 KO MRSA n=8, WT super-infected n=8, PD-1 KO super-infected n=8). D) Histological scoring of lung sections from WT and PD-1 KO mice looking at the parenchyma, airways, and arteries (WT MRSA n= 6, PD-1 KO MRSA n=5, WT super-infected n=7, PD-1 KO super-infected n=5). p values: *<0.05, **<0.01, *<0.001, ****<0.0001.**

2.4.4 Lung infiltrating cells in global PD-1 KO super-infected mice remain unchanged compared to their WT counterparts, however they are reduced in an antibody blockade model.

Due to the minimal role of PD-1 in susceptibility to super-infection in terms of burden, morbidity, and injury markers, we wanted to determine if there were changes at the cellular level. The total number of lung-infiltrating cells in our global PD-1 KO super-infected group was not significantly changed compared to its WT counterpart (Fig. 2.4a). Interestingly, we did see a reduction in infiltrating cell number between global PD-1 KO and WT animals infected with influenza (Fig. 2.4a). When we compared these results with our PD-1 antibody blockade we found that in contrast to global PD-1 KO mice, there was a significant reduction in total infiltrating cell number in the anti-PD-1 treated group (Fig. 2.4b). When we broke down the infiltrating cell numbers into more specific subsets, we again saw no significant change in either monocyte or neutrophil number between PD-1 KO and WT mice (Fig. 2.4c and e). However, we did see a significant reduction in neutrophil number in the PD-1 KO mice infected with influenza alone (Fig. 2.4e). Our antibody blockade experiments also showed a reduction in the number of neutrophils, but not monocytes, in the anti-PD-1 super-infected mouse group, compared to WT mice (Fig. 2.4d and f). Blocking of PD-L1 had no significant change in total cell, monocyte, or neutrophil numbers

in super-infected groups (Appendix Fig. A.1.3c). These data suggest that targeting PD-1 via antibody blockade during super-infection, rather than with a global PD-1 KO mouse model, does result in a change in cellular infiltrate, but this does not result in a significant change in susceptibility to bacterial burden and morbidity.

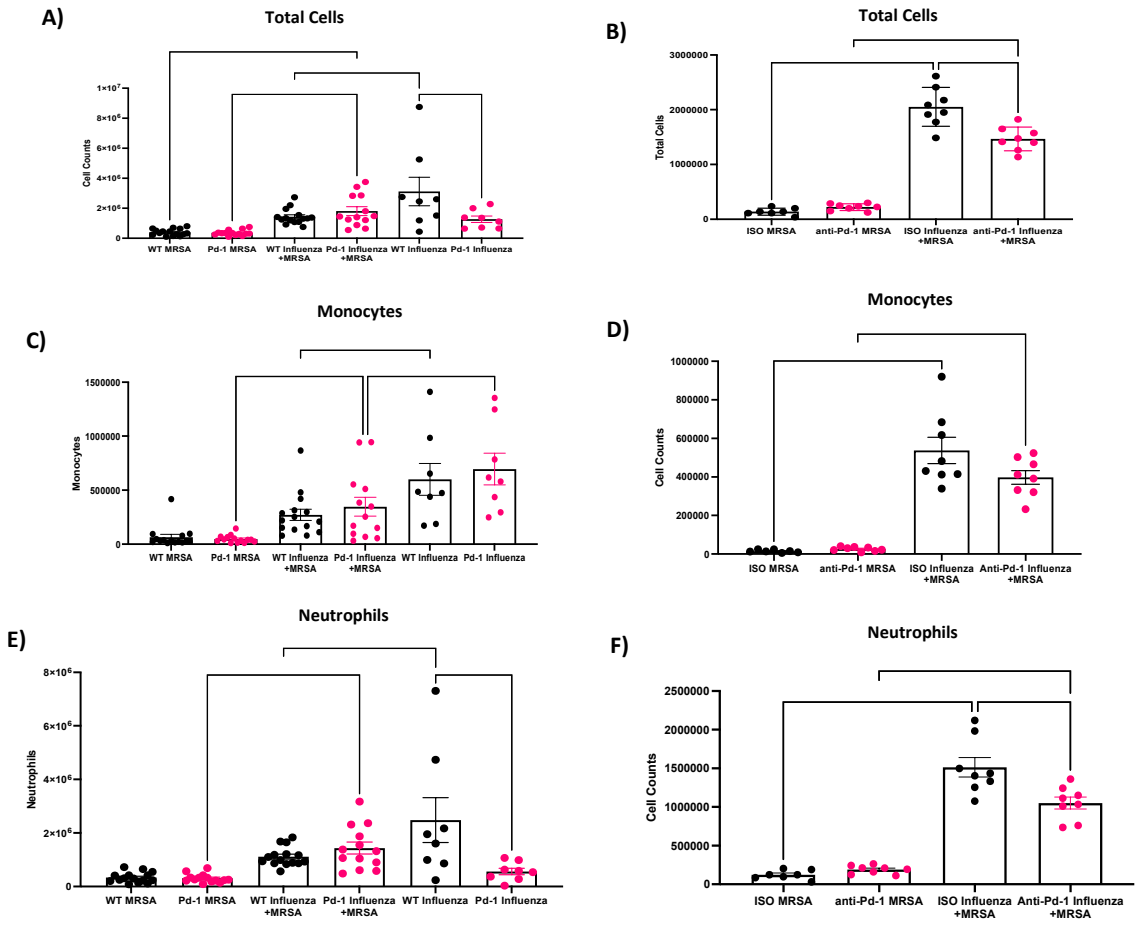

Figure 2.4 Super-infected PD-1 KO mice have similar levels of infiltrating cells compared to WT mice, but, treating with an antibody against PD-1 led to a significant reduction in total cells. A-F)Total infiltrating cell counts, number of monocytes, as well as number of neutrophils were determined by cytospins using bronchoalveolar lavage fluid collected from infected mouse lungs at time of harvest (PD-1 KO studies→total cells, monocytes, and neutrophils: WT MRSA n= 15, PD-1 KO MRSA n=14, WT super-infected n=15, PD-1 KO super-infected n=13, WT Influenza n=8, PD-1 KO Influenza n=8; anti PD-1 blockade→ total cells, monocytes, and neutrophils ISO MRSA n=7, anti-PD-1 MRSA n=8, ISO super-infected n=8, anti-PD-1 super-infected n=8). P values: *<0.05, **<0.01, *<0.001, ****<0.0001.**

2.4.5 Global knock out of PD-1 results in changes in the T cell compartment in various disease states.

We further assessed changes in the cellular compartment caused by the absence of PD-1 via flow cytometry during super-infection. Using our global PD-1 KO super-infection model, we first determined if $CD4^+$ T cell subsets changed in the absence of PD-1 following our different infection scenarios. Within our infection groups, we saw no change in the percentage of cells expressing GATA3, a canonical transcription factor for Th2 cells, between our WT or PD-1KO mice (Fig. 2.5a). When we looked at the changes in cells that expressed FoxP3, the Treg cell transcription factor, we did see a significant reduction in our PD-1 KO super-infected and influenza alone groups when we compared them to WT counterparts (Fig. 2.5b). Cells expressing Rorgt, the Th17 transcription factor, were reduced across all treatment groups, however, there was significantly fewer of these cells in the MRSA alone PD-1KO mice (Fig. 2.5c). One of the prevailing ideas in the field of inhibitory receptors is that multiple inhibitory receptors work together resulting in a more powerful downregulation of immune mechanisms. With this in mind we also looked at changes in the percentage of cells that express the other inhibitor receptors: Lag3, Cd244, and Tim3. Cells expressing Cd244 and Lag3 increased in WT and PD-1KO super-infected and influenza alone infected groups (Fig. 2.5d). Interestingly, in our MRSA alone and super-infected groups Tim3 was decreased in our WT and PD-1KO mice, however, it was significantly elevated in influenza alone WT infected mice compared to their PD-1KO counterparts (Fig. 2.5d). We further assessed changes in the $CD8^+$ T cell compartment in the absence of PD-1 across treatment groups. Although all PD-1 KO mice seemed to have lower levels of tetramer positive cells, this was not significantly different that their WT counterparts in all three of the infection conditions (Fig. 2.5e). Again, as we did with the $CD4^+$ T cells, we looked at

changes in the percentage of cells expressing inhibitory markers and again we saw an increase in these cell types in influenza alone and super-infected WT and PD-1KO groups, with the exception being in Tim3 where we did see an elevation in our super-infected WT and PD-1 KO groups (Fig. 2-5f). Lastly, we looked at changes in protein concentration of molecules associated with T cell activity during infection. We found that Ifnγ is significantly elevated in PD-1 KO super-infection and IL-4 expression is significantly decreased as compared to WT mice (Fig. 2.5g). Together these data suggest that knocking out PD-1 does affect both $CD4^+$ and $CD8^+$ T cells when looking at PD-1 KO groups across infectious states from MRSA, super-infection, and influenza. In particular an increase in percentage of cells expressing other inhibitory factors was seen when PD-1 KO groups were compared to each other, which could potentially act to compensate for the loss of PD-1.

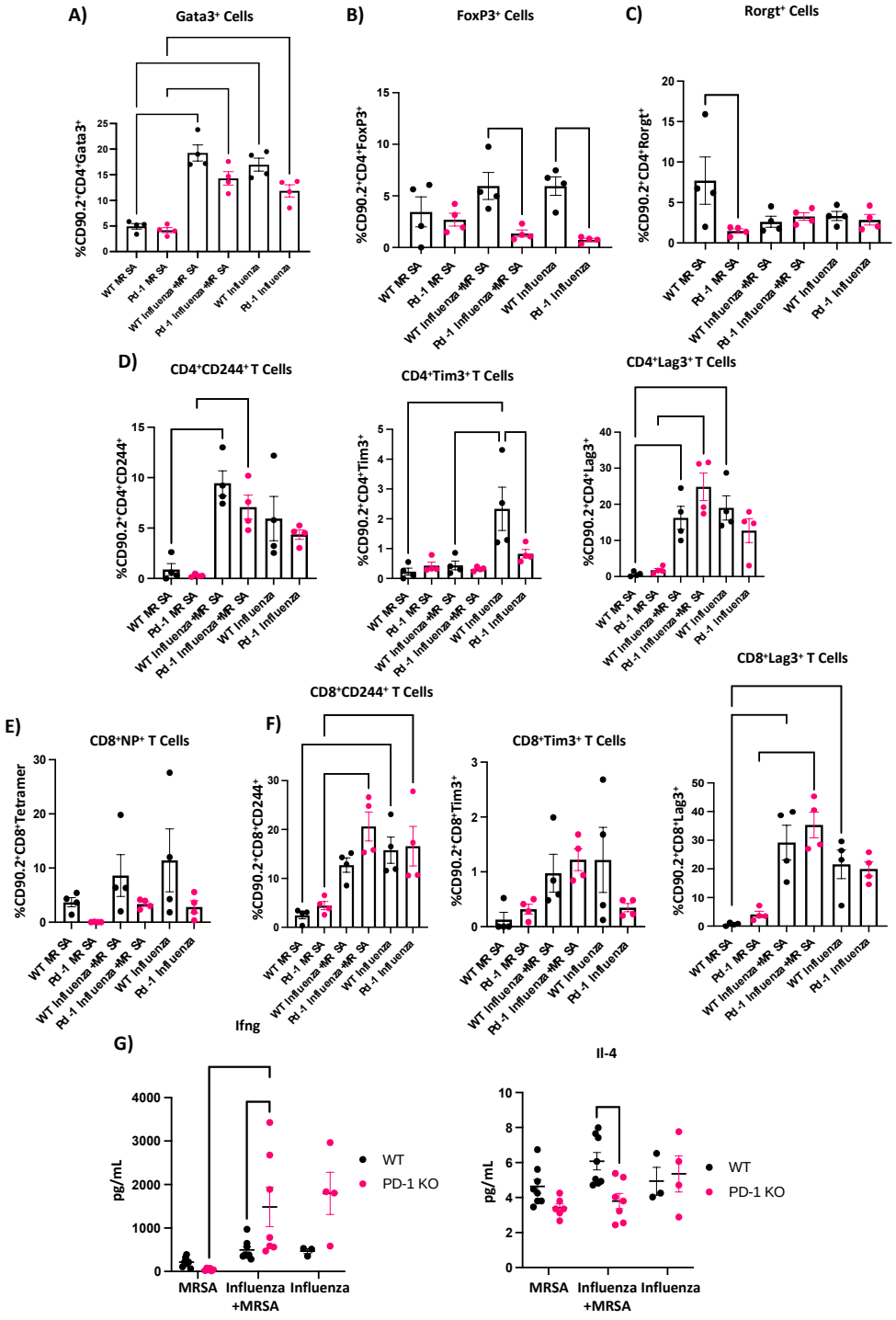

Figure 2.5 PD-1 KO mice exhibit changes in expression of markers related to cell subset and inhibitory marker expression between treatment groups. A) Percentage of $CD45^+$ $CD90.2^+$ $CD4^+$ $Gata3^+$ Th2 cells determined from flow cytometry in mouse lungs (n=4). B) Percentage of $CD45^+$ $CD90.2^+$ $CD4^+$ $FoxP3^+$ Treg

cells determined from flow cytometry in mouse lungs (n=4). C) Percentage of $CD45^+$ $CD90.2^+$ $CD4^+$ $Rorgt^+$ Th17 cells determined from flow cytometry in mouse lungs (n=4). D) Percentage of $CD45^+$ $CD90.2^+$ $CD4^+$ T cells expressing inhibitory markers Tim3, Cd244, or Lag3 determined from flow cytometry in mouse lungs (n=4). E) Percentage of $CD45^+$ $CD90.2^+$ $CD8^+$ NP^+ T cells determined from flow cytometry in mouse lungs (n=4). F) Percentage of $CD45^+$ $CD90.2^+$ $CD8^+$ T cells expressing inhibitory markers Tim3, Cd244, or Lag3 determined from flow cytometry in mouse lungs (n=4). G) Protein expression of Ifnγ and IL-4 in PD-1 KO or WT MRSA alone, influenza alone, or super-infected mice (Ifnγ and IL-4: MRSA alone: WT n=8, PD-1 KO n= 6, Influenza alone: WT n=3, PD-1 KO n=4, super-infection: WT n=8, PD-1 KO n=7).p values: *<0.05, **<0.01, *<0.001, ****<0.0001.**

2.4.6 Targeting the PD-1 pathway results in changes to the myeloid compartment.

The important role that the myeloid compartment plays during bacterial infections, led us to investigate if PD-1 alters the myeloid compartment. We did this by looking at the different myeloid cell subsets via flow cytometry. There was minimal change seen in percentage of neutrophils, monocytes, macrophages, dendritic cells or eosinophils when PD-1 was knocked out when compared to their WT counterparts within groups (Appendix Fig. A.1.4). When we looked at percentage of cells expressing other inhibitory markers, we did see an increase in exudative macrophages expressing Tim3 in influenza and super-infected groups, and a reduction in Pd-l1 expressing cells in exudative macrophages in our superinfected and influenza alone infected WT and PD-1KO groups (Fig. 2.6a). More changes in percentage of cells expressing inhibitory markers were seen in neutrophils. Neutrophils expressing Cd244 were elevated in PD-1 KO influenza alone and super-infected mice, however they were reduced significantly in MRSA alone infected mice (Fig. 2.6b). PD-12 and Tim3 expressing neutrophils were significantly decreased in PD-1 KO mice that were infected with influenza alone or super-infected (Fig. 2.6b). As we did with T

cells we determined if protein concentration of molecules associated with the myeloid compartment are changed between treatment groups. We found that the inflammatory cytokines Il-1α and Tnfα are both significantly reduced in PD-1 KO MRSA alone infected mice (Fig. 2.6c). Lastly, we looked at cytokines important in differentiation of macrophages, M-CSF, as well as migration of inflammatory cells to sites of infection, Cxcl10 and MCP-3. Each of these cytokines was significantly reduced in our PD-1KO MRSA alone infected mice, suggesting that the myeloid compartment is potentially hindered during bacterial infections alone (Fig. 2.6d). These results suggest that global deletion of PD-1 plays a role on myeloid cells during super-infection, however, it may play a more robust role during MRSA alone infections.

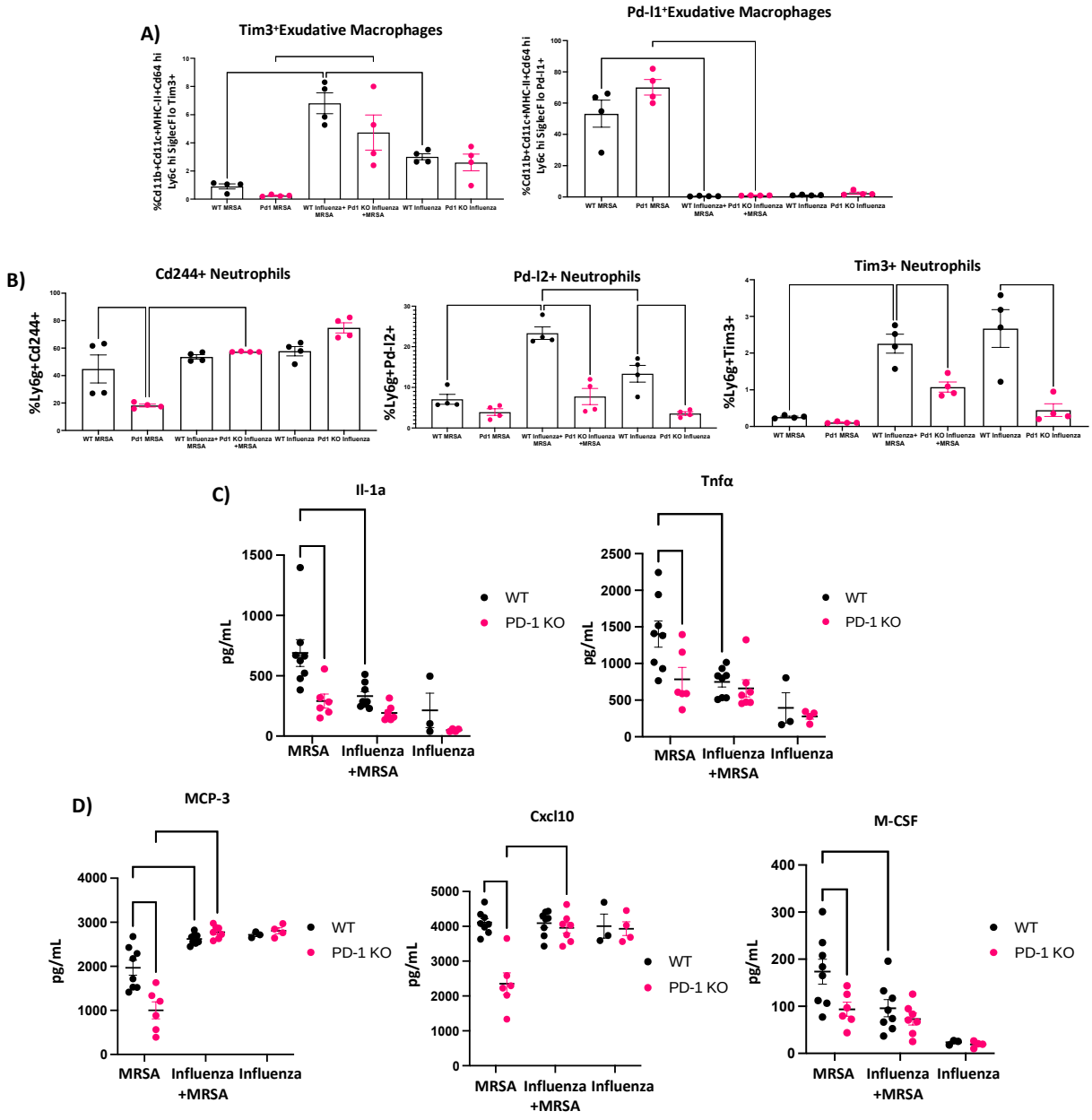

Figure 2.6 PD-1 KO mice exhibit only slight changes in expression of markers related to changes in myeloid cell subset expression across treatment groups as comapred to WT mice, howver they do exhibit changes in inhibitory marker expression, as well as migration, differentiation and inflammatory potential during a MRSA alone infection. A) Percentage of $CD45^+$ $CD11b^+$ $CD11c^+$ $MHC\text{-}II^+$ $CD64^+$ $Ly6c^+$ cells expressing inhibitory markers Tim3 and Pd-l1(n=4). B) Percentage of $CD45^+$ $Ly6g^+$ cells expressing inhibitory markers Cd244, Pd-l2, and Tim3 (n=4). C-D) Protein expression of Il-1^{α}, Tnfα, MCP-3, Cxcl10, and M-CSF in PD-1 KO or WT MRSA alone, influenza alone, or super-infected mice (Il-1^{α}, Tnfα, MCP-3, Cxcl10, and M-CSF:

MRSA alone: WT n=8, PD-1 KO n= 6, Influenza alone: WT n=3, PD-1 KO n=4, super-infection: WT n=8, PD-1 KO n=7). P values: *<0.05, **<0.01, *<0.001, ****<0.0001.**

2.5 Discussion

With the emergence of drug resistant bacterial strains, the development of novel therapeutics is of particular importance especially in the context of secondary bacterial infections where the immune system is in a weakened state. Research on super-infections has uncovered several pathways that are associated with susceptibility and establishment of secondary infections. Much of this research has focused on the role that influenza plays on shaping the subsequent anti-bacterial response[27, 92, 95, 113, 114]. The research presented here focuses on the role of inhibitory markers and their pathways on multiple cells types in susceptibility to secondary infections following an acute viral challenge.

Studies on inhibitory pathways during acute viral infections have implicated inhibitory mechanisms, such as PD-1, in driving susceptibility to infection[53, 54, 56]. In our study we determined that PD-1 expressing cells are found at higher levels in super-infected and influenza alone infected mice on multiple cell types of the myeloid and adaptive immune cell compartment when compared to MRSA alone groups. This increase in PD-1 expressing cells that we observed in our groups is most likely due to the presence of viral antigen driving upregulation as was the case in previous studies on acute viral respiratory infections[53, 56]. Interestingly, global targeting of the PD-1 pathway during super-infection resulted in no difference to susceptibility when MRSA burden and morbidity was assessed. This observation may be due to our use of global PD-1 KOs, which creates an environment where PD-1 is ablated at all stages of infection on all cell types. Of note, these

results were recapitulated when we used antibody blockade against PD-1 as well as Pd-l1. Super-infections are complex and dynamic infections so a targeted approach to knock down PD-1 in specific cell subsets may change the outcome observed in these studies.

The role of PD-1 during infection is to act as a brake on the immune system effectively shutting down the immune response and protecting the area from immunopathology. In the present study we did find an increase in protein in the BALF as well as a decrease in relative gene expression of markers associated with epithelial integrity in our PD-1 KO super-infected mice. These data suggest that the lungs of PD-1 KO mice during super-infection appear to be altered in ways that drive a more immunopathological phenotype. Interestingly, these alterations played little role in susceptibility to MRSA colonization which has been shown to correlate with lung damage.

Super-infections are characterized by several immune cell types of both the innate and adaptive immune system acting on each other and in several circumstances acting to hinder each other. The presence of PD-1 on several cell subsets led us to study what role knocking out PD-1 during super-infection plays at the cellular level. The results presented herein suggest that the global loss of PD-1 did not result in an increase in inflammatory mechanisms infiltrating into the lung space during super-infection. Interestingly, when we looked further at the composition of immune cells in the lungs of infected mice of both the innate and adaptive immune systems, we did see changes in T cell subsets. We did not see this type of change in myeloid cell composition. One of the most striking observations from our studies suggests that knocking out PD-1 results in a higher percentage of cells expressing other inhibitory markers in both the myeloid and adaptive cell compartments when comparing within PD-1 KO mice across infectious groups. This could potentially be due to the prevailing idea that these inhibitory mechanisms act in concert with each other, resulting in compensation when one is lost and the preservation of an inhibitory phenotype.

Further research on the PD-1 pathway should be conducted to specifically target PD-1 on distinct cell types rather than with a global knock out model.

3.0 Heterotypic Influenza Infections Mitigate Susceptibility to Secondary Bacterial Infection

3.1 Summary

Influenza-associated bacterial super-infections have devastating impacts on the lung and can result in increased risk of mortality, compared with single infection. New strains of influenza circulate throughout the population yearly, promoting the establishment of immune memory. Nearly all individuals have some degree of influenza memory prior to adulthood. Due to this, we sought to understand the role of immune memory during bacterial super-infections. An influenza heterotypic immunity model was established using influenza A/PR/8/34 and A/X31. We report here that influenza experienced mice are more resistant to secondary bacterial infection with methicillin-resistant *Staphylococcus aureus*, as determined by wasting, bacterial burden, pulmonary inflammation, and lung leak, despite significant ongoing lung remodeling. Multidimensional flow cytometry and lung transcriptomics revealed significant alterations in the lung environment in influenza-experienced mice compared with naïve animals. These include changes in the lung monocyte and T cell compartments, characterized by increased expansion of influenza tetramer-specific $CD8^+$ T cells. The protection that was seen in the infection-experienced (memory) mouse model is associated with the reduction in inflammatory mechanisms, making the lung less susceptible to damage and subsequent bacterial colonization. These findings provide insight into how influenza heterotypic immunity re-shapes the immune response and the overall lung environment, including to a re-challenge event, which is highly relevant to the context of human infection.

3.2 Introduction

Seasonal influenza infections account for significant numbers of hospitalizations and increased morbidity and mortality annually, especially in the young, immunocompromised, and the elderly. The WHO estimates that yearly influenza infections led to 290,000-600,000 deaths globally prior to the COVID-19 pandemic [115]. Influenza infection begins by primarily targeting epithelial cells as sites for viral replication [116]. Once epithelial cells become infected, a cascade of innate and adaptive immunological mechanisms is initiated resulting in clearance of the virus. This process of viral clearance creates a highly inflamed lung environment that can lead to excessive damage to the lung epithelium and an increased risk of development of a secondary bacterial infection and subsequent pneumonia [31, 35, 117, 118, 119]. Influenza-associated secondary bacterial infections heighten the risk of mortality, as is evidenced by histology records from the 1918 influenza pandemic, which indicate the presence of bacterial infections in the lungs of approximately 95% of those who succumbed to infection [1, 15]. Mouse models have provided evidence of dysregulated immune responses to the bacteria, which are thought to be caused by the preceding anti-viral response [25, 27, 29, 32, 33, 34, 95, 120, 121, 122, 123]. These mechanisms in the lung environment allow for influenza and bacteria to act in a synergistic way, with influenza promoting subsequent bacterial colonization and outgrowth [124]. Due to the extensive damage that influenza-associated secondary bacterial infections can have on the host lung, it is imperative to understand the mechanisms that shape the host-pathogen response to these types of infections.

Influenza evades host immunity by readily mutating its surface proteins, neuraminidase (NA) and hemagglutinin (HA), in response to evolutionary pressure that is driven in part by host antibodies directed against HA and NA [125, 126]. This helps drive the yearly emergence of novel influenza strains. Although the antibody response may be evaded by heterotypic influenza strains,

the host also establishes a memory immune cell compartment distinct from the antibody response that is able to mobilize and respond against multiple influenza strains [125, 126]. Both the innate and adaptive immune systems can produce memory immune cells against a variety of pathogens [127, 128]. The importance of the immune response following priming and repeated exposure to antigens has been studied extensively at both the basic and translational level for vaccine and therapeutic purposes [129, 130, 131, 132]. There is evidence that priming by influenza reprograms immune cells over time, specifically myeloid cells, to display enhanced antibacterial functions [133]. Both $CD8^+$ and $CD4^+$ memory T cells have been shown to be of particular importance in the memory response to heterologous strains of influenza because they are able to react against internally conserved pieces of the virus that are less likely to undergo mutations driven by evolutionary pressure, ensuring quick mobilization and responses against infection [134, 135, 136]. There are several memory T cell subsets: central memory (Tcm), effector memory (Tem), and resident memory (Trm). The different subsets of memory T cells are defined by both their localization and surface marker expression. Due to their location at the site of infection, i.e. within the lung, Trm cells have been implicated in the augmented clearance of viral respiratory infections including influenza [137]. Nearly all humans have some level of pre-existing memory against influenza from early life exposures. Although memory cells are imperative for clearance of heterotypic viral strains, a fine balance in the inflammatory response must be achieved to limit the amount of damage to the lung tissue.

Currently, most of the studies in the field on influenza-associated bacterial infections focus on the acute stage in naïve mice, whereas our study takes into account pre-existing influenza memory akin to human influenza immunity. To better understand the role of memory in influenza-associated bacterial infections, we used a mouse model to mimic a heterotypic influenza infection, using H3N2 and re-challenging approximately two months later with H1N1 followed in six days

by infection with methicillin-resistant *Staphylococcus aureus* (MRSA). With spectral flow cytometry and transcriptomics we studied the role that antigen experience has on susceptibility to secondary bacterial infections. The model we used here is intended to provide a more clinically relevant representation of how heterotypic influenza strains infect the human population annually and how the immune response is shaped over time. These data provide insight into how viral infections reprogram the lung to respond to subsequent infections and the repercussions this has for susceptibility to secondary infections, further highlighting the importance of antigen-experienced cells in the response to lung pathogens.

The following study was published August 1, 2022 in The Journal of Immunology. "Heterotypic Influenza Infection Mitigates Susceptibility to Secondary Bacterial Infection" by Ellyse M. Cipolla, Molin Yue, Kara L. Nickolich, Brydie R. Huckestein, Danielle Antos, Wei Chen, and John F. Alcorn.

3.3 Materials and Methods

3.3.1 Mouse Model and Sample Collection

On day zero, six to eight-week old male WT C57BL/6 mice (Taconic Farms, Germantown, NY) were infected with 10^5 pfu of mouse adapted influenza A/X31 H3N2 or PBS vehicle. After 53-54 days the mice were re-challenged with 100 pfu of a heterotypic strain of mouse adapted influenza A/PR/8/34 H1N1. 6 days after influenza re-challenge (day 59/60) the mice were challenged with $5x10^7$ colony forming units (cfu) of USA300 MRSA suspended in PBS and harvested a day later. All infections were given via oropharyngeal aspiration. Mice were

maintained under pathogen-free conditions at UPMC Children's Hospital of Pittsburgh and all animal studies were conducted with approval from the University of Pittsburgh Institutional Animal Care and Use Committee. All studies used age- and sex-matched mice. Mice were euthanized via pentobarbital injection followed by exsanguination by severing the renal artery. No mice died prior to euthanasia.

3.3.2 Bronchoalveolar Lavage Fluid Collection and Differential Cell Counting

Upon harvest, mice were cannulated and lavaged with 1ml of PBS for bronchoalveolar lavage fluid (BALF) collection. BALF was spun down and pelleted and supernatant was collected and stored for downstream analysis. Pelleted cells were treated with ACK lysing buffer (Gibco Fisher Scientific, Hampton, NH) to remove red blood cells. The cell pellet was then resuspended in 500µl of PBS and total cell count was determined by hemocytometer. 200µLs of resuspended cells were then concentrated on a microscope slide using a cytocentrifuge (ThermoFisher Scientific, Waltham, MA) and stained with Diff-Quik staining solution (Fisher Scientific, Hampton, NH) to determine monocyte, neutrophil, eosinophil, and lymphocyte counts.

3.3.3 Bacterial Plating

Right upper lung lobes from mice were collected and homogenized in 1ml of PBS. After homogenization, 10-fold dilutions were dot plated on culture plates. Plates were then incubated at 37^{o} Celsius overnight, and cfu was assessed by bacterial colony counting.

3.3.4 Flow Cytometry

Mouse lungs were aseptically dissected using sterile scissors. Lungs were then digested for an hour at 37^{o} Celsius in 1mg/ml collagenase media (DMEM Gibco Fisher Scientific, Hampton, NH). After an hour, lungs were mashed through 70 micron filters to obtain a single cell suspension. The single cell suspension was treated with ACK lysing buffer (Gibco Fisher Scientific, Hampton, NH) to remove red blood cells. After red blood cell lysis, cells were resuspended in PBS. Single cell suspensions were stained as follows for spectral flow cytometry analysis. For the T cell memory panel, cells were stained with anti-Cd45 (30-F11,BD Pharmingen, San Diego, CA), Cd4 (RM4-5,BD Biosciences, Franklin Lakes, NJ), Cd103 (M290,Invitrogen-ThermoFisher Scientific, Waltham, MA), Cd49a (HA31/8,BD Biosciences, Franklin Lakes, NJ), Cd69 (H1.2F3, BioLegend, San Diego, CA), Pd-l2 (TY25,BioLegend, San Diego, CA), Pd-l1 (10F.9G2,BioLegend, San Diego, CA), Cx3cr1 (SA011F11,BioLegend, San Diego, CA), Lag3 (C9B7W,BioLegend, San Diego, CA), Cd8 (53-6.7,Invitrogen-ThermoFisher Scientific, Waltham, MA), Cd11a (M17/4,BioLegend, San Diego, CA), Cd127 (SB/199,Invitrogen-ThermoFisher Scientific, Waltham, MA), Klrg1 (2F1,BD Biosciences, Franklin Lakes, NJ), Foxp3 (FJK-16s,Invitrogen-ThermoFisher Scientific, Waltham, MA), Tetramer (I-A(b) Influenza A NP 311-325 QVYSLIRPNENPAHK), Tim3 (RMT3-23,BioLegend, San Diego, CA), CD244.2 (m2B4(B6)458.1,BioLegend, San Diego, CA), PD-1 (29F.1A12,BioLegend, San Diego, CA), Cd90.2 (30-H12,BD Biosciences, Franklin Lakes, NJ), Cd62L (MEL-14,BD Biosciences, Franklin Lakes, NJ), and Cd44 (IM7,BD Biosciences, Franklin Lakes, NJ). NP366 tetramers were obtained from the NIH tetramer core facility (Bethesda, MD) and were stained at 37^{o} Celsius for 30 minutes prior to viability stain. For the myeloid panel, cells were stained with anti-CD45 (30-F11,Invitrogen-ThermoFisher Scientific ,Waltham, MA), Pd-l2 (TY25,BioLegend,San Diego,

CA), F4/80 (T45-2342,BD Biosciences, Franklin Lakes, NJ), Cd64a/b (X54-5/7.1,BD Biosciences, Franklin Lakes, NJ), Pd-l1 (10F.9G2,BioLegend, San Diego, CA), Cd103 (2E7,Invitrogen-ThermoFisher Scientific ,Waltham, MA), Ly6c (HK1.4,BioLegend, San Diego, CA), Cd11b (M1/70,BD Biosciences, Franklin Lakes, NJ), MHC-II (M5/114.15.2,BD Biosciences, Franklin Lakes, NJ), Cd80 (16-10A1,BD Biosciences, Franklin Lakes, NJ), Cd86 (GL1,BD Biosciences, Franklin Lakes, NJ), B220 (RA3-6B2,Invitrogen-ThermoFisher Scientific , Waltham, MA), Tcrb (H57-597,BioLegend, San Diego, CA), SiglecF (1RNM44N,Invitrogen-ThermoFisher Scientific, Waltham, MA), Cd24 (M1/69,BioLegend, San Diego, CA), PD-1 (RMP1-30,BioLegend, San Diego, CA), Cd244.2 (m2B4(B6)458.1,BioLegend, San Diego, CA), Nk1.1 (PK136,BioLegend, San Diego, CA), Cd11c (N418,Invitrogen-ThermoFisher Scientific. Waltham, MA), Tim3 (B8.2C12,BioLegend, San Diego, CA), and Arg-1 (A1exF5,Invitrogen-ThermoFisher Scientific, Waltham, MA). The viability dye, Zombie NIR (BioLegend, San Diego, CA), was used to exclude live cells from dead cells in both panels. Our mastermix for cell staining contained Super Bright Complete Staining Buffer (ThermoFisher Scientific, Waltham, MA) as well as True-Stain Monocyte Blocker (BioLegend, San Diego, CA) for the myeloid panel. Intracellular staining was performed at room temperature using the eBioscience™ Foxp3/Transcription Factor Staining Buffer Set (ThermoFisher Scientific, Waltham, MA) as directed by the manufacturer. All samples were run on the Cytek Aurora (Cytek Biosciences, Fremont, CA). Flow cytometric analysis was performed using FlowJo with UMAP [138] and FlowSOM [139] integrated plug-ins (Tree Star, Ashland, OR). Absolute cell counts were determined following manufacturer's instructions using UltraComp eBeads™ Plus Compensation Beads (Invitrogen-ThermoFisher Scientific, Waltham, MA).

3.3.5 Histology

Left lung lobes from mice were inflated with and preserved in 10% neutral buffered formalin solution. Formalin fixed tissues were then transferred to 70% ethanol and shipped to StageBio (Mount Jackson, VA), where they were paraffin embedded and sectioned for histopathological analysis. Upon sectioning, hematoxylin and eosin (H&E) staining was performed. Histological scoring was performed on H&E stained slides using a scale from 1 to 4 with 1 being no damage and 4 being severely damaged. Cellular infiltration and tissue damage was assessed for the lung parenchyma, peribronchial, and perivascular regions. Scoring was performed sample blinded by two separate investigators. Percent of metaplasia was measured using Fiji software and calculating threshold values for areas of metaplasia and dividing by threshold of total damaged imaged area , which was graphed separately[140].

3.3.6 RNA extraction and qPCR

Mouse lungs were isolated and snap-frozen in liquid nitrogen or suspended in Allprotect Tissue Reagent (Qiagen, Hilden, Germany). RNA was extracted as directed using the Qiagen Rneasy Mini Kit (Qiagen, Hilden, Germany). cDNA was synthesized using the iScript cDNA synthesis kit (Bio-Rad, Hercules, CA). qPCR was conducted using SsoAdvanced universal probes supermix (Bio-Rad, Hercules, CA) and target specific TaqMan real-time PCR assay primer probes (ThermoFisher Scientific, Waltham, MA). Viral burden was determined by quantitative real-time RT-PCR on lung RNA for viral matrix protein (M1) as described previously [111, 112]. Forward Primer:5′-GGACTGCAGCGTAGACGCTT-3′, Reverse Primer:5′-

CATCCTGTTGTATATGAGGCCCAT-3′,Probe:5′-/56-FAM/CTCAGTTAT/ZEN/TCTGCTGGTGCACTTGCCA/3IABkFQ/−3′.

3.3.7 Protein Assays and Lincoplex

The Pierce™ BCA protein assay kit (ThermoFisher Scientific, Waltham, MA) was used as directed to determine protein levels in BALF. Cytokine production was measured in lung homogenates via Bioplex using the Luminex™ Magpix™ multiplexing platform with the Bio-Plex Pro Mouse Cytokine 23-plex assay (Bio-Rad, Hercules, CA) as directed. Mouse lung homogenates were used to determine IgM protein using an IgM uncoated ELISA kit as directed (Invitrogen-ThermoFisher Scientific, Waltham, MA).

3.3.8 Bulk-RNA Sequencing

RNA for sequencing was isolated from total mouse lungs as described above. Library preparation and sequencing was performed at UPMC Children's Hospital of Pittsburgh. Samples were run on the Illumina NEXT-Seq 500 platform: 1x75bp single-end reads and 20 million reads per sample.

3.3.9 Bioinformatics

Bulk-RNA seq reads were aligned using CLC Genomics Workbench 22 (Qiagen, Hilden, Germany). Once aligned, raw counts were extracted and exported to R workspace where the data was further processed with the DESEQ2 and clusterprofiler packages [141, 142]. We used Cell-type

Identification by Estimating Relative Subsets of RNA Transcripts, CibersortX, to estimate and define cell-types via RNA transcript information from our bulk-RNA memory versus acute super-infected sequencing data using a single-cell reference dataset [143, 144]. In brief, a signature matrix was built from a publicly available single-cell dataset from PBS and 48-hour influenza infected mouse lung tissue that consisted of 6,528 cells [145] with 50% sampled without replacement for our 10 cell types of interest. Default parameters were used for the signature matrix building and CIBERSORTx analysis was conducted on our bulk-RNA sequencing dataset. Relative mode and number of permutations was set at 100 and cell type proportions, Pearson correlation coefficient, p value, and root mean squared error was calculated (RMSE). All sequencing data will be uploaded to Gene Expression Omnibus upon publication.

3.3.10 Statistical Analysis

Data were analyzed using GraphPad Prism software (San Diego, CA). Experiments were repeated 3-6 times as indicated. All data are presented as mean $\pm$ SEM, unless otherwise noted. Mann-Whitney test or one-way ANOVA followed by multiple comparisons were used for statistical significance with a p value of equal or less than 0.05. Mouse studies were repeated at least three times, in most cases.

3.4 Results

3.4.1 Preceding heterotypic influenza infection is protective against subsequent secondary bacterial infection.

To determine the role that immune memory plays in influenza associated super-infections we primed wild-type (WT) C57BL/6 mice with influenza A/X31 H3N2 (X-31) on day zero followed by re-challenge with a heterotypic influenza strain, A/PR/8/34 H1N1 (PR8), and inoculation with methicillin-resistant *Staphylococcus aureus* USA300 (MRSA) six days after PR8 infection (Fig. 3.1a). We used the mouse adapted strains X-31 and PR8 in these studies because they share genetic similarities in internal proteins, and have previously been used to model memory in influenza mouse models [146, 147]. Super-infected mice that had pre-existing heterotypic influenza immunity were better protected upon bacterial infection, with less weight loss and bacterial burden than matched acute infection controls, but they did have similar levels of weight loss and bacterial burden to mice infected with MRSA alone (Fig. 3.1b and c). When lung infiltrating cells were assessed, super-infected memory mice had lower levels of total infiltrating cells comparable to those of MRSA alone infected mice, and upon further assessment it was determined that monocytes made up more of the total cell distribution (Fig. 3.1d). Previous research on influenza-associated bacterial super-infections have elucidated several potential mechanisms behind these types of infections, with one of the prevailing ideas being that the anti-viral mechanisms in the lung environment dampen the anti-bacterial response [15, 31, 148, 149]. We observed that memory super-infected mice at the time of MRSA challenge had non-detectable levels of PR8 gene expression in their lungs indicating that the anti-viral memory mechanisms controlled the infection, potentially ensuring a more effective anti-bacterial response to secondary bacterial infection (Fig. 3.1e).

Finally, we observed a reduction in levels of Type I, II, and III interferons during super-infection. Interferons are are important signaling molecules during viral infection and have been shown to interfere with antibacterial responses and outcomes (survival) in secondary bacterial infections [25, 92, 150, 151] (Fig. 3.1f). These data suggest that mice with influenza memory have an advantage over matched naïve acute infection counterparts upon challenge with MRSA, due to a more controlled and targeted anti-viral response.

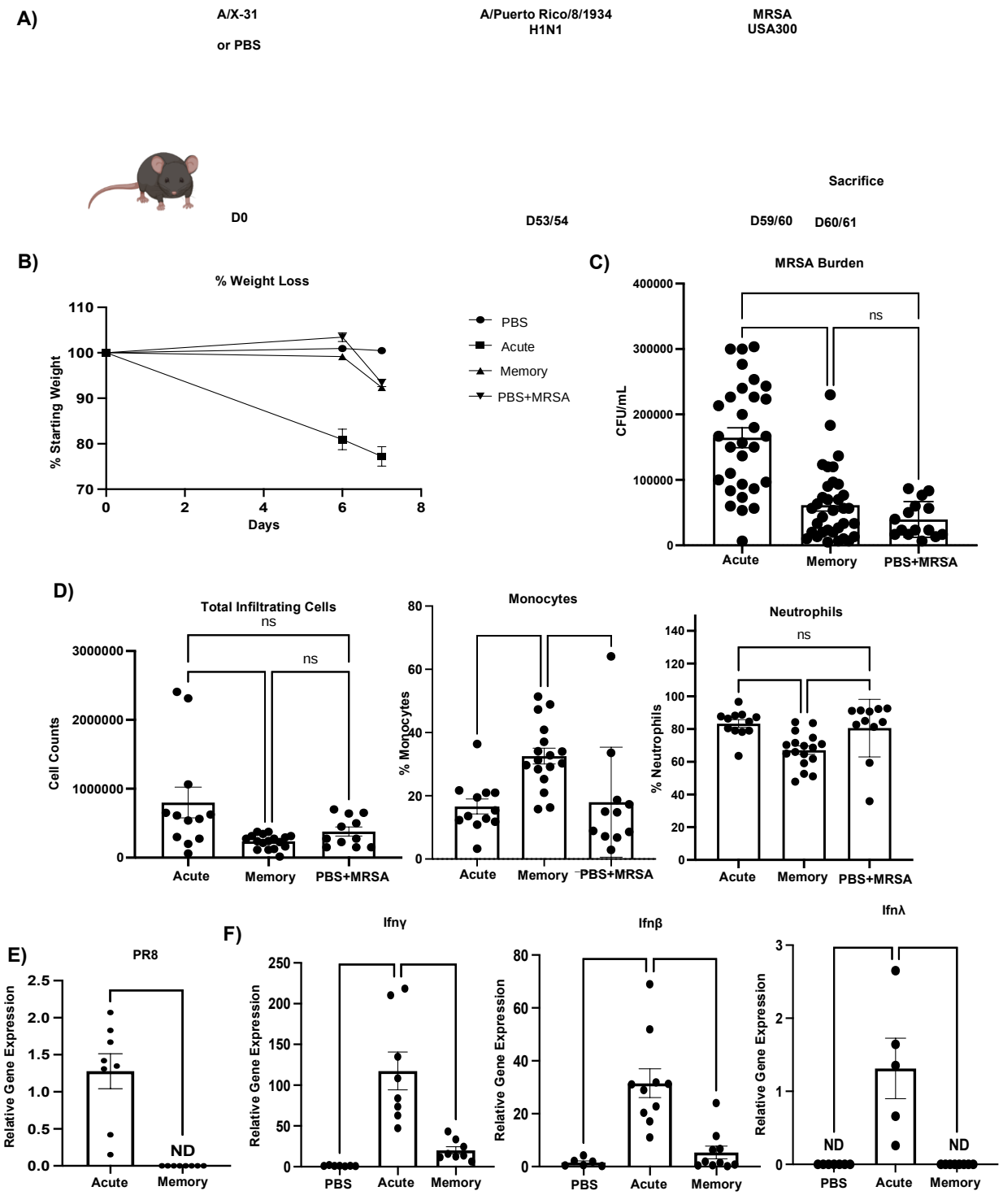

Figure 3.1 Influenza memory experienced mice are better protected against secondary bacterial infection with *Staphylococcus aureus* compared to acute counterparts. A) Infection scheme for memory super-infected C57BL/6 mice. Mice were infected on day 0 with A/X-31 H3N2 (X-31) and at 53 to 54 days post-infection (p.i.)

mice were given A/Puerto Rico/8/1934 H1N1 (PR8). MRSA USA300 (MRSA) was given on day 59 or 60 p.i. and mice were harvested on day 60 or 61 p.i. B) Percent of weight loss was calculated starting from secondary infection with PR8 for each of the treatment groups and compared to mice that received PBS only and MRSA only, with day 6 being the date that MRSA was given on (PBS= 15, acute n=17, memory n=23, PBS+MRSA n=15). C) Number of MRSA colonies plated from infected mouse lung homogenates (acute n=30, memory n=34, PBS+MRSA n=15). D) Total infiltrating cell counts, percent of monocytes, as well as percent of neutrophils were determined by cytospins using bronchoalveolar lavage fluid collected from infected mouse lungs at time of harvest (acute n=12, memory n=16, PBS+Memory n=11). E) Presence of viral protein was assessed in cDNA from total mouse lung via relative gene expression analysis of PR8 (Matrix protein) (acute n=8, memory n=8). F) Relative gene expression of interferon classes (Ifn-λ3, Ifn-γ, and Ifn-β) from total mouse lung cDNA. ND=non-detectable. P values: *<0.05, **<0.01 *<0.001, ****<0.0001. Mouse figure was created with BioRender.com.**

3.4.2 Lung injury is present in acute and memory influenza challenged mice.

Since viral burden was effectively controlled in heterotypic influenza challenged mice, we investigated if lung injury was altered in our model. Memory and acute super-infected mice were equally susceptible to lung damage following PR8 and MRSA challenge; however, the memory mice displayed areas of epithelial remodeling and metaplasia (Fig. 3.2a and b). These results were compared against mice infected with MRSA alone, which had minimal damage (Appendix Fig. A.2.1). Percent damage and percent metaplasia were further assessed using Fiji software and compared against influenza alone memory experienced mice (Appendix Fig. A.2.1b). Interestingly, when we looked at other measures to assess tissue integrity, we found that memory mice had attenuated levels of IgM and protein in their BALF when compared to their acute counterparts (Fig. 3.2c). The respiratory system has several mechanisms to defend itself against pathogens and to ensure a balance in the lung environment, because of these protective factors we

also examined the expression of genes associated with lung function, protection, and remodeling. Memory experienced mice displayed elevated expression levels of important molecules involved in the mucociliary escalator, including mucin 5b (*Muc5b*) and mucin 5ac (*Muc5ac*) (Fig. 3.2d). Further, secretoglobin family 1a member 1 (*Scgb1a1*), a key club cell protein, and forkhead box j1 (*Foxj1*), a key transcription factor in ciliated epithelial cells, were elevated in memory super-infection versus acute infection (Fig. 3.2e). Interestingly, we did see reductions in gene expression of epithelial remodeling markers in the memory mice most notably in collagen 1 a 1 (col1a1) and α – smooth muscle actin (*Acta2*), but saw no change in tight junction protein (*Tjp1*) (Fig. 3.2f). These data indicate that heterotypic memory to influenza drives changes in the lung environment that differ from their previously naïve acute counterparts and may hinder opportunistic bacterial infections.

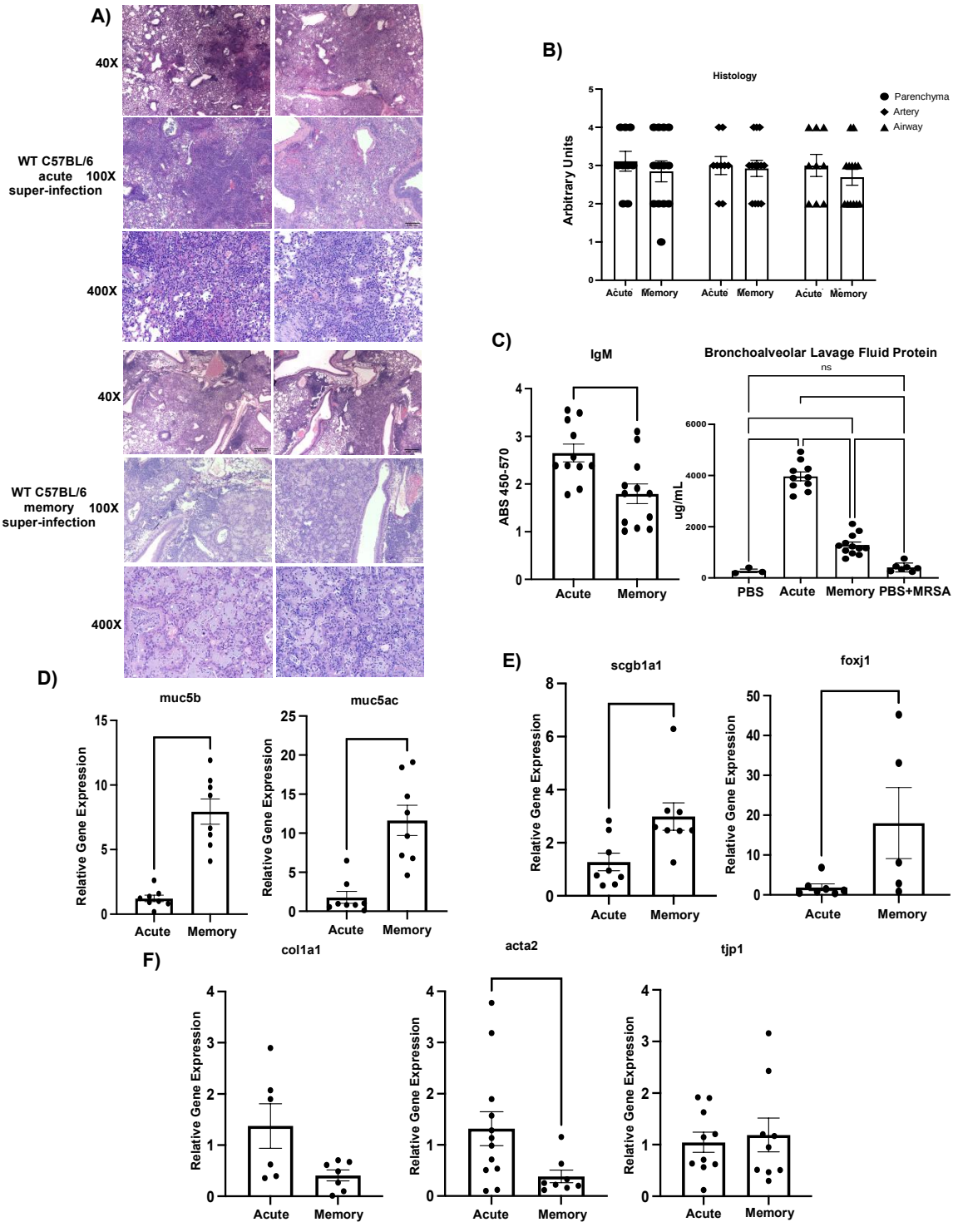

Figure 3.2 Lung damage is evident in acute and memory challenge. A) Representative histology sections of acute (n=2) and memory (n=2) super-infected WT C57BL/6 mice from formalin inflated mouse lungs stained with H&E at 40X,100X, and 200X. Black arrows denote areas of metaplasia in memory mice. B) Blinded

histology scores from paraffin embedded lung tissue sections. Lung injury scoring was carried out on three areas of the lung: parenchyma, artery, and airway (acute n=9, memory n=13).C) IgM was quantified from mouse lung homogenates using an IgM ELISA (acute n=11, memory n=12). BAL protein was quantified from BAL collected at day of harvest (PBS n=3, acute n=10, memory n=12, PBS+MRSA n=7). D-F) RNA was extracted from mouse lungs and made into cDNA which we then used to probe for various genetic targets (*Muc5b, Muc5ac, Scgb1a1*: acute n=8, memory n=8; foxj1: PBS n=6,acute n=7, memory n=5; *Col1a1*:acute n=6, memory n=7; acta2: acute n=12, memory n=8; *Tjp1*: acute n=11, memory n=9). P values: *<0.05, **<0.01 *<0.001, ****<0.0001.**

3.4.3 Lung transcriptomics indicate an altered inflammatory microenvironment and epithelial biology in influenza memory infected mice.

To study the broad-spectrum changes in the lung environment of influenza memory super-infected mice and matched naïve acute mice, we compared gene expression changes via bulk-RNA sequencing analysis. We performed a deconvolution analysis on data obtained at day seven, using a single-cell reference dataset of combined PBS and 48-hour influenza infected mice [145]. Deconvolution analysis revealed changes in the proportions of genes associated with granulocytes, mononuclear phagocytic cells, epithelial cells, and α-sma between memory and acute infected groups (Fig. 3.3a). Influenza super-infected memory experienced mice had a transcriptomic signature driven more by epithelial cells and less by granulocytes compared with acute infection controls. Sequencing analysis showed clustering of samples within groups (Fig. 3.3b). When up- or down-regulated genes were assessed in memory versus acute infection we found that memory mice displayed a reduction in genes typically associated with inflammation and control of inflammatory mechanisms such as interferon gamma (*Ifng*), granzyme B (*Gzmb*), and interleukin

10 (*Il10*) (Fig. 3.3c). Next, we performed gene ontology analysis on our sample groups and found that the pathways activated in memory are associated with the epithelium and mucociliary mechanisms, whereas those that are suppressed deal with response to virus, and immune effector processes as well as the inflammatory response (Fig. 3.3d). Gene ontology biological pathway analyses revealed that the top enriched pathways dealt with leukocyte migration, response to interferon-beta, response to chemokine, and chemotaxis (Fig. 3.3e). Together these data demonstrate that the controlled lung environment of influenza memory experienced mice is characterized by changes towards a state of lower inflammation and a balance in inflammatory mechanisms potentially accounting for a better immune response to a secondary bacterial infection.

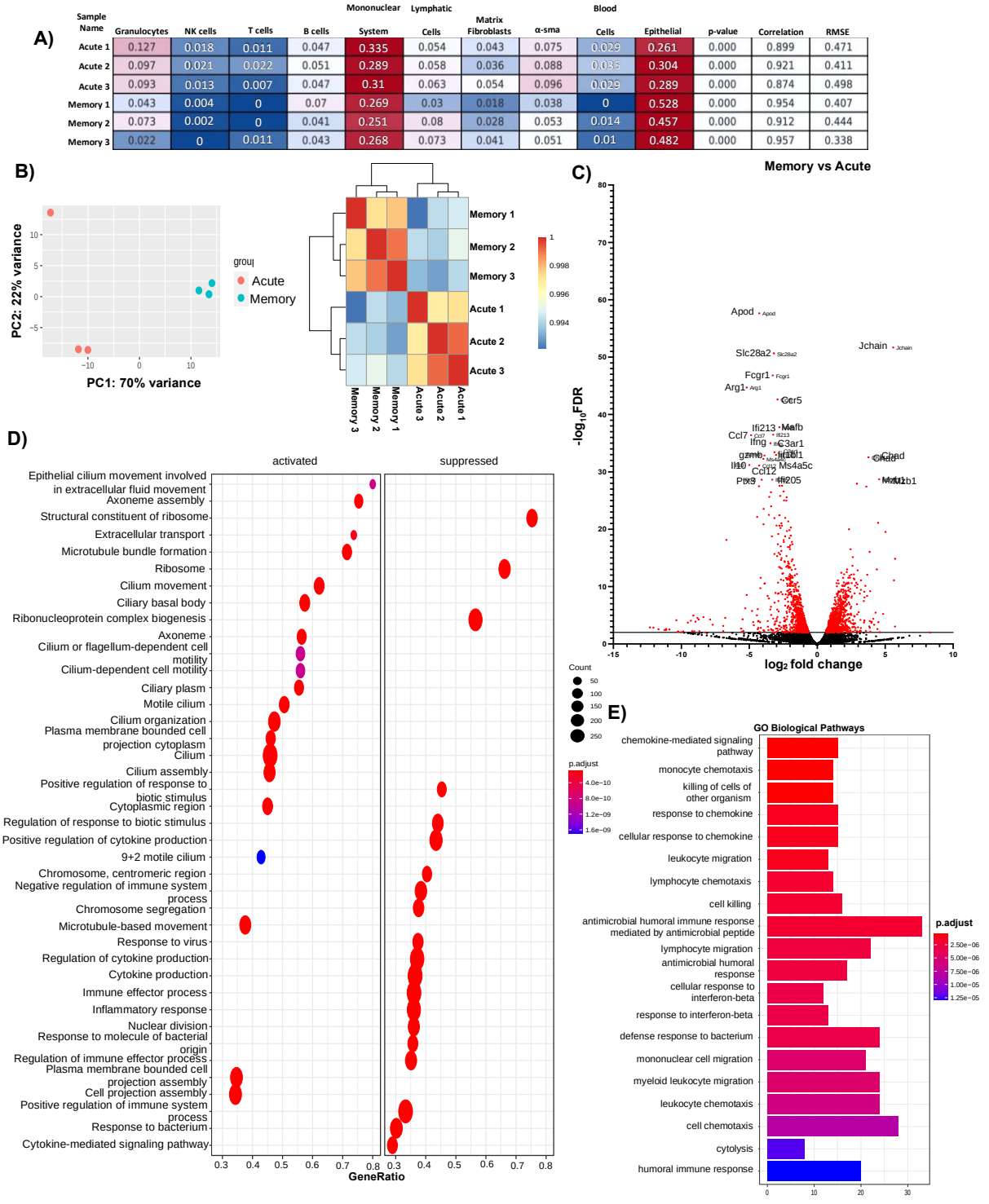

Sample Name	Granulocytes	NK cells	T cells	B cells	Mononuclear System	Lymphatic Cells	Matrix Fibroblasts	α-sma	Blood Cells	Epithelial	p-value	Correlation	RMSE
Acute 1	0.127	0.018	0.011	0.047	0.335	0.054	0.043	0.075	0.029	0.261	0.000	0.899	0.471
Acute 2	0.097	0.021	0.022	0.051	0.289	0.058	0.036	0.088	0.035	0.304	0.000	0.921	0.411
Acute 3	0.093	0.013	0.007	0.047	0.31	0.063	0.054	0.096	0.029	0.289	0.000	0.874	0.498
Memory 1	0.043	0.004	0	0.07	0.269	0.03	0.018	0.038	0	0.528	0.000	0.954	0.407
Memory 2	0.073	0.002	0	0.041	0.251	0.08	0.028	0.053	0.014	0.457	0.000	0.912	0.444
Memory 3	0.022	0	0.011	0.043	0.268	0.073	0.041	0.051	0.01	0.482	0.000	0.957	0.338

Figure 3.3 The immune signature of memory experienced mice shows a shift in inflammatory pathways and highlights a trend towards a less inflamed lung environment.

Illumina reads were aligned using CLC Genomics Workbench 22 and raw counts were extracted for bulk RNA seq analysis using DESEQ2 and clusterProfiler R software packages (acute n=3, memory n=3). A) CibersortX was used to perform deconvolution on bulk-RNA sequencing data using a single reference dataset that contained 48-hour influenza and PBS-treated mouse lung data. Numbers in boxes reflect the proportion of cells in each group. B) PCA plot and clustering heatmap from bulk RNA-seq analysis showing how the acute and memory infected groups cluster. C) Volcano plot of differentially expressed genes in memory versus acute infected mice. Red dots denote genes with a $-\log_{10}$FDR >2. Genes highlighted are the top 20 genes with $-\log_{10}$FDR >2. D) Gene Ontology analysis of activated and suppressed pathways in memory vs acute infected mice with p values>0.05. E) Gene set enrichment analysis (GSEA) on biological pathways in memory versus acute infected mice, based on genes with p values<0.05.

3.4.4 Heterotypic influenza memory alters the lung T cell compartment during bacterial super-infection.

To further characterize the changes in the mouse lung inflammatory environment driven by the presence of pre-existing influenza memory, we examined pulmonary immune cell subsets. T cell populations play a vital role in clearance of influenza infections, therefore, we looked at how the T cell compartment changes in influenza super-infected memory versus acute super-infected mice. Using clustering (FlowSOM) and dimensionality reduction (UMAP) methods, we tracked changes in marker expression in T cell populations from mouse lungs. From our gating strategy we found that (Appendix Fig. A.2.2), in an acute super-infection there are a higher proportion of $CD4^+$ $FoxP3^+$ regulatory T cells, this significant change was seen in both percentage of parent gate as well as absolute cell counts (Fig. 3.4a-c). The shift towards a lower proportion of

regulatory T cells in the memory lung environment could indicate an earlier controlled inflammatory response towards viral infection, allowing for an unimpeded switch towards immune mechanisms generated in response to bacterial infections. Further, we observed an increase in the proportion of $CD8^+$ NP^+ tetramer-positive T cells, an immunodominant epitope, in memory experienced mice when compared to the acute infected mice. This was again confirmed by significant differences in cell proportions and absolute cell counts consistent with increased memory expansion (Fig. 3.4a, b, d). The reduction in $CD4^+$ $FoxP3^+$ regulatory T cells and increase in $CD8^+$ NP^+ tetramer-positive T cells was also seen when we compared influenza alone memory and acute infected mice, adding further support to our hypothesis that influenza alters the immune response (Appendix Fig. A.2.2).

A)

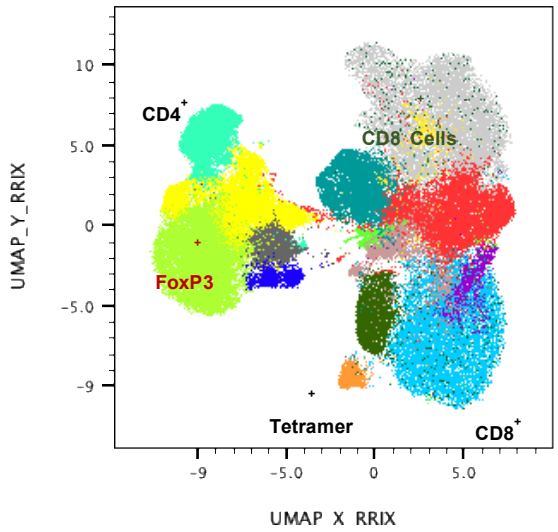

Subset Name	Count
Activated CD8+ T cells	50488
Memory Precursor CD8+ T cells	23582
CD8+Tetramer+ T cells	899
CD90.2+CD4-CD8- cells	717
Short lived effector CD8+ T cells	4604
CD90.2+CD4-CD8- cells	2158
CD103+CD8+ T cells	688
CD90.2+CD4-CD8- cells	7546
CD4+ T cells	12737
FoxP3+ T regulatory cells	2856
Naïve CD8+ T cells	48595
FoxP3+ T regulatory cells	1647
Naïve CD8+ T cells	453
CD4+ T cells	19905
Naïve CD4+ T cells	5709

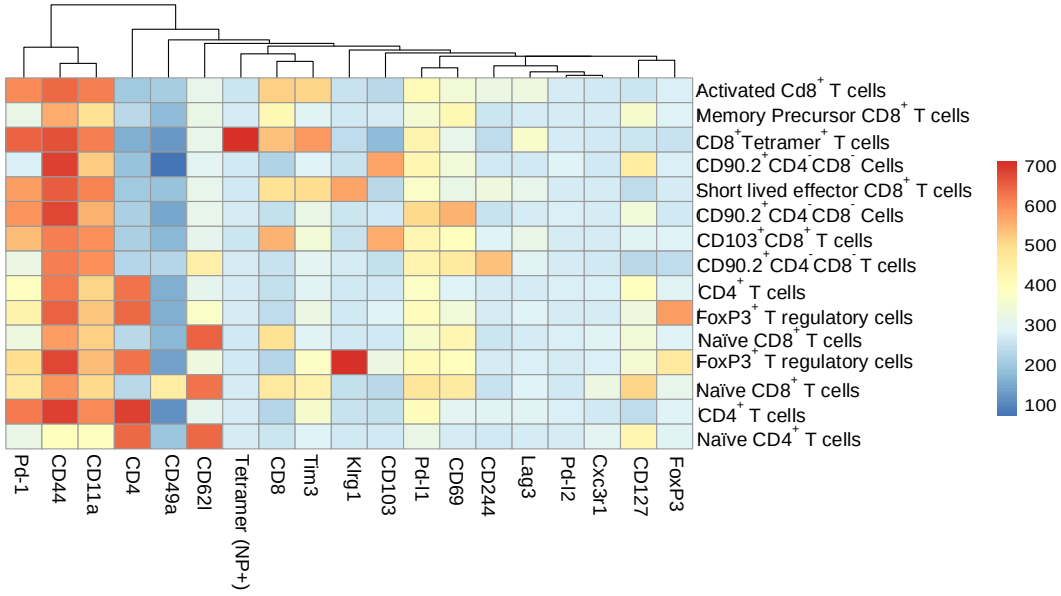

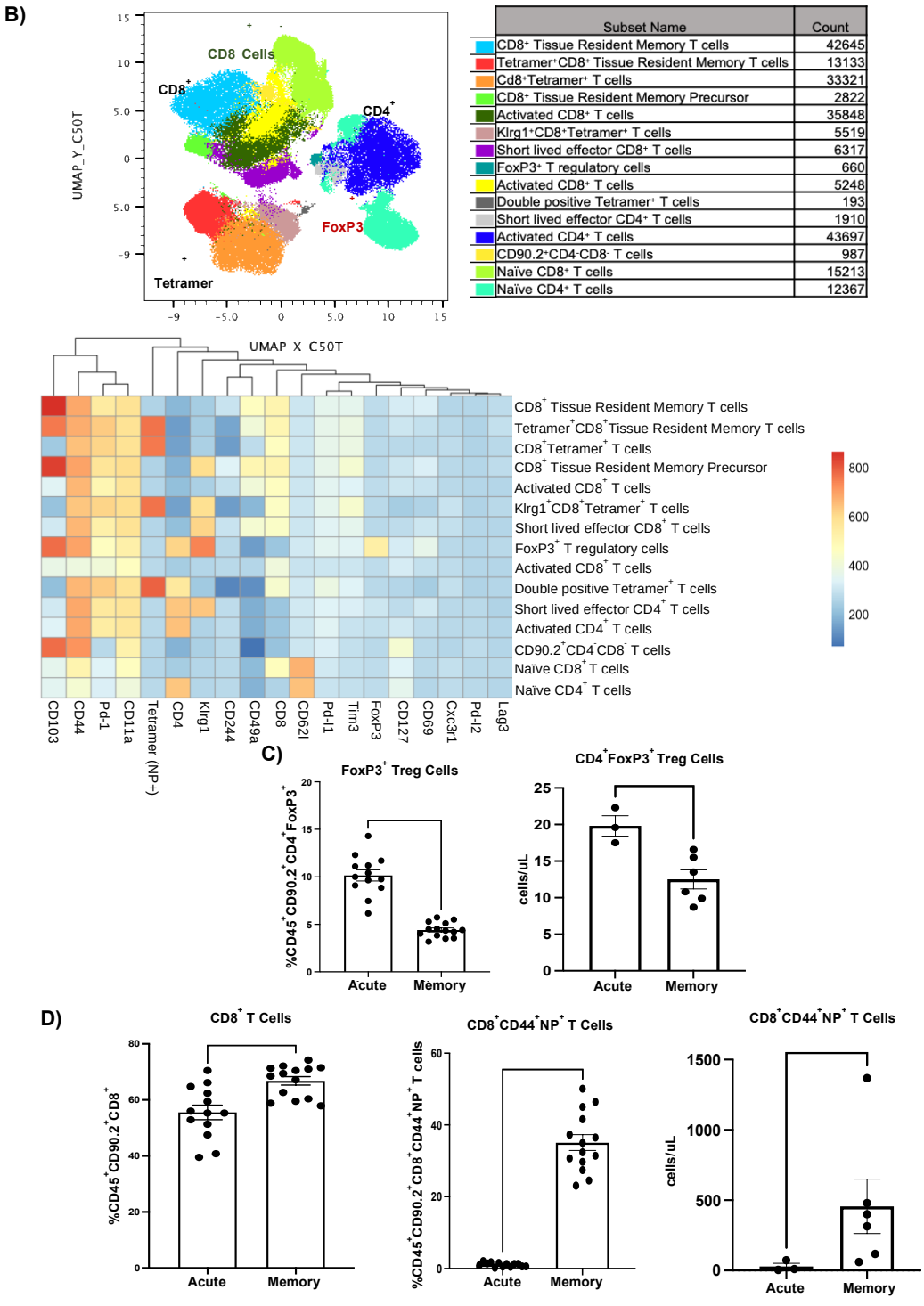

Figure 3.4 Memory experienced mice have a distinct T cell landscape characterized by an increase in NP+ tetramer specific CD8$^+$ T cells. A) Flow cytometry analysis on previously naïve acute super-infected mouse lungs. Samples were initially gated on CD45$^+$ CD90.2$^+$ live cells. Once gated samples were concatenated (n=4)

and populations were visualized using FlowSOM and UMAP plugins in FlowJo. FlowSOM populations were further analyzed by conventional gating techniques to determine breakdown of T cell types. B) Flow cytometry analysis on memory super-infected mouse lungs (n=5). Gating and visualization of T cell types were determined as noted above for A. C) Percentage and absolute cell count of $CD45^+$ $CD90.2^+$ $CD4^+$ $FoxP3^+$ Treg cells determined from flow cytometry in mouse lungs (percentage $FoxP3^+$ acute n=13, memory n=14, absolute number $FoxP3^+$ acute n=3, memory n=6). D) Percentage of $CD45^+$ $CD90.2^+$ $CD8^+$ T cells and NP^+ T cells with absolute cell counts determined by flow cytometry in mouse lungs (percentage acute n=13, memory n=14, absolute cell counts acute n=3, memory n=6). P values: *<0.05, **<0.01 *<0.001, ****<0.0001.**

We next looked at the expression of cytokines associated with T cell migration, proliferation, and regulation. We found that protein levels of pro-inflammatory cytokines IL-12p40 and IL-12p70 were significantly elevated in influenza memory experienced super-infected mouse lungs (Fig. 3.5a). Other cytokines that significantly changed in the lungs of memory or acute super-infected mice were CXCL10, IL-6, and IL-10, all of which are significantly decreased in memory experienced mice based on either protein expression or gene expression (Fig. 3.5b-d). Lastly, we saw a trend toward higher levels of IL-17a and IL-22, based on gene expression, although this was not significant. However, we did see a significant increase in expression of the Type 17 immune promoting cytokines IL-23 and IL-1β (Fig. 3.5e). These data demonstrate that the T cell compartment in memory experienced mice is characterized by an influx of tetramer positive $CD8^+$ T cells that are better able to control influenza infection, thus creating an environment that is potentially oriented towards improved bacterial immunity.

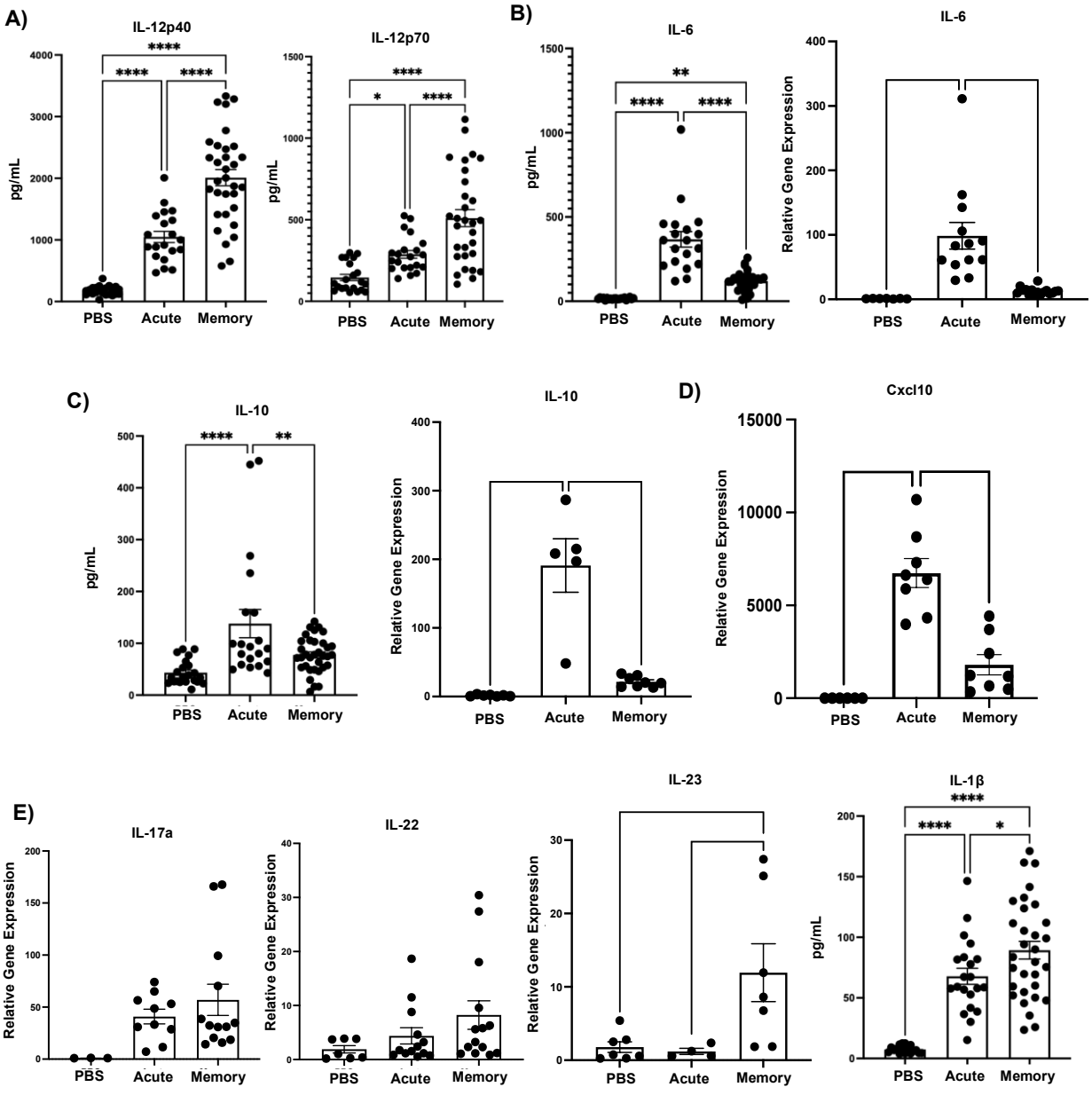

Figure 3.5 Memory experienced mice have reduced levels of cytokines that act as indicators of severe influenza infection, but display elevated levels of cytokines with roles in bacterial clearance. A-E) Relative gene expression and protein levels in memory versus acute super-infected mouse lungs. (IL-12p40: PBS n=23,acute n=20, memory n=32; IL-12p70: PBS n=21, acute n=21, memory n=30; IL-6: PBS n=21, acute n=19, memory n=29; IL-6 message: PBS n=7, acute n=13, memory n=16; IL-10: PBS n=22, acute n=20, memory n=34; CXCL10 message: PBS n=6, acute n=8, memory n=8; Il-17a message: PBS n=3, acute n=10,

memory n=13; IL-22 message: PBS n=7, acute n=13, memory n=14; IL-23 message: PBS n=7, acute n=4, memory n=7; IL-1β: PBS n=18, acute n=21, memory n=31). P values: *<0.05, **<0.01, *<0.001, ****<0.0001.**

3.4.5 Heterotypic influenza memory alters the innate immune cell compartment during bacterial super-infection.

Finally, we explored the impact of heterotypic influenza memory on innate immune cell populations, which are crucial for defense against bacterial infections. We used FlowSOM and UMAP to visualize changes in the myeloid compartment of mice with an established memory compartment. We found that neutrophils make up the largest proportion of myeloid cells in both super-infected treatment groups (Fig. 3.6a and b). Using our myeloid gating strategy (Appendix Fig. A.2.3), we also found that the total number of NK cells, monocytes, macrophages, and eosinophils were significantly reduced in the influenza super-infected memory mice as compared to their acute counterparts (Fig. 3.6c). Interestingly, no change was seen in the total number of neutrophils between both groups (Fig. 3.6c). Further flow cytometry analysis was conducted on acute and memory influenza alone infected mice, which we used to determine influenza-specific changes that occur in myeloid subsets (Appendix Fig. A.2.3). Influenza memory resulted in increases in proportions of NK cells, eosinophils, and monocytes (Appendix Fig. A.2.3). Next, we assessed changes in common cytokines and markers associated with myeloid cells and their function via both gene and protein expression. We first looked at two mediators of the inflammatory response, the alarmins IL-1α and IL-33. Both of these cytokines were significantly elevated in the lungs of memory mice via protein gene expression (Fig. 3.6d). When we examined markers that were significantly downregulated in the influenza super-infected memory mice, we

observed a decrease in protein expression of monocyte chemoattractant protein-1 (MCP-1), macrophage inflammatory protein-1 beta (MIP-1β), macrophage inflammatory protein-1 alpha (MIP-1α), and eotaxin (Fig. 3.6e), all of which suggests a less inflamed environment. Lastly, we found that arginase-1 (*Arg1*), cathepsin g (*Ctsg*), nitric oxide synthase 2 (*Nos2*), and amphiregulin (*Areg*) gene expression were also downregulated in memory mice (Fig. 3.6f). The promotion of an inflammatory balance in the lung environment through the stages of infection from influenza to secondary bacterial infection in the heterotypic memory mice may create an environment that is suitable for bacterial clearance.

A)

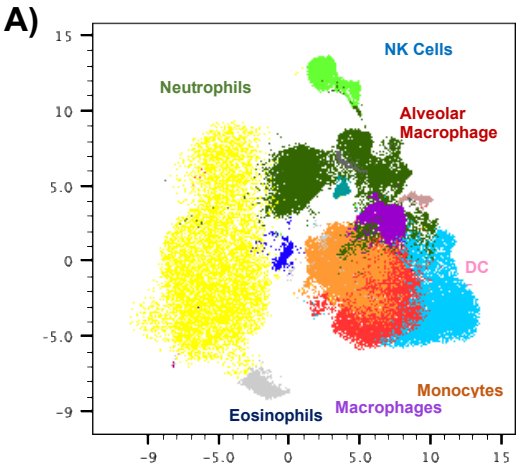

Subset Name	Count
Monocytes	34999
Macrophages	49855
Macrophages	18879
NK Cells	3965
Myeloid Cells	22570
Alveolar Macrophages	581
Dendritic Cells (DCs)	2736
Eosinophils	777
Neutrophils	173871
Neutrophils	272
Neutrophils	1704
Mature Neutrophils	480

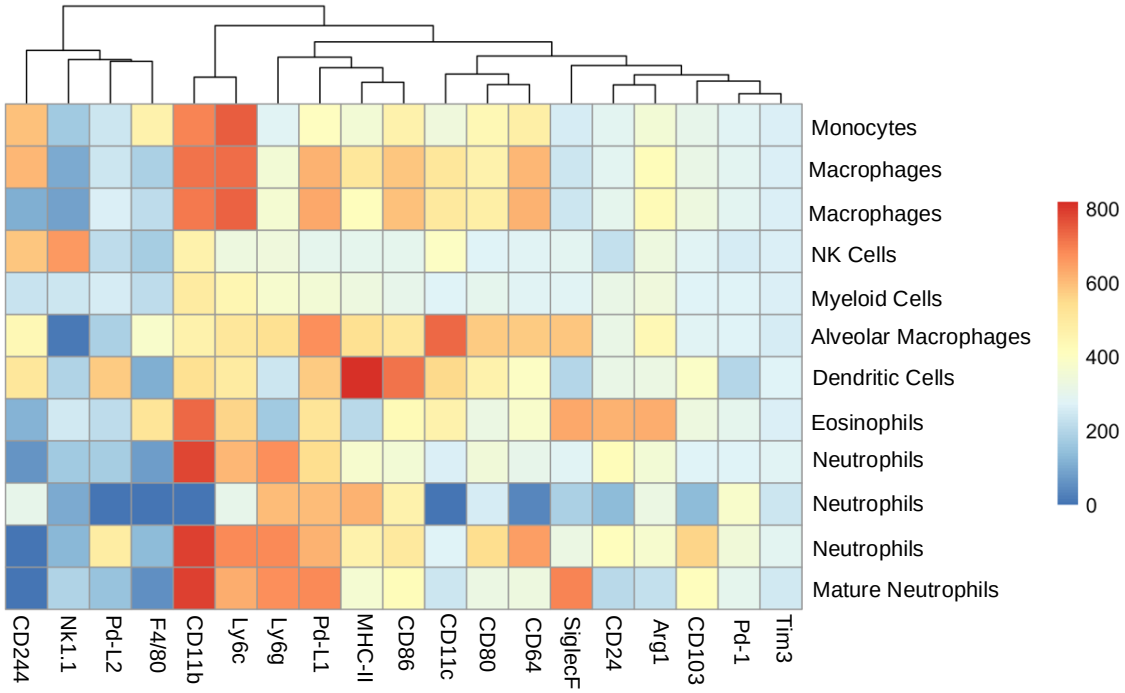

B)

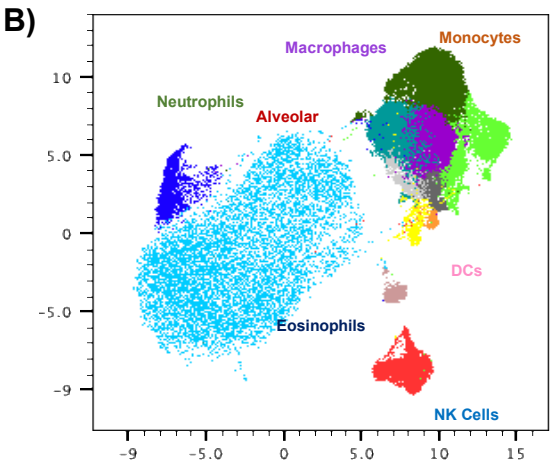

Subset Name	Count
Neutrophils	139934
NK Cells	3806
Alveolar Macrophages	343
Monocytes	5855
Monocytes	9665
Eosinophils	562
Macrophages	8695
Macrophages	4631
Myeloid Cells	587
Dendritic Cells (DCs)	986
Dendritic Cells (DCs)	512
Neutrophils	2192

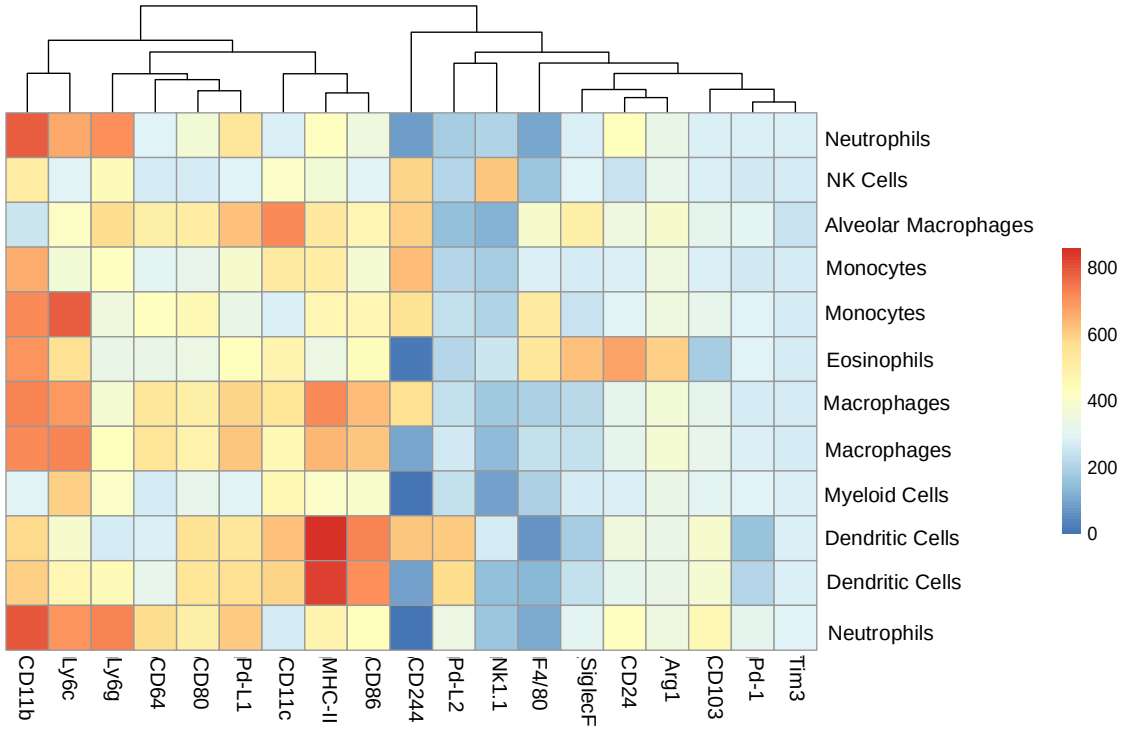

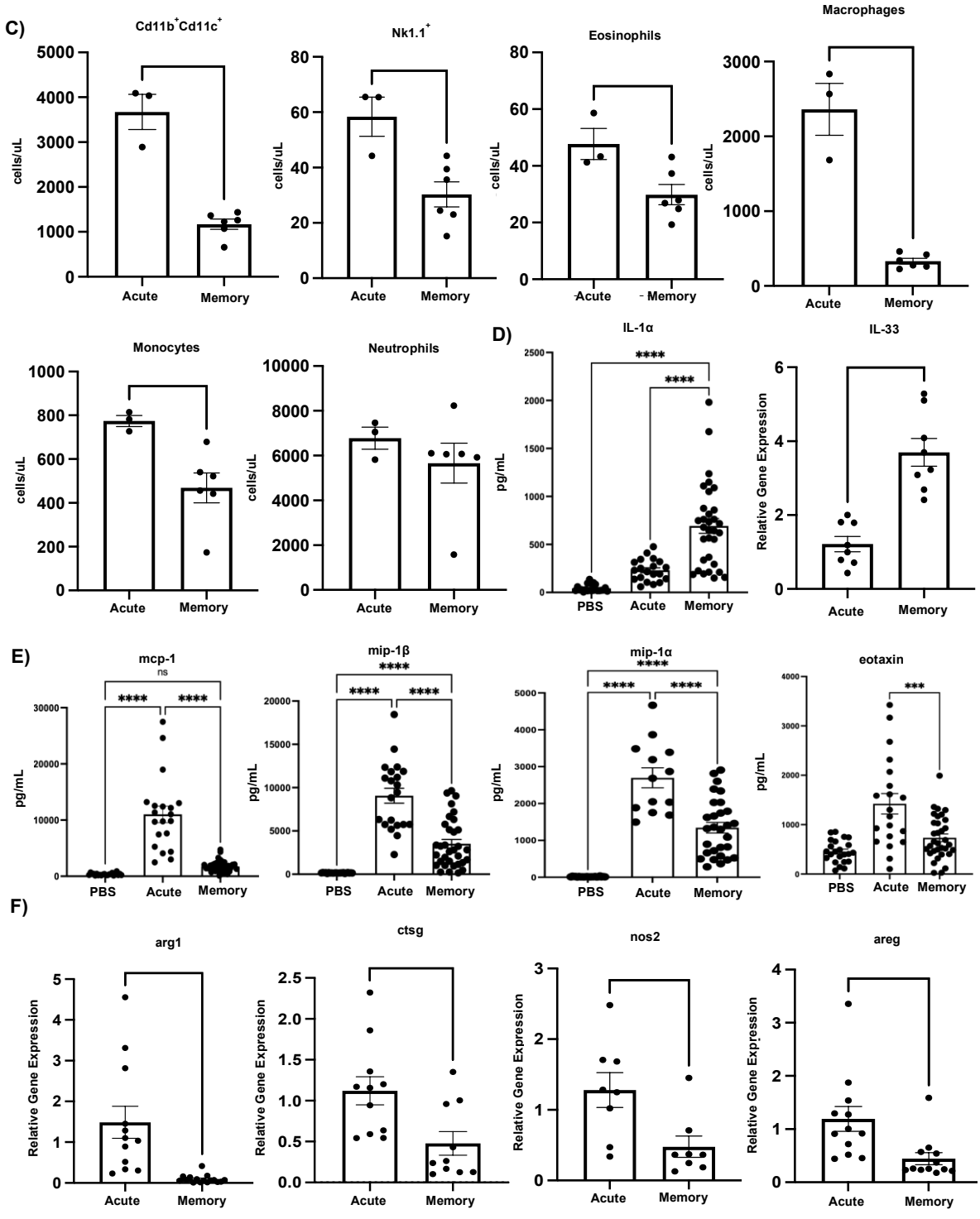

Figure 3.6 The myeloid cell landscape in memory experienced mice is characterized by a reduction in the number of cell types. A) Flow cytometry analysis on acute super-infected mouse lungs. Samples were initially gated on CD45^{+} TCRβ^{-}B220^{-}Live cells. Once gated samples were concatenated (n=5) then downsampled and

populations were visualized using FlowSOM and UMAP plugins in FlowJo. FlowSOM populations were further analyzed by conventional gating techniques to determine breakdown of myeloid cell types. B) Flow cytometry analysis on memory super-infected mouse lungs (n=4). Gating and visualization were determined as noted above for A. C) Absolute cell counts of myeloid cell subsets from flow cytometry analysis (acute n=3, memory n=6). D) Protein expression of IL-1*α* (PBS n=22, acute n=20, memory n=32) and relative gene expression of IL-33 (acute n=8, memory n=8) in mouse lungs. E) Protein expression of cytokines associated with the myeloid compartment (MCP-1: PBS n=22, acute n=20, memory n=34; MIP-1β: PBS n=22, acute n=21, memory n=33; MIP-1*α*: PBS n=22 , acute n=13, memory n=29; eotaxin: PBS n=23 , acute n=20, memory n=33). F) Relative gene expression of molecules associated with myeloid cell function (*Arg1*: acute n=12, memory n=16; *Ctsg*: acute n=11, memory n=10; *Nos2*: acute n=8, memory n=8; *Areg*: acute n=12, memory n=12). P values: *<0.05, **<0.01 *<0.001, ****<0.0001.**

3.5 Discussion

The importance of understanding how bacterial and viral infections synergize is widely applicable across many respiratory viral diseases including the recent Covid-19 pandemic [152]. Influenza-associated secondary bacterial infections are multi-faceted infections that employ multiple immune cell players of both the adaptive and innate immune systems to cover the broad spectrum of the host response from viral infection to bacterial infection. It is widely established that during an acute secondary bacterial infection the anti-viral response hinders the anti-bacterial mechanisms that are required to protect against opportunistic pathogens such as MRSA [14, 15, 16, 31, 33, 34, 92, 95, 121, 149, 153, 154, 155]. Secondary bacterial infection also results in heightened immunopathology driven by an overactive immune landscape, ultimately creating an ideal environment for opportunistic pathogens [122]. The results presented herein expand on the prevailing views in the field generated in previously infected(?) animals and suggest that memory to influenza

infections creates a balanced lung environment at the time of secondary bacterial infection susceptibility, resulting in a more effective anti-bacterial response.

The epithelium represents the first line of defense against respiratory pathogens and assault from environmental stressors. Influenza directly targets the epithelial barrier leading to extensive damage and impairment of the mucocilliary escalator resulting in an environment that heavily favors bacterial adherence and colonization [153, 156]. In the present study we found that influenza super-infected memory experienced mice have an altered lung epithelial environment as compared to their previously naïve acute infection counterparts. Interestingly, our data show that influenza super-infected memory lungs still undergo significant damage due to influenza infection. However, we observed preservation of epithelial gene expression of structural and functional markers in influenza super-infected memory mouse lungs. We saw an increase in the expression of Scgb1a1 (also known as club cell secretory protein), which has been shown to promote alveolar macrophage survival and response to inflammation [157]. Deconvolution analysis also suggested that memory mice expressed a higher proportion of the lung gene signature associated with the epithelium. Further, we observed upregulation of markers associated with cilium and ciliary movement, as well as mucus production. Taken together these data suggest that influenza memory does not prevent lung injury, rather the epithelium is re-programmed in a manner that favors the enhancement of bacterial clearance. Barrier integrity is also targeted by aberrant immune mechanisms including enhanced cytokine production in response to influenza that in cases of severe viral infections can cause severe edema [158]. Lung leak was also limited in the context of heterotypic influenza super-infected memory. Aberrant immune activation, such as cytokine storm, is key to influenza-related lung injury. Our data suggests that there is a reduction in

production of cytokines that are detrimental and associated with immunopathology, in particular MCP-1, MIP-1α, CXCL10, and IL-6 [158, 159, 160, 161].

A critical immune response to viral infection Is the production of interferons, a highly inducible first line defense against influenza infection. The interferon group is made up of three classes: type I (IFN-α and IFN-β), type II (IFN-γ), and type III (IFN-λ). Previous studies have shown that interferons enhance susceptibility during bacterial super-infection. These effects have been attributed to decreased Type 17 immune activation and destabilization in function and recruitment of phagocytic cells [25, 26, 27, 28, 29, 92, 120]. Our data suggest that at the time of super-infection, influenza memory experienced mice have reduced levels in expression of interferons, which based on prior studies would indicate that anti-bacterial mechanisms are preserved. One of the major roles that interferons play in the immune system is to induce production of other chemokines such as cxcl10, an important molecule associated with the trafficking of immune cell types including activated T cells [161]. Although, this immune cell trafficking to the site of infection is imperative for resolution of infection, too many pro-inflammatory cells in the lung environment can lead to detrimental outcomes. In this study, we observed a decrease in the relative gene expression of CXCL10, which could indicate decreased inflammation in the lung environment of memory experienced mice, and which adds further support to the reduction seen in infiltrating cells at time of super-infection.

An effective anti-bacterial response is marked by increased numbers of activated phagocytic cells. Support for a more effective anti-bacterial response to MRSA infection in our heterotypic memory experienced super-infected mice is demonstrated by the increase in the IL-1 family of cytokines, including IL-1β, IL-1α, and IL-33. It has been shown that restoration of IL-33 during an influenza associated bacterial super-infection is beneficial for bacterial clearance of

both *S. aureus* and MRSA, due to the role it plays in neutrophil recruitment to the infected lung [162]. IL-1β production is impaired by preceding influenza infection during secondary bacterial super-infections. This results in a detrimental outcome for the host because of the ability of IL-1b to promote the Type 17 pathway, which is important during antibacterial responses against numerous extracellular pathogens including *S. aureus* [114]. The IL-12 family has also been implicated in protection against bacterial infections. In our model, we found that three members of the IL-12 family (IL-12p40, IL-12p70 and IL-23) were increased. IL-12p70 and IL-23 have been shown to play a role in bacterial super-infections in human cells due to their alteration by influenza, resulting in impairment of the Ifn-γ and Type 17 pathways, respectively [163]. Another study suggested that IL-12p40 is crucial to early protection against bacterial infections due to its role in neutrophil recruitment [164]. However, this study also determined that IFN-γ was important in their model and we saw neither an increase in the relative gene expression of IFN-γ or neutrophil recruitment in our memory mice at the time of super-infection. Although, we did not see a significant increase in Type 17 cytokines, IL-17a and IL-22 in our influenza super-infected memory versus acute infected mice, we did see increased IL-1β, IL-23 and decreased IFN-γ, suggesting promotion of Type 17 immunity. Together these data indicate that heterotypic memory mice display increases in pathways related to bacterial defense. These pathways should be studied further to elucidate direct mechanisms by which they are regulated.

The lung is a dynamic organ that requires a state of homeostasis characterized by a balance in proinflammatory and anti-inflammatory factors [165]. Influenza infection results in a highly inflamed lung environment that is characterized by an influx in immune cells and increase in their soluble mediators. To return to homeostasis, the lung initiates anti-inflammatory mechanisms. One of the key anti-inflammatory mechanisms of the immune system consists of $Foxp3^+$ regulatory T

cells. These cells expand in response to an inflamed mucosal environment to dampen the immune response and they have been shown to acquire memory recall for targeted pathogen responses during re-challenge events [166, 167] which are imperative to restore homeostasis. In our study we saw a reduction in the proportion and numbers of FoxP3^{+} regulatory T cells in heterotypic memory experienced mice, as well as a reduction in the production of the anti-inflammatory cytokine IL-10. IL-10 has further been implicated in impairment of immune defense against influenza-associated secondary bacterial infections with *Streptococcus pneumoniae* and *Staphylococcus aureus* [113, 168, 169]. These data suggest that the lung environment of the influenza super-infected memory mice is targeted against the virus early on in re-challenge, which is reflected in the lower number of regulatory T cells present at time of bacterial infection. Our data further support this notion with the increase seen in tetramer specific T cells in memory mice and reduction in innate immune cells that are elevated in acute infections and are associated with aberrant pro-inflammatory responses.

In order to promote an environment that is beneficial for bacterial clearance and limits immunopathology caused by aberrant immune activation, a balancing act must be struck between anti-viral and anti-bacterial host defense. As shown herein, this balance can be accomplished in memory experienced mice by a quick and controlled response against the influenza infection, ultimately limiting the deleterious impact of anti-viral mechanisms on anti-bacterial immunity. This finding is highly relevant to the human condition where nearly all humans have some level of pre-existing immunity against influenza and is suggestive of an important role for pre-existing heterotypic influenza memory in limiting super-infection susceptibility. Although our studies are limited to two influenza strains, PR8 and X-31, recognition of conserved epitopes and subsequent heterotypic immunity has been found in multiple mouse adapted strains of influenza and even in

mouse models infected with some human strains, the use of which could further enhance the results found here [170, 171]. Further research on the role that heterotypic memory plays to enable susceptibility or protection against secondary bacterial infections is necessary and could provide further avenues of therapeutic intervention.

4.0 Conclusion and Future Directions

Influenza associated bacterial super-infections represent an ongoing area of therapeutic interest due to their devastating impacts and long-term consequences on the lung. Due to the multifaceted nature of this disease, current therapies for treatment rely heavily on treating the virus with antivirals or giving broadly neutralizing antibiotics. Both of these therapies rely heavily on timing of administration for effectiveness as well as the probability of the bacterial species to respond to the antibiotic. Here we presented novel research that furthers our understanding of the role of the immune system in establishment and susceptibility to secondary bacterial super-infections.

Our studies with the inhibitory marker PD-1 showed minimal changes in susceptibility to super-infection, as evidenced by the lack of significant change in MRSA burden during super-infection. In chronic and cancer models, where stimulation of the immune system is constant, inhibiting pathways that downregulate the immune response results in better control of infection[172]. Some studies on acute infections have resulted in a slightly different outcome with the observation that downregulation of these pathways results in heightened immune responses by T cells, but at the cost of immunopathology[172]. Interestingly, in our model we did see data that hinted at more damage in PD-1 KO super-infected mice as compared to their WT counterparts. Many disease models that have been published with the use of checkpoint inhibitors have stressed the timing of therapy [173]. From our research, we concluded that loss of PD-1 on all cell types during the course of infection is a potential caveat in our studies. With this in mind, we have obtained PD-$1^{fl/fl}$ mice from Drs. Arlene Sharpe and Dario Vignali, which we will use in the future to study the role of PD-1 on specific cell subsets, with particular interest on myeloid cells. We are particularly

interested in studying the role on macrophages ($Cx3cr1^{CreER}$) and neutrophils ($Mrp8^{Cre}$). PD-1 expression is dependent upon stimulation; therefore, we could use our mouse memory model to study the long-term impacts of PD-1 on regulation of the immune memory compartment and super-infection susceptibility.

The study of immune memory during influenza challenge has shaped our understanding of the role of the immune system in the face of evolved viral strains. This knowledge has led to new potential targets for development of universal vaccines to effectively defend against mutated influenza viruses. In our studies we looked further at the role that immune memory plays following influenza infection, specifically how it shapes super-infection susceptibility. Our studies determined that immune memory plays a role in bacterial super-infection. The exact mechanism that drives the reduction in MRSA burden in our model is still to be elucidated. Our data pinpoint several pathways of interest to pursue in the future. Two cytokines of interest that were increased during memory super-infection were Il-1β and Il-12p40. With antibody blockade we can target both of these cytokines and their signaling pathways to determine if they have any role in MRSA reduction. We also are currently diving deeper into understanding the role of B cells in our model, with a particular interest in antigen presenting B cells and how they influence the establishment of the memory compartment. Using mouse models, we can target B cells to determine the role they play in establishment of the memory response to secondary bacterial super-infections. Two mouse models that we are interested in using to study these responses are muMT, which lack mature B cells, and MD4 mice, which lack antigen presenting B cells.

In conclusion, we are still at the early stages of understanding the role of inhibitory pathways as well as memory in susceptibility to influenza associated secondary bacterial super-infections. Ongoing studies in both of these areas could help us further understand super-infection

susceptibility, with the goal of eventually targeting one of these pathways for therapeutic purposes. Regarding influenza, there has been ongoing interest in designing universal vaccines which could stimulate the memory cell compartment enabling broad spectrum immunity across strains. Our research suggests that the influenza immune memory compartment is also protective against secondary bacterial infections; therefore, if a universal vaccine can be synthesized it may also confer protection against secondary bacterial infections.

Appendix A Supplementary Figures and Tables

Appendix A.1 The role of Inhibitory Marker PD-1 in Susceptibility to Influenza Associated Secondary Bacterial Infections.

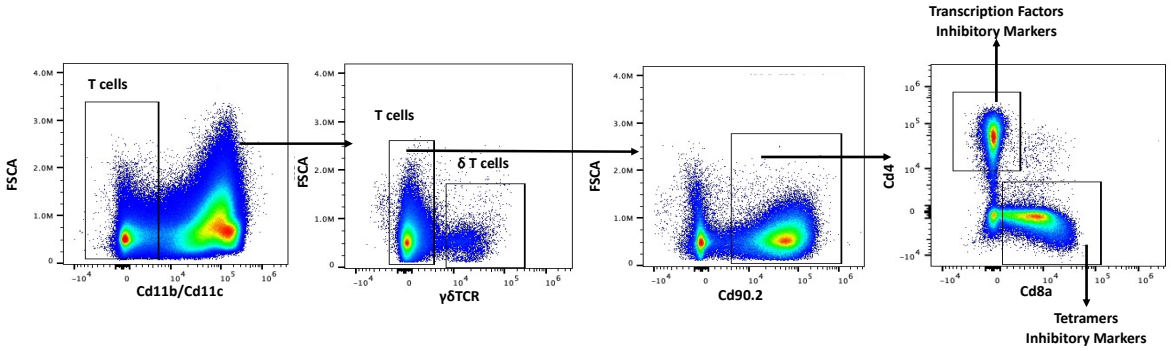

Appendix Figure A.1.1 T cell flow cytometry gating strategy. T cells were initially gated on Cd45^{+} Live cells then gated further into their individual subsets.

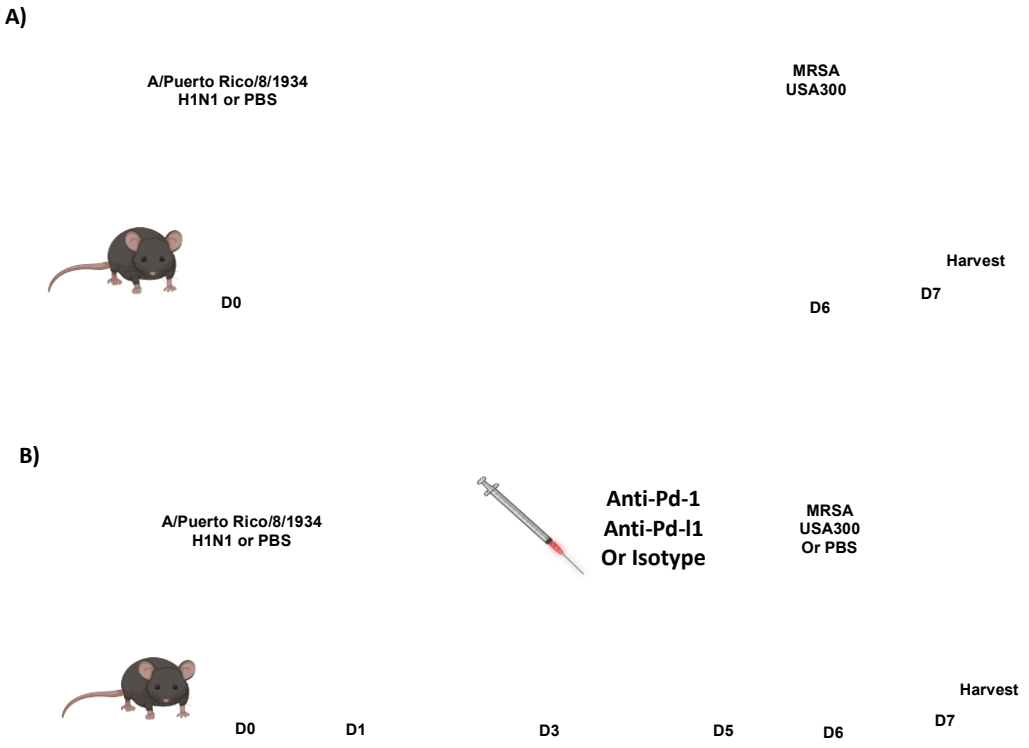

Appendix Figure A.1.2Mouse model of global PD-1 KO and antibody blockade of PD-1 and Pd-l1. A)WT C57Bl/6 and global PD-1 KO micewere infected on day zero with eithe PBS or influenza strain PR8. Following influenza infection, mice were challenged with MRSA USA300 or PBS at day six. On day seven mice were euthanized and lungs, and bronchoalveolar lavage fluid was collected for downstream analysis. B) WT C57Bl/6 mice were infected with PBS or influenza strain PR8. Antibody injections of either PD-1, its ligand Pd-l1, or their corresponding isotype controls were given at 200ug doses on days one, three, and five (all antibodies came from BioXCell, Lebanon NH). On day six mice were given PBS or MRSA strain USA300. Mice were harvested ond ay seven for downstream analysis.

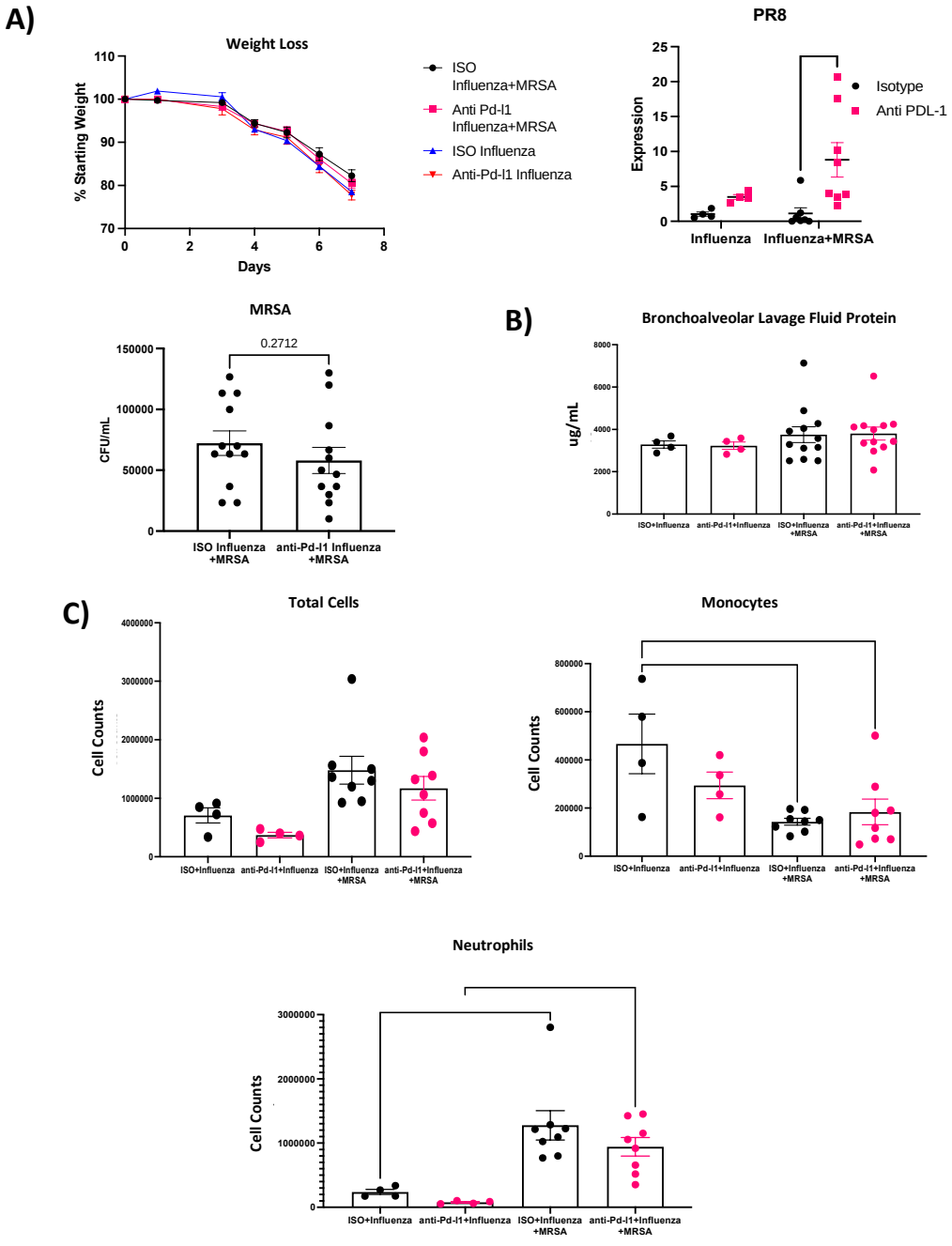

Appendix Figure A.1.3 Antibody blockde against PD-L1 has a minimal impact on susceptibility to super-infection. A) Percent of weight loss in anti-PD-L1 or isotype treated WT C57Bl/6 was calculated starting from day zero, then again on day six when MRSA was given, and lastly on day seven the day of harvest (Influenza: ISO n=4, anti-Pd-l1 n=4; super-infected: ISO n=12, anti-Pd-l1 n=12). Relative gene expression of Presence of viral protein was assessed in cDNA from total mouse lung via relative gene expression analysis of PR8

(Matrix protein) (Influenza: ISO n=4, anti-Pd-l1 n=4; super-infected: ISO n=7, anti-Pd-l1 n=8). Number of MRSA colonies plated from infected mouse lung homogenates (super-infected: ISO n= 12, anti-PD-l1 n=12). B) BAL protein from Isotype and anti-Pd-L1 treated mice were quantified from BAL collected at day of harvest (Influenza: ISO n=4, anti-Pd-l1 n=4; super-infected: ISO n=12, anti-Pd-l1 n=12). C) Total infiltrating cell counts, number of monocytes, as well as number of neutrophils were determined by cytospins using bronchoalveolar lavage fluid collected from infected mouse lungs at time of harvest (Influenza: ISO n=4, anti-Pd-l1 n=4; super-infected: ISO n=8, anti-Pd-l1 n=8). P values:*<0.05, **<0.01,*<0.001,****<0.0001.**

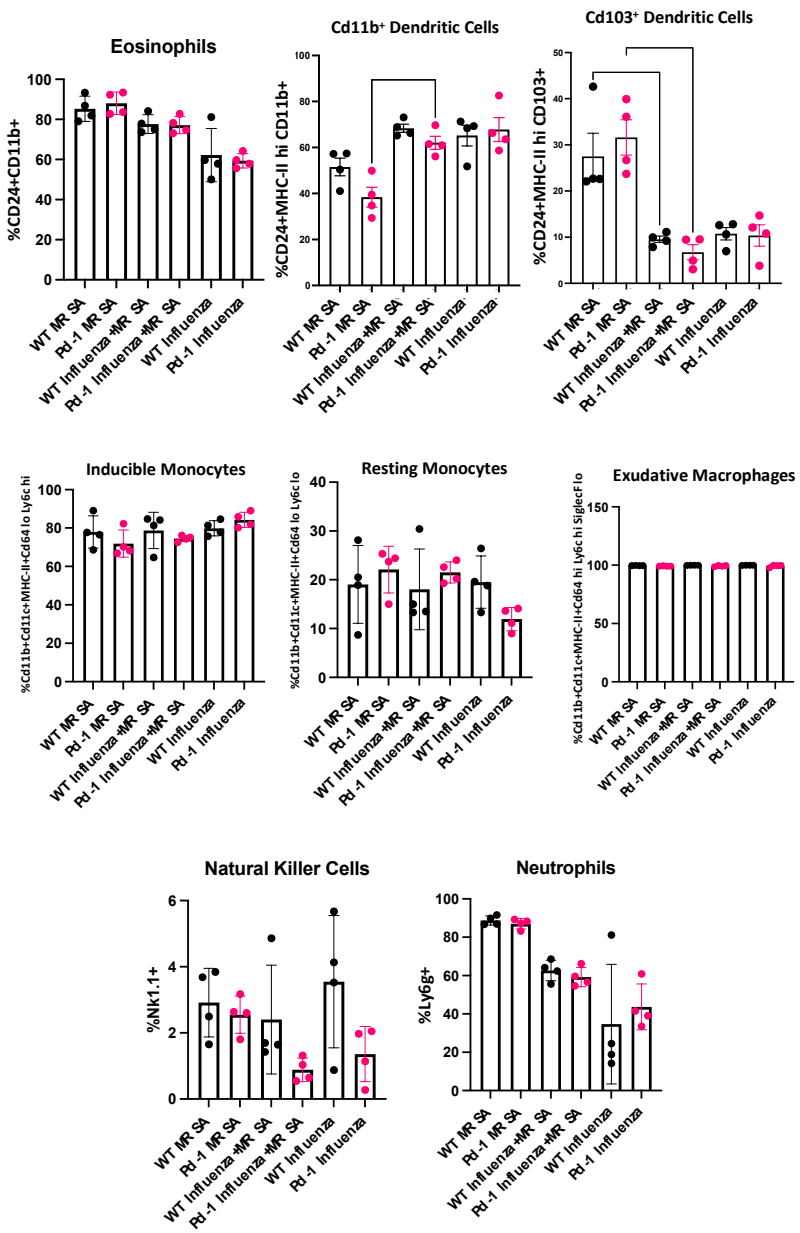

Appendix Figure A.1.4 Global knock out of PD-1 plays a minimal role on changes in myeloid ell subset.

Flow cytometry staining of myeloid cell subsets in PD-1 KO and WT super-infected, MRSA alone, or Influenza alone groups. Samples were initially gated on $CD45^{+}$ $TCR\beta^{-}B220^{-}$Live cells (n=4).

Appendix A.2 Heterotypic Influenza Infections Mitigate Susceptibility to Secondary Bacterial Infection

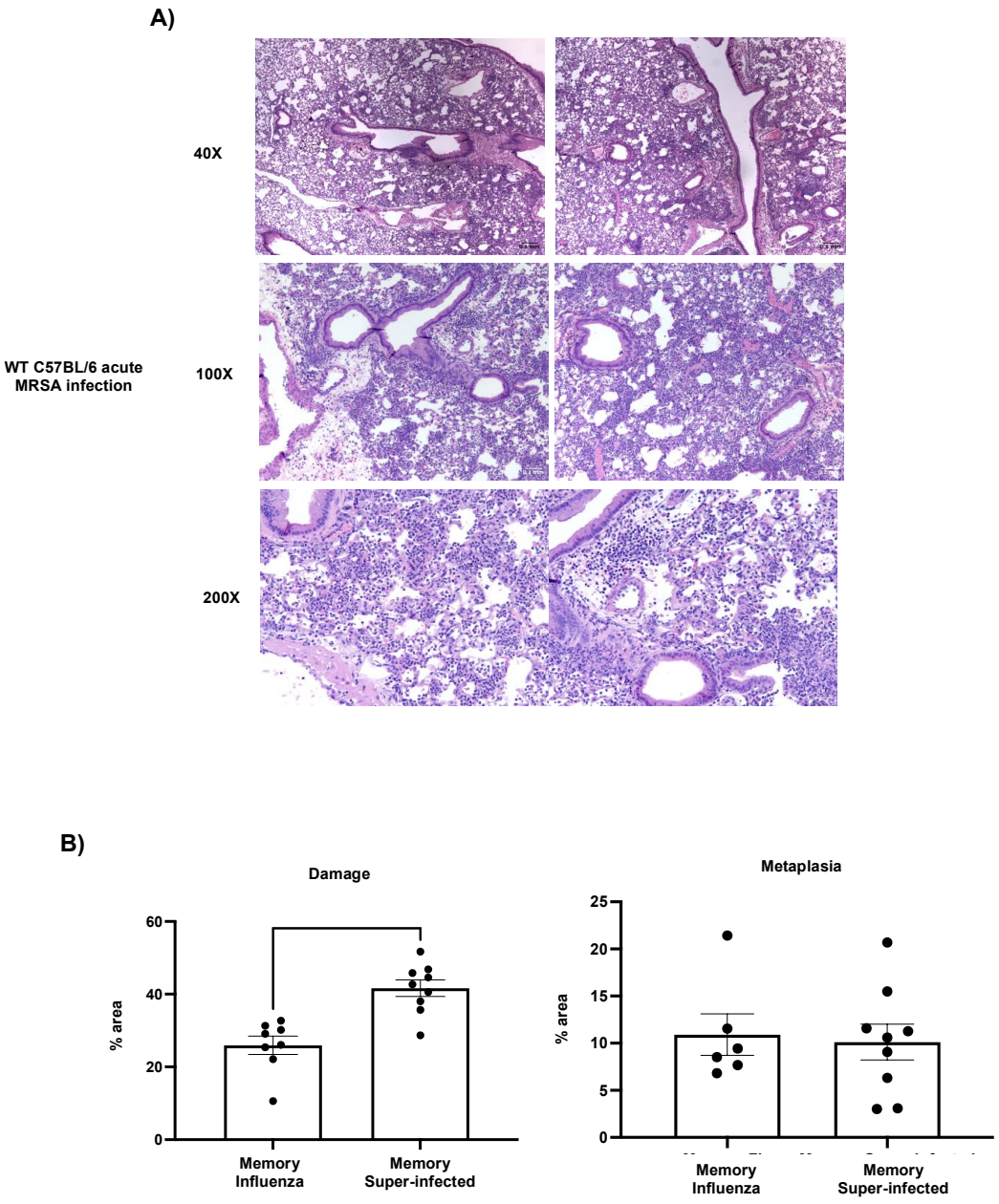

Appendix Figure A.2.1 Visualization of lung damage MRSA alone infected mice and quantification of damage and metaplasia in memory experienced mice. A) Representative histology sections of acute (n=2) and memory (n=2) influenza infected WT C57Bl/6 mice from formalin inflated mouse lungs stained with H&E at

40X,100X, and 200X. B) Percent of damage and metaplasia in influenza alone and super-infected memory groups quantified by calculating thresholds of damaged areas and areas of metaplasia using Fiji software (influenza n=8, super-infected n=9). P values: *<0.05, **<0.01, *<0.001, ****<0.0001.**

A)

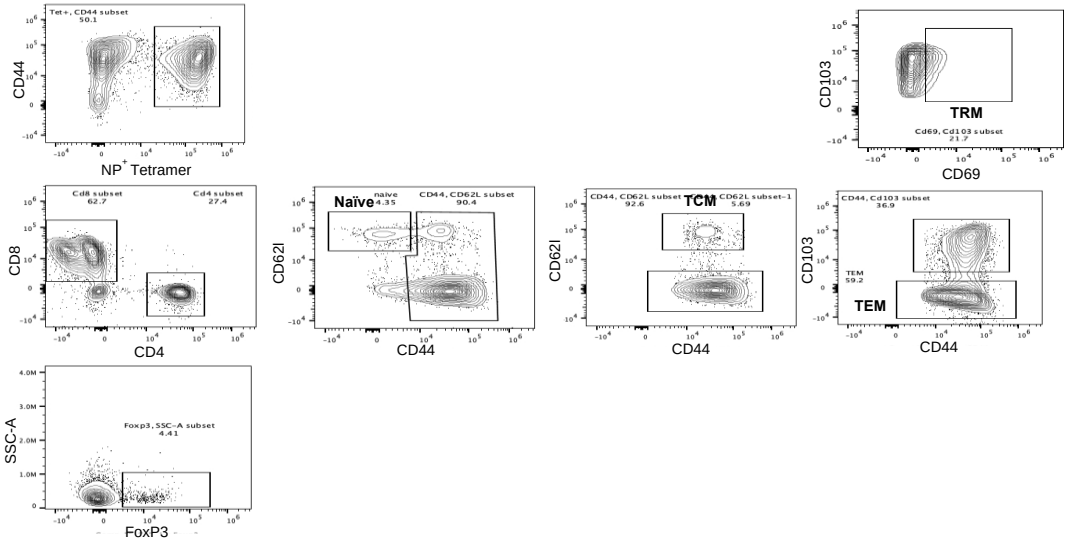

B)

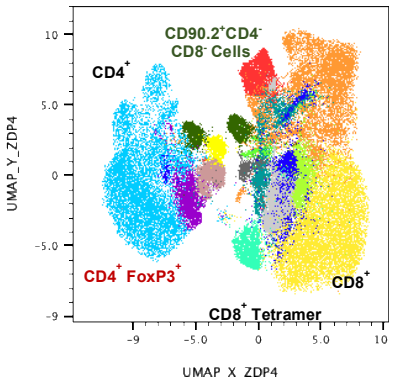

Subset Name	Count
Activated CD4+ T cells	44774
CD90.2+CD4-CD8- T cells	4296
Naïve CD8+ T cell	34154
CD90.2+CD4-CD8- T cells	426
CD90.2+CD4-CD8- T cells	2602
FoxP3+ T regulatory Cell	2394
Activated CD4+ T cells	1972
CD90.2+CD4-CD8- T cells	2660
FoxP3+ T regulatory Cell	1171
CD90.2+CD4-CD8- T cells	732
Activated CD8+ T cells	5800
CD90.2+CD4-CD8- T cells	2540
Activated CD8+ T cells	52824
Memory Precursor CD8+ T cells	1682
CD8+ Tetramer+ T cells	2101

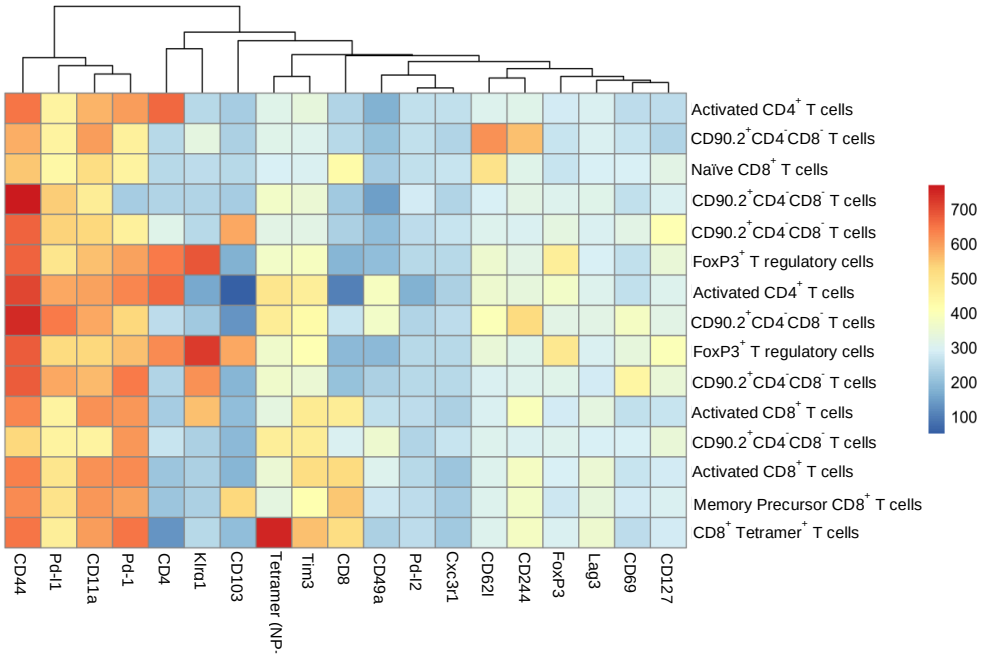
Activated CD4+ T cells
CD90.2+CD4-CD8- T cells
Naïve CD8+ T cells
CD90.2+CD4-CD8- T cells
CD90.2+CD4-CD8- T cells
FoxP3+ T regulatory cells
Activated CD4+ T cells
CD90.2+CD4-CD8- T cells
FoxP3+ T regulatory cells
CD90.2+CD4-CD8- T cells
Activated CD8+ T cells
CD90.2+CD4-CD8- T cells
Activated CD8+ T cells
Memory Precursor CD8+ T cells
CD8+ Tetramer+ T cells
CD44
Pd-l1
CD11a
Pd-1
CD4
Klrg1
CD103
Tetramer (NP-
Tim3
CD8
CD49a
Pd-l2
Cxc3r1
CD62l
CD244
FoxP3
Lag3
CD69
CD127
700
600
500
400
300
200
100

C)

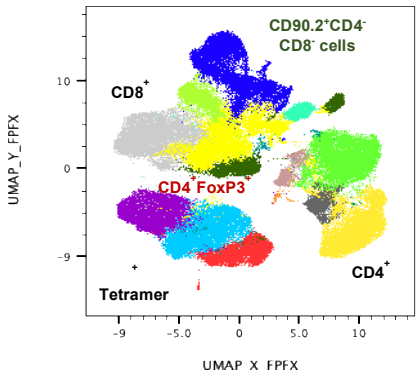

Subset Name	Count
CD8+ Tetramer+ T cells	27203
Klrg1+ CD8+ Tetramer+ T cells	5949
CD8+ Tetramer+ T cells	113
Activated CD4+ T cells	24576
Short Lived effector CD8+ T cells	4261
FoxP3+ T regulatory Cells	1309
CD8+ Tetramer+ Tissue Resident Memory T cells	13572
CD90.2+Cd4-CD8- T cells	282
Activated CD8+ T cells	21746
Activated CD4+ T cells	2211
CD8+ Tissue Resident Memory T cells	24046
Naïve CD8+ T cell	19600
Naïve CD4+ T cell	16168
Activated CD8+ T cells	3066
CD90.2+Cd4-CD8- T cells	1866

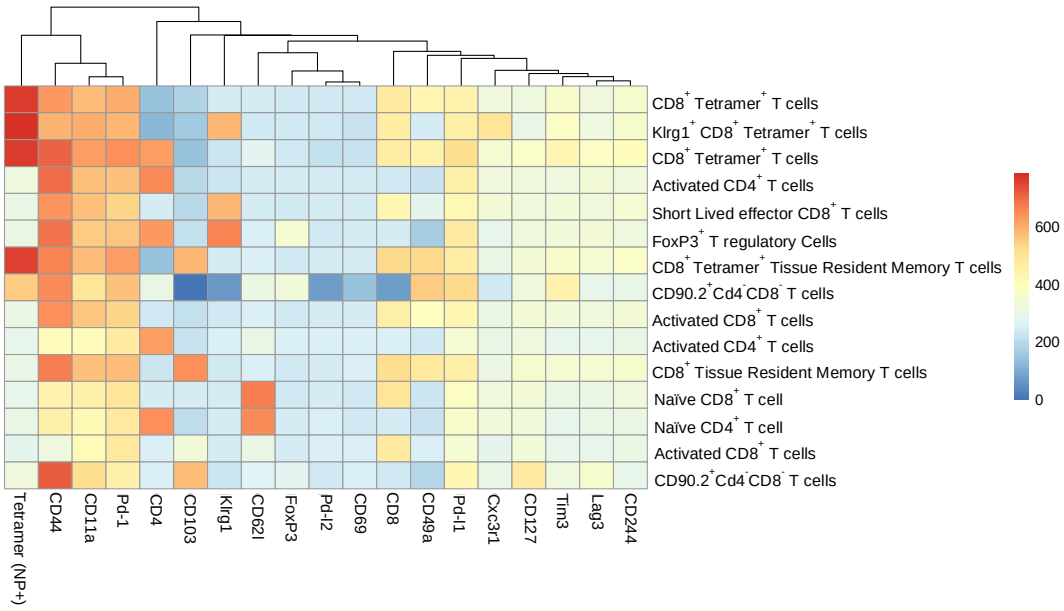

Appendix Figure A.2.2 Gating strategy for T cell compartment analysis and flow cytometry analysis for acute and memory influenza alone infections. T cells were initially gated on CD90.2$^+$CD45$^+$Live cells and further gated to parse out changes in CD4$^+$ and CD8$^+$ T cells. B) Flow cytometry analysis on acute influenza infected mouse lungs. Once gated samples were concatenated (n=3) and populations were visualized using FlowSOM and UMAP plugins in FlowJo. FlowSOM populations were further analyzed by conventional gating techniques to determine breakdown of T cell types. C) Flow cytometry analysis on memory influenza alone infected mice (n=4).

A)

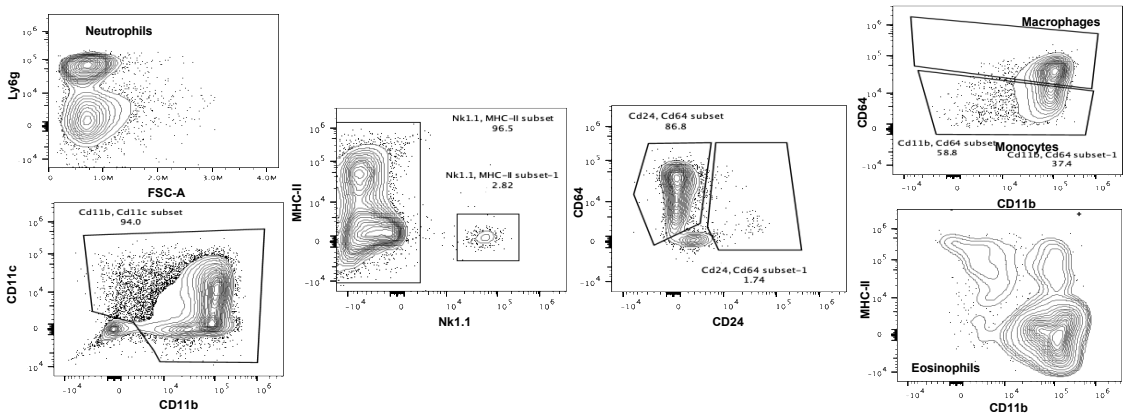

B)

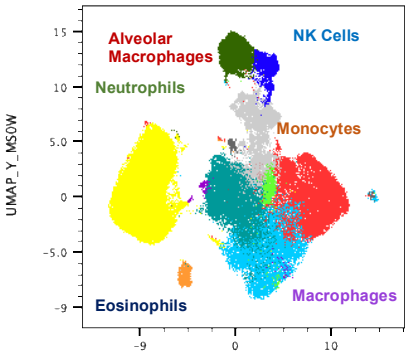

Subset Name	Count
Macrophages	17073
Macrophages	44428
Eosinophils	965
Monocytes	773
NK cells	964
Monocytes	5799
Macrophages	409
Macrophages	19910
Neutrophils	375
Alveolar Macrophages	31214
Myeloid Cells	7259
NK Cells	403

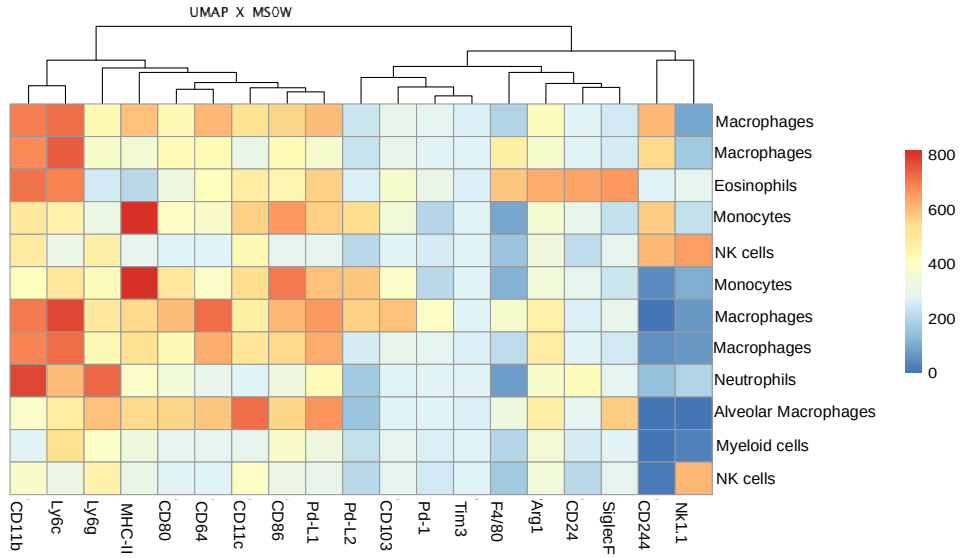

C)

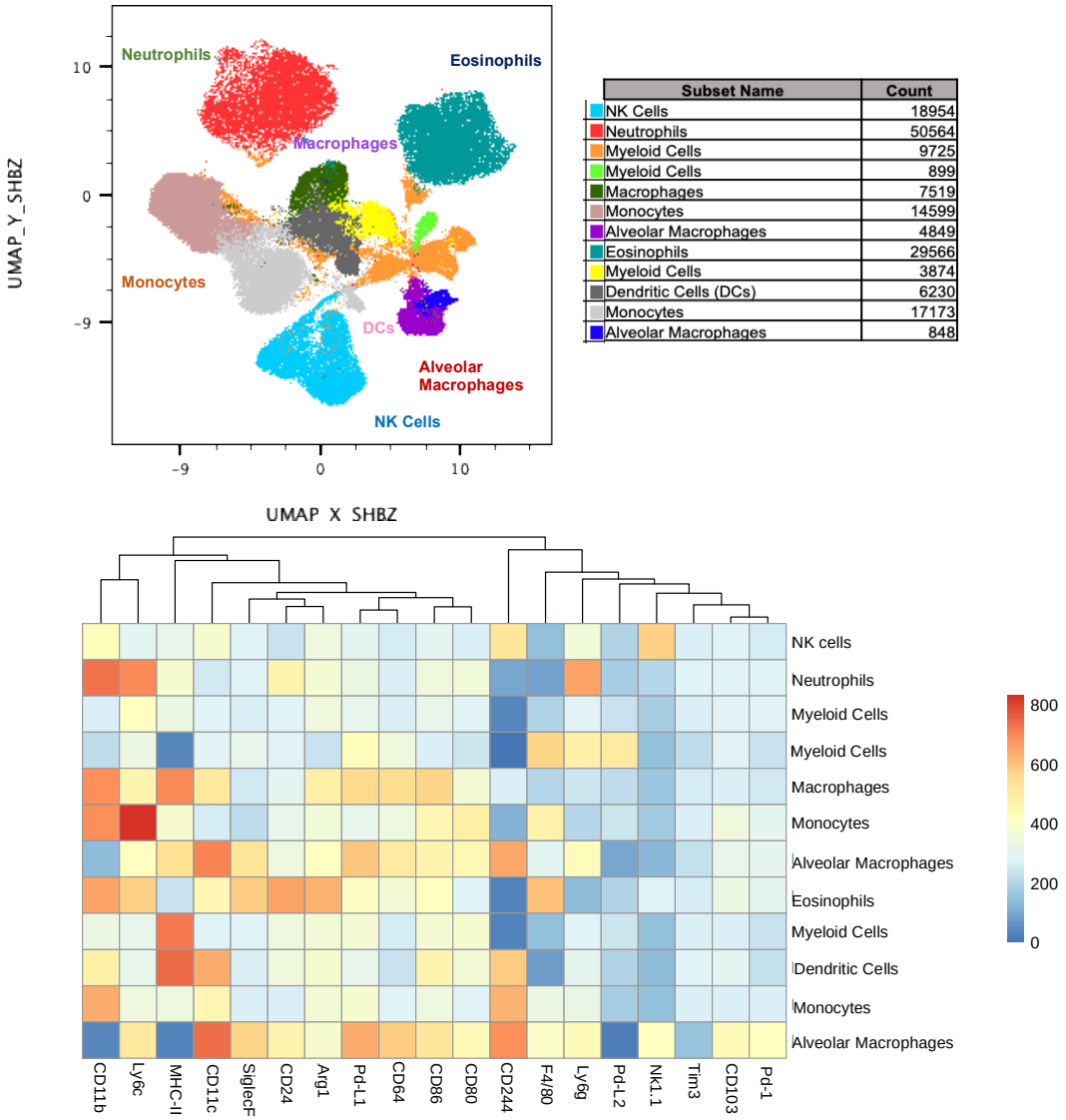

Appendix Figure A.2.3 Gating strategy for myeloid cell subset analysis and flow cytometry analysis for acute and memory influenza alone infections. A) Myeloid cells were initially gated on TCRB^{-}B220^{-}CD45^{+}Live cells and further gated to determine changes in myeloid cell subsets. B) Flow cytometry analysis on acute influenza infected mouse lungs. Once gated samples were concatenated (n=3) and downsampled then visualized using FlowSOM and UMAP plugins in FlowJo. FlowSOM populations were further analyzed by conventional gating techniques to determine breakdown of myeloid cell types. C) Flow cytometry analysis on memory influenza alone infected mice (n=4).

Appendix B Supplementary Materials and Methods

Appendix B.1

Mouse real-time PCR primers used in all experiments, purchased as a proprietary primer probe set as TaqMan "Assay on Demand".

Table 1 "Assay on Demand" Probes

Gene Name	Assay ID
tjp1	Mm00493699_m1
scgb1a1	Mm00442046_m1
sftpc	Mm00488144_m1
Ifnγ	Mm01168134_m1
Ifnα	Mm03030145-gH
Ifnβ	Mm00439546_s1
Ifnλ3	Mm00663660_g1
muc5b	Mm00466376_m1
muc5ac	Mm01276725_g1
foxj1	Mm01267279_m1
col1a1	Mm01302040_g1
acta2	Mm01546133_m1
Il-6	Mm00446190_m1
Il-10	Mm00439614_m1
cxcl10	Mm00445235_m1
Il-17a	Mm00439618_m1
Il-23	Mm00518984_m1
Il-1β	Mm00434228_m1
Il-22	Mm0044421_m1
Il-1α	Mm00439620_m1
Il-33	Mm00505403_m1
arg1	Mm00475988_m1
ctsg	Mm00456011_m1
nos2	Mm00440502_m1
areg	Mm01354339_m1

Appendix B.2 Staphylococcus Aureus Media Recipe

1) Mix the following in a 1L Erlenmeyer flask:

7.5g agar

15g yeast extract

10g casamino acids

1.24g Na_2HPO_4

0.205g KH_2PO_4

10mg $MgSO_4 \cdot 7H_2O$

3.75mg $MnSO_4 \cdot H_2O$

3.2mg $FeSO_4 \cdot 7H_2O$

3.2mg citric acid

450mL distilled water

2) pH to 7.3

3) Autoclave

4) Meanwhile mix:

11.6g sodium pyruvate

50mL distilled water

5)Filter-sterilize sodium pyruvate mixture and add to autoclaved portion once it has cooled slightly.

6) Distribute 10mL of media to sterile plates under cell culture hood, swirling to spread evenly and popping any bubbles with a sterile glass pipet tip.

To make broth, follow all above steps and exclude the addition of agar.

Bibliography

1. Morens, D.M., Taubenberger, J.K. & Fauci, A.S. Predominant role of bacterial pneumonia as a cause of death in pandemic influenza: implications for pandemic influenza preparedness. *J Infect Dis* **198**, 962-970 (2008).

2. Morris, D.E., Cleary, D.W. & Clarke, S.C. Secondary Bacterial Infections Associated with Influenza Pandemics. *Front Microbiol* **8**, 1041 (2017).

3. Manohar, P. *et al.* Secondary Bacterial Infections in Patients With Viral Pneumonia. *Front Med (Lausanne)* **7**, 420 (2020).

4. Denney, L. & Ho, L.P. The role of respiratory epithelium in host defence against influenza virus infection. *Biomed J* **41**, 218-233 (2018).

5. Peteranderl, C., Herold, S. & Schmoldt, C. Human Influenza Virus Infections. *Semin Respir Crit Care Med* **37**, 487-500 (2016).

6. Chen, X. *et al.* Host Immune Response to Influenza A Virus Infection. *Front Immunol* **9**, 320 (2018).

7. Muruganandah, V. & Kupz, A. Immune responses to bacterial lung infections and their implications for vaccination. *Int Immunol* **34**, 231-248 (2022).

8. Geitani, R., Moubareck, C.A., Xu, Z., Karam Sarkis, D. & Touqui, L. Expression and Roles of Antimicrobial Peptides in Innate Defense of Airway Mucosa: Potential Implication in Cystic Fibrosis. *Front Immunol* **11**, 1198 (2020).

9. Aberdein, J.D., Cole, J., Bewley, M.A., Marriott, H.M. & Dockrell, D.H. Alveolar macrophages in pulmonary host defence the unrecognized role of apoptosis as a mechanism of intracellular bacterial killing. *Clin Exp Immunol* **174**, 193-202 (2013).

10. Pidwill, G.R., Gibson, J.F., Cole, J., Renshaw, S.A. & Foster, S.J. The Role of Macrophages in *Staphylococcus aureus* infection. *Front Immunol* **11**, 620339 (2020).

11. Giacalone, V.D., Margaroli, C., Mall, M.A. & Tirouvanziam, R. Neutrophil Adaptations upon Recruitment to the Lung: New Concepts and Implications for Homeostasis and Disease. *Int J Mol Sci* **21** (2020).

12. Tsai, H.C., Velichko, S., Hung, L.Y. & Wu, R. IL-17A and Th17 cells in lung inflammation: an update on the role of Th17 cell differentiation and IL-17R signaling in host defense against infection. *Clin Dev Immunol* **2013**, 267971 (2013).

13. Rathore, J.S. & Wang, Y. Protective role of Th17 cells in pulmonary infection. *Vaccine* **34**, 1504-1514 (2016).

14. Rynda-Apple, A., Robinson, K.M. & Alcorn, J.F. Influenza and Bacterial Superinfection: Illuminating the Immunologic Mechanisms of Disease. *Infect Immun* **83**, 3764-3770 (2015).

15. McCullers, J.A. The co-pathogenesis of influenza viruses with bacteria in the lung. *Nat Rev Microbiol* **12**, 252-262 (2014).

16. Smith, A.M. & McCullers, J.A. Secondary bacterial infections in influenza virus infection pathogenesis. *Curr Top Microbiol Immunol* **385**, 327-356 (2014).

17. Zhang, W.J. *et al.* Lethal synergism between influenza infection and staphylococcal enterotoxin B in mice. *J Immunol* **157**, 5049-5060 (1996).

18. van der Sluijs, K.F. *et al.* Influenza-induced expression of indoleamine 2,3-dioxygenase enhances interleukin-10 production and bacterial outgrowth during secondary pneumococcal pneumonia. *J Infect Dis* **193**, 214-222 (2006).

19. McCullers, J.A. Insights into the interaction between influenza virus and pneumococcus. *Clin Microbiol Rev* **19**, 571-582 (2006).

20. Metzger, D.W. & Sun, K. Immune dysfunction and bacterial coinfections following influenza. *J Immunol* **191**, 2047-2052 (2013).

21. Cauley, L.S. & Vella, A.T. Why is coinfection with influenza virus and bacteria so difficult to control? *Discov Med* **19**, 33-40 (2015).

22. Kash, J.C. *et al.* Lethal synergism of 2009 pandemic H1N1 influenza virus and Streptococcus pneumoniae coinfection is associated with loss of murine lung repair responses. *mBio* **2** (2011).

23. McCullers, J.A. & Bartmess, K.C. Role of neuraminidase in lethal synergism between influenza virus and Streptococcus pneumoniae. *J Infect Dis* **187**, 1000-1009 (2003).

24. Siegel, S.J., Roche, A.M. & Weiser, J.N. Influenza promotes pneumococcal growth during coinfection by providing host sialylated substrates as a nutrient source. *Cell Host Microbe* **16**, 55-67 (2014).

25. Nakamura, S., Davis, K.M. & Weiser, J.N. Synergistic stimulation of type I interferons during influenza virus coinfection promotes Streptococcus pneumoniae colonization in mice. *J Clin Invest* **121**, 3657-3665 (2011).

26. Shahangian, A. *et al.* Type I IFNs mediate development of postinfluenza bacterial pneumonia in mice. *J Clin Invest* **119**, 1910-1920 (2009).

27. Sun, K. & Metzger, D.W. Inhibition of pulmonary antibacterial defense by interferon-gamma during recovery from influenza infection. *Nat Med* **14**, 558-564 (2008).

28. Rich, H.E. *et al.* Murine Type III interferons are functionally redundant and correlate with bacterial burden during influenza/bacterial super-infection. *PLoS One* **16**, e0255309 (2021).

29. Rich, H.E. *et al.* Interferon Lambda Inhibits Bacterial Uptake during Influenza Superinfection. *Infect Immun* **87** (2019).

30. Didierlaurent, A. *et al.* Sustained desensitization to bacterial Toll-like receptor ligands after resolution of respiratory influenza infection. *J Exp Med* **205**, 323-329 (2008).

31. Robinson, K.M., Kolls, J.K. & Alcorn, J.F. The immunology of influenza virus-associated bacterial pneumonia. *Curr Opin Immunol* **34**, 59-67 (2015).

32. Small, C.L. *et al.* Influenza infection leads to increased susceptibility to subsequent bacterial superinfection by impairing NK cell responses in the lung. *J Immunol* **184**, 2048-2056 (2010).

33. Kudva, A. *et al.* Influenza A inhibits Th17-mediated host defense against bacterial pneumonia in mice. *J Immunol* **186**, 1666-1674 (2011).

34. Lee, B. *et al.* STAT1 Is Required for Suppression of Type 17 Immunity during Influenza and Bacterial Superinfection. *Immunohorizons* **1**, 81-91 (2017).

35. Cipolla, E.M., Huckestein, B.R. & Alcorn, J.F. Influenza sequelae: from immune modulation to persistent alveolitis. *Clin Sci (Lond)* **134**, 1697-1714 (2020).

36. Paget, C. & Trottein, F. Mechanisms of Bacterial Superinfection Post-influenza: A Role for Unconventional T Cells. *Front Immunol* **10**, 336 (2019).

37. Rumpret, M. *et al.* Functional categories of immune inhibitory receptors. *Nat Rev Immunol* **20**, 771-780 (2020).

38. Shao, Q. *et al.* Tissue Tregs and Maintenance of Tissue Homeostasis. *Front Cell Dev Biol* **9**, 717903 (2021).

39. Sharpe, A.H. & Pauken, K.E. The diverse functions of the PD1 inhibitory pathway. *Nat Rev Immunol* **18**, 153-167 (2018).

40. Patsoukis, N., Wang, Q., Strauss, L. & Boussiotis, V.A. Revisiting the PD-1 pathway. *Sci Adv* **6** (2020).

41. Aroldi, F. *et al.* Lag3: From Bench to Bedside. *Cancer Treat Res* **183**, 185-199 (2022).

42. Yi, M. *et al.* Combination strategies with PD-1/PD-L1 blockade: current advances and future directions. *Mol Cancer* **21**, 28 (2022).

43. Wolf, Y., Anderson, A.C. & Kuchroo, V.K. TIM3 comes of age as an inhibitory receptor. *Nat Rev Immunol* **20**, 173-185 (2020).

44. Robert, C. *et al.* Pembrolizumab versus Ipilimumab in Advanced Melanoma. *N Engl J Med* **372**, 2521-2532 (2015).

45. Robert, C. *et al.* Five-Year Outcomes With Nivolumab in Patients With Wild-Type *BRAF* Advanced Melanoma. *J Clin Oncol* **38**, 3937-3946 (2020).

46. Barber, D.L. *et al.* Restoring function in exhausted CD8 T cells during chronic viral infection. *Nature* **439**, 682-687 (2006).

47. Velu, V. *et al.* Enhancing SIV-specific immunity in vivo by PD-1 blockade. *Nature* **458**, 206-210 (2009).

48. Channappanavar, R., Twardy, B.S. & Suvas, S. Blocking of PDL-1 interaction enhances primary and secondary CD8 T cell response to herpes simplex virus-1 infection. *PLoS One* **7**, e39757 (2012).

49. Sharpe, A.H., Wherry, E.J., Ahmed, R. & Freeman, G.J. The function of programmed cell death 1 and its ligands in regulating autoimmunity and infection. *Nat Immunol* **8**, 239-245 (2007).

50. Ahn, E. *et al.* Role of PD-1 during effector CD8 T cell differentiation. *Proc Natl Acad Sci U S A* **115**, 4749-4754 (2018).

51. Green, K.A., Okazaki, T., Honjo, T., Cook, W.J. & Green, W.R. The programmed death-1 and interleukin-10 pathways play a down-modulatory role in LP-BM5 retrovirus-induced murine immunodeficiency syndrome. *J Virol* **82**, 2456-2469 (2008).

52. David, P. *et al.* The PD-1/PD-L1 Pathway Affects the Expansion and Function of Cytotoxic CD8. *Front Immunol* **10**, 54 (2019).

53. Erickson, J.J. *et al.* Acute Viral Respiratory Infection Rapidly Induces a CD8+ T Cell Exhaustion-like Phenotype. *J Immunol* **195**, 4319-4330 (2015).

54. Erickson, J.J., Rogers, M.C., Hastings, A.K., Tollefson, S.J. & Williams, J.V. Programmed death-1 impairs secondary effector lung $CD8^+$ T cells during respiratory virus reinfection. *J Immunol* **193**, 5108-5117 (2014).

55. Rutigliano, J.A. *et al.* Highly pathological influenza A virus infection is associated with augmented expression of PD-1 by functionally compromised virus-specific CD8+ T cells. *J Virol* **88**, 1636-1651 (2014).

56. Erickson, J.J. *et al.* Viral acute lower respiratory infections impair CD8+ T cells through PD-1. *J Clin Invest* **122**, 2967-2982 (2012).

57. Pauken, K.E. *et al.* The PD-1 Pathway Regulates Development and Function of Memory $CD8^+$ T Cells following Respiratory Viral Infection. *Cell Rep* **31**, 107827 (2020).

58. Diao, B. *et al.* Reduction and Functional Exhaustion of T Cells in Patients With Coronavirus Disease 2019 (COVID-19). *Front Immunol* **11**, 827 (2020).

59. De Biasi, S. *et al.* Marked T cell activation, senescence, exhaustion and skewing towards TH17 in patients with COVID-19 pneumonia. *Nat Commun* **11**, 3434 (2020).

60. Frebel, H. *et al.* Programmed death 1 protects from fatal circulatory failure during systemic virus infection of mice. *J Exp Med* **209**, 2485-2499 (2012).

61. Das, S. *et al.* Expression of B7-H1 on gastric epithelial cells: its potential role in regulating T cells during Helicobacter pylori infection. *J Immunol* **176**, 3000-3009 (2006).

62. Anderson, K.M., Czinn, S.J., Redline, R.W. & Blanchard, T.G. Induction of CTLA-4-mediated anergy contributes to persistent colonization in the murine model of gastric Helicobacter pylori infection. *J Immunol* **176**, 5306-5313 (2006).

63. Wu, Y.Y. *et al.* Increased programmed death-ligand-1 expression in human gastric epithelial cells in Helicobacter pylori infection. *Clin Exp Immunol* **161**, 551-559 (2010).

64. Lázár-Molnár, E. *et al.* Programmed death-1 (PD-1)-deficient mice are extraordinarily sensitive to tuberculosis. *Proc Natl Acad Sci U S A* **107**, 13402-13407 (2010).

65. Shen, L. *et al.* The characteristic profiles of PD-1 and PD-L1 expressions and dynamic changes during treatment in active tuberculosis. *Tuberculosis (Edinb)* **101**, 146-150 (2016).

66. Barber, D.L., Mayer-Barber, K.D., Feng, C.G., Sharpe, A.H. & Sher, A. CD4 T cells promote rather than control tuberculosis in the absence of PD-1-mediated inhibition. *J Immunol* **186**, 1598-1607 (2011).

67. Huang, X. *et al.* PD-1 expression by macrophages plays a pathologic role in altering microbial clearance and the innate inflammatory response to sepsis. *Proc Natl Acad Sci U S A* **106**, 6303-6308 (2009).

68. Brahmamdam, P. *et al.* Delayed administration of anti-PD-1 antibody reverses immune dysfunction and improves survival during sepsis. *J Leukoc Biol* **88**, 233-240 (2010).

69. Zhang, Y. *et al.* PD-L1 blockade improves survival in experimental sepsis by inhibiting lymphocyte apoptosis and reversing monocyte dysfunction. *Crit Care* **14**, R220 (2010).

70. Patera, A.C. *et al.* Frontline Science: Defects in immune function in patients with sepsis are associated with PD-1 or PD-L1 expression and can be restored by antibodies targeting PD-1 or PD-L1. *J Leukoc Biol* **100**, 1239-1254 (2016).

71. Triantafyllou, E. *et al.* PD-1 blockade improves Kupffer cell bacterial clearance in acute liver injury. *J Clin Invest* **131** (2021).

72. Netea, M.G., Schlitzer, A., Placek, K., Joosten, L.A.B. & Schultze, J.L. Innate and Adaptive Immune Memory: an Evolutionary Continuum in the Host's Response to Pathogens. *Cell Host Microbe* **25**, 13-26 (2019).

73. Netea, M.G. *et al.* Trained immunity: A program of innate immune memory in health and disease. *Science* **352**, aaf1098 (2016).

74. Ribes, S. *et al.* Intraperitoneal prophylaxis with CpG oligodeoxynucleotides protects neutropenic mice against intracerebral Escherichia coli K1 infection. *J Neuroinflammation* **11**, 14 (2014).

75. Muñoz, N. *et al.* Mucosal administration of flagellin protects mice from Streptococcus pneumoniae lung infection. *Infect Immun* **78**, 4226-4233 (2010).

76. van der Meer, J.W., Barza, M., Wolff, S.M. & Dinarello, C.A. A low dose of recombinant interleukin 1 protects granulocytopenic mice from lethal gram-negative infection. *Proc Natl Acad Sci U S A* **85**, 1620-1623 (1988).

77. Sun, J.C., Beilke, J.N. & Lanier, L.L. Adaptive immune features of natural killer cells. *Nature* **457**, 557-561 (2009).

78. Sun, J.C. & Lanier, L.L. NK cell development, homeostasis and function: parallels with $CD8^+$ T cells. *Nat Rev Immunol* **11**, 645-657 (2011).

79. Brillantes, M. & Beaulieu, A.M. Memory and Memory-Like NK Cell Responses to Microbial Pathogens. *Front Cell Infect Microbiol* **10**, 102 (2020).

80. Sheppard, S. & Sun, J.C. Virus-specific NK cell memory. *J Exp Med* **218** (2021).

81. Chan, L.C. *et al.* Protective immunity in recurrent. *Proc Natl Acad Sci U S A* **115**, E11111-E11119 (2018).

82. Martin, M.D. & Badovinac, V.P. Defining Memory CD8 T Cell. *Front Immunol* **9**, 2692 (2018).

83. Palm, A.E. & Henry, C. Remembrance of Things Past: Long-Term B Cell Memory After Infection and Vaccination. *Front Immunol* **10**, 1787 (2019).

84. McKinstry, K.K. *et al.* Memory CD4+ T cells protect against influenza through multiple synergizing mechanisms. *J Clin Invest* **122**, 2847-2856 (2012).

85. Clemens, E.B., van de Sandt, C., Wong, S.S., Wakim, L.M. & Valkenburg, S.A. Harnessing the Power of T Cells: The Promising Hope for a Universal Influenza Vaccine. *Vaccines (Basel)* **6** (2018).

86. Reijnders, T.D.Y., Schuurman, A.R. & van der Poll, T. The Immune Response to Respiratory Viruses: From Start to Memory. *Semin Respir Crit Care Med* **42**, 759-770 (2021).

87. Wu, T. *et al.* Lung-resident memory CD8 T cells (TRM) are indispensable for optimal cross-protection against pulmonary virus infection. *J Leukoc Biol* **95**, 215-224 (2014).

88. Pizzolla, A. *et al.* Resident memory $CD8^+$ T cells in the upper respiratory tract prevent pulmonary influenza virus infection. *Sci Immunol* **2** (2017).

89. Shenoy, A.T. *et al.* Lung $CD4^+$resident memory T cells remodel epithelial responses to accelerate neutrophil recruitment during pneumonia. *Mucosal Immunol* **13**, 334-343 (2020).

90. Slütter, B. *et al.* Dynamics of influenza-induced lung-resident memory T cells underlie waning heterosubtypic immunity. *Sci Immunol* **2** (2017).

91. Hayward, S.L. *et al.* Environmental cues regulate epigenetic reprogramming of airway-resident memory CD8. *Nat Immunol* **21**, 309-320 (2020).

92. Lee, B. *et al.* Influenza-induced type I interferon enhances susceptibility to gram-negative and gram-positive bacterial pneumonia in mice. *Am J Physiol Lung Cell Mol Physiol* **309**, L158-167 (2015).

93. Rynda-Apple, A. *et al.* Regulation of IFN-γ by IL-13 dictates susceptibility to secondary postinfluenza MRSA pneumonia. *Eur J Immunol* **44**, 3263-3272 (2014).

94. Shepardson, K.M. *et al.* Differential Type I Interferon Signaling Is a Master Regulator of Susceptibility to Postinfluenza Bacterial Superinfection. *mBio* **7** (2016).

95. Robinson, K.M. *et al.* Influenza A virus exacerbates Staphylococcus aureus pneumonia in mice by attenuating antimicrobial peptide production. *J Infect Dis* **209**, 865-875 (2014).

96. Robinson, K.M. *et al.* The inflammasome potentiates influenza/Staphylococcus aureus superinfection in mice. *JCI Insight* **3** (2018).

97. Ingram, J.T., Yi, J.S. & Zajac, A.J. Exhausted CD8 T cells downregulate the IL-18 receptor and become unresponsive to inflammatory cytokines and bacterial co-infections. *PLoS Pathog* **7**, e1002273 (2011).

98. Blevins, L.K. *et al.* Coinfection with Streptococcus pneumoniae negatively modulates the size and composition of the ongoing influenza-specific $CD8^+$ T cell response. *J Immunol* **193**, 5076-5087 (2014).

99. Houser, K. & Subbarao, K. Influenza vaccines: challenges and solutions. *Cell Host Microbe* **17**, 295-300 (2015).

100. Finelli, L. *et al.* Influenza-associated pediatric mortality in the United States: increase of Staphylococcus aureus coinfection. *Pediatrics* **122**, 805-811 (2008).

101. Joseph, C., Togawa, Y. & Shindo, N. Bacterial and viral infections associated with influenza. *Influenza Other Respir Viruses* **7 Suppl 2**, 105-113 (2013).

102. Black, S. *et al.* Efficacy, safety and immunogenicity of heptavalent pneumococcal conjugate vaccine in children. Northern California Kaiser Permanente Vaccine Study Center Group. *Pediatr Infect Dis J* **19**, 187-195 (2000).

103. Kaźmierczak, Z., Górski, A. & Dąbrowska, K. Facing antibiotic resistance: Staphylococcus aureus phages as a medical tool. *Viruses* **6**, 2551-2570 (2014).

104. Pauken, K.E. & Wherry, E.J. Overcoming T cell exhaustion in infection and cancer. *Trends Immunol* **36**, 265-276 (2015).

105. Wherry, E.J. T cell exhaustion. *Nat Immunol* **12**, 492-499 (2011).

106. Ohaegbulam, K.C., Assal, A., Lazar-Molnar, E., Yao, Y. & Zang, X. Human cancer immunotherapy with antibodies to the PD-1 and PD-L1 pathway. *Trends Mol Med* **21**, 24-33 (2015).

107. Day, C.L. *et al.* PD-1 expression on HIV-specific T cells is associated with T-cell exhaustion and disease progression. *Nature* **443**, 350-354 (2006).

108. Zajac, A.J. *et al.* Viral immune evasion due to persistence of activated T cells without effector function. *J Exp Med* **188**, 2205-2213 (1998).

109. Zelinskyy, G. *et al.* Virus-specific CD8+ T cells upregulate programmed death-1 expression during acute friend retrovirus infection but are highly cytotoxic and control virus replication. *J Immunol* **187**, 3730-3737 (2011).

110. McNally, B., Ye, F., Willette, M. & Flaño, E. Local blockade of epithelial PDL-1 in the airways enhances T cell function and viral clearance during influenza virus infection. *J Virol* **87**, 12916-12924 (2013).

111. Crowe, C.R. *et al.* Critical role of IL-17RA in immunopathology of influenza infection. *J Immunol* **183**, 5301-5310 (2009).

112. Van der Velden, J. *et al.* Differential requirement for c-Jun N-terminal kinase 1 in lung inflammation and host defense. *PLoS One* **7**, e34638 (2012).

113. Robinson, K.M. *et al.* The role of IL-27 in susceptibility to post-influenza Staphylococcus aureus pneumonia. *Respir Res* **16**, 10 (2015).

114. Robinson, K.M. *et al.* Influenza A exacerbates Staphylococcus aureus pneumonia by attenuating IL-1β production in mice. *J Immunol* **191**, 5153-5159 (2013).

115. WHO. Global Influenza Programme: Burden of disease. 2021 [cited]Available from: https://www.who.int/teams/global-influenza-programme/surveillance-and-monitoring/burden-of-disease

116. Matrosovich, M.N., Matrosovich, T.Y., Gray, T., Roberts, N.A. & Klenk, H.D. Human and avian influenza viruses target different cell types in cultures of human airway epithelium. *Proc Natl Acad Sci U S A* **101**, 4620-4624 (2004).

117. Atkin-Smith, G.K., Duan, M., Chen, W. & Poon, I.K.H. The induction and consequences of Influenza A virus-induced cell death. *Cell Death Dis* **9**, 1002 (2018).

118. LOURIA, D.B., BLUMENFELD, H.L., ELLIS, J.T., KILBOURNE, E.D. & ROGERS, D.E. Studies on influenza in the pandemic of 1957-1958. II. Pulmonary complications of influenza. *J Clin Invest* **38**, 213-265 (1959).

119. van de Sandt, C.E. *et al.* Human CD8(+) T Cells Damage Noninfected Epithelial Cells during Influenza Virus Infection In Vitro. *Am J Respir Cell Mol Biol* **57**, 536-546 (2017).

120. Li, W., Moltedo, B. & Moran, T.M. Type I interferon induction during influenza virus infection increases susceptibility to secondary Streptococcus pneumoniae infection by negative regulation of γδ T cells. *J Virol* **86**, 12304-12312 (2012).

121. Ghoneim, H.E., Thomas, P.G. & McCullers, J.A. Depletion of alveolar macrophages during influenza infection facilitates bacterial superinfections. *J Immunol* **191**, 1250-1259 (2013).

122. Damjanovic, D., Lai, R., Jeyanathan, M., Hogaboam, C.M. & Xing, Z. Marked improvement of severe lung immunopathology by influenza-associated pneumococcal superinfection requires the control of both bacterial replication and host immune responses. *Am J Pathol* **183**, 868-880 (2013).

123. Narayana Moorthy, A. *et al.* In vivo and in vitro studies on the roles of neutrophil extracellular traps during secondary pneumococcal pneumonia after primary pulmonary influenza infection. *Front Immunol* **4**, 56 (2013).

124. Li, N. *et al.* Influenza viral neuraminidase primes bacterial coinfection through TGF-β-mediated expression of host cell receptors. *Proc Natl Acad Sci U S A* **112**, 238-243 (2015).

125. Valkenburg, S.A. *et al.* Protection by universal influenza vaccine is mediated by memory CD4 T cells. *Vaccine* **36**, 4198-4206 (2018).

126. Doherty, P.C., Turner, S.J., Webby, R.G. & Thomas, P.G. Influenza and the challenge for immunology. *Nat Immunol* **7**, 449-455 (2006).

127. Xing, Z. *et al.* Innate immune memory of tissue-resident macrophages and trained innate immunity: Re-vamping vaccine concept and strategies. *J Leukoc Biol* **108**, 825-834 (2020).

128. Auladell, M. *et al.* Recalling the Future: Immunological Memory Toward Unpredictable Influenza Viruses. *Front Immunol* **10**, 1400 (2019).

129. He, X.S. *et al.* Baseline levels of influenza-specific CD4 memory T-cells affect T-cell responses to influenza vaccines. *PLoS One* **3**, e2574 (2008).

130. Wilk, M.M. & Mills, K.H.G. CD4 Trm Cells Following Infection and Immunization: Implications for More Effective Vaccine Design. *Front Immunol* **9**, 1860 (2018).

131. Goel, R.R. *et al.* mRNA vaccines induce durable immune memory to SARS-CoV-2 and variants of concern. *Science* **374**, abm0829 (2021).

132. Van Braeckel-Budimir, N., Varga, S.M., Badovinac, V.P. & Harty, J.T. Repeated Antigen Exposure Extends the Durability of Influenza-Specific Lung-Resident Memory CD8(+) T Cells and Heterosubtypic Immunity. *Cell Rep* **24**, 3374-3382 e3373 (2018).

133. Aegerter, H. *et al.* Influenza-induced monocyte-derived alveolar macrophages confer prolonged antibacterial protection. *Nat Immunol* **21**, 145-157 (2020).

134. Yewdell, J.W., Bennink, J.R., Smith, G.L. & Moss, B. Influenza A virus nucleoprotein is a major target antigen for cross-reactive anti-influenza A virus cytotoxic T lymphocytes. *Proc Natl Acad Sci U S A* **82**, 1785-1789 (1985).

135. Gotch, F., McMichael, A., Smith, G. & Moss, B. Identification of viral molecules recognized by influenza-specific human cytotoxic T lymphocytes. *J Exp Med* **165**, 408-416 (1987).

136. Pizzolla, A. & Wakim, L.M. Memory T Cell Dynamics in the Lung during Influenza Virus Infection. *J Immunol* **202**, 374-381 (2019).

137. Herndler-Brandstetter, D. *et al.* KLRG1 + Effector CD8+ T Cells Lose KLRG1, Differentiate into All Memory T Cell Lineages, and Convey Enhanced Protective Immunity. *Immunity* **48**, 716-729.e718 (2018).

138. McInnes, L., Healy, J. & Melville, J. UMAP: Uniform Manifold Approximation and Projection for Dimension Reduction. *arXiv:1802.03426* (Feb 2018).

139. Van Gassen, S. *et al.* FlowSOM: Using self-organizing maps for visualization and interpretation of cytometry data. *Cytometry A* **87**, 636-645 (2015).

140. Schindelin, J. *et al.* Fiji: an open-source platform for biological-image analysis. *Nat Methods* **9**, 676-682 (2012).

141. Love, M.I., Huber, W. & Anders, S. Moderated estimation of fold change and dispersion for RNA-seq data with DESeq2. *Genome Biol* **15**, 550 (2014).

142. Yu, G., Wang, L.G., Han, Y. & He, Q.Y. clusterProfiler: an R package for comparing biological themes among gene clusters. *OMICS* **16**, 284-287 (2012).

143. Newman, A.M. *et al.* Determining cell type abundance and expression from bulk tissues with digital cytometry. *Nat Biotechnol* **37**, 773-782 (2019).

144. Newman, A.M. *et al.* Robust enumeration of cell subsets from tissue expression profiles. *Nat Methods* **12**, 453-457 (2015).

145. Steuerman, Y. *et al.* Dissection of Influenza Infection In Vivo by Single-Cell RNA Sequencing. *Cell Syst* **6**, 679-691.e674 (2018).

146. Rutigliano, J.A. *et al.* Protective memory responses are modulated by priming events prior to challenge. *J Virol* **84**, 1047-1056 (2010).

147. Kreijtz, J.H. *et al.* Primary influenza A virus infection induces cross-protective immunity against a lethal infection with a heterosubtypic virus strain in mice. *Vaccine* **25**, 612-620 (2007).

148. Wang, C. *et al.* Influenza-Induced Priming and Leak of Human Lung Microvascular Endothelium upon Exposure to Staphylococcus aureus. *Am J Respir Cell Mol Biol* **53**, 459-470 (2015).

149. Iverson, A.R. *et al.* Influenza virus primes mice for pneumonia from Staphylococcus aureus. *J Infect Dis* **203**, 880-888 (2011).

150. Jewell, N.A. *et al.* Lambda interferon is the predominant interferon induced by influenza A virus infection in vivo. *J Virol* **84**, 11515-11522 (2010).

151. Barman, T.K. *et al.* Sequential targeting of interferon pathways for increased host resistance to bacterial superinfection during influenza. *PLoS Pathog* **17**, e1009405 (2021).

152. Shafran, N. *et al.* Secondary bacterial infection in COVID-19 patients is a stronger predictor for death compared to influenza patients. *Sci Rep* **11**, 12703 (2021).

153. Pittet, L.A., Hall-Stoodley, L., Rutkowski, M.R. & Harmsen, A.G. Influenza virus infection decreases tracheal mucociliary velocity and clearance of Streptococcus pneumoniae. *Am J Respir Cell Mol Biol* **42**, 450-460 (2010).

154. Oliva, J. & Terrier, O. Viral and Bacterial Co-Infections in the Lungs: Dangerous Liaisons. *Viruses* **13** (2021).

155. Jia, L. *et al.* Mechanisms of Severe Mortality-Associated Bacterial Co-infections Following Influenza Virus Infection. *Front Cell Infect Microbiol* **7**, 338 (2017).

156. Plotkowski, M.C., Puchelle, E., Beck, G., Jacquot, J. & Hannoun, C. Adherence of type I Streptococcus pneumoniae to tracheal epithelium of mice infected with influenza A/PR8 virus. *Am Rev Respir Dis* **134**, 1040-1044 (1986).

157. Xu, M., Yang, W., Wang, X. & Nayak, D.K. Lung Secretoglobin Scgb1a1 Influences Alveolar Macrophage-Mediated Inflammation and Immunity. *Front Immunol* **11**, 584310 (2020).

158. Liu, Q., Zhou, Y.H. & Yang, Z.Q. The cytokine storm of severe influenza and development of immunomodulatory therapy. *Cell Mol Immunol* **13**, 3-10 (2016).

159. Coates, B.M. *et al.* Inflammatory Monocytes Drive Influenza A Virus-Mediated Lung Injury in Juvenile Mice. *J Immunol* **200**, 2391-2404 (2018).

160. Hall, M.W. *et al.* Innate immune function and mortality in critically ill children with influenza: a multicenter study. *Crit Care Med* **41**, 224-236 (2013).

161. Dufour, J.H. *et al.* IFN-gamma-inducible protein 10 (IP-10; CXCL10)-deficient mice reveal a role for IP-10 in effector T cell generation and trafficking. *J Immunol* **168**, 3195-3204 (2002).

162. Robinson, K.M. *et al.* Novel protective mechanism for interleukin-33 at the mucosal barrier during influenza-associated bacterial superinfection. *Mucosal Immunol* **11**, 199-208 (2018).

163. Loughran, S.T. *et al.* Influenza infection directly alters innate IL-23 and IL-12p70 and subsequent IL-17A and IFN-γ responses to pneumococcus in vitro in human monocytes. *PLoS One* **13**, e0203521 (2018).

164. Yamamoto, N. *et al.* Essential role for the p40 subunit of interleukin-12 in neutrophil-mediated early host defense against pulmonary infection with Streptococcus pneumoniae: involvement of interferon-gamma. *Microbes Infect* **6**, 1241-1249 (2004).

165. Moldoveanu, B. *et al.* Inflammatory mechanisms in the lung. *J Inflamm Res* **2**, 1-11 (2009).

166. Betts, R.J. *et al.* Influenza A virus infection results in a robust, antigen-responsive, and widely disseminated Foxp3+ regulatory T cell response. *J Virol* **86**, 2817-2825 (2012).

167. Brincks, E.L. *et al.* Antigen-specific memory regulatory CD4+Foxp3+ T cells control memory responses to influenza virus infection. *J Immunol* **190**, 3438-3446 (2013).

168. van der Sluijs, K.F. *et al.* IL-10 is an important mediator of the enhanced susceptibility to pneumococcal pneumonia after influenza infection. *J Immunol* **172**, 7603-7609 (2004).

169. Barthelemy, A. *et al.* Influenza A virus-induced release of interleukin-10 inhibits the anti-microbial activities of invariant natural killer T cells during invasive pneumococcal superinfection. *Mucosal Immunol* **10**, 460-469 (2017).

170. Floc'h, F. & Werner, G.H. Heterotypic protective immune reactions in mice infected with distinct serotypes of human influenza virus. *Ann Microbiol (Paris)* **129**, 509-524 (1978).

171. Kreijtz, J.H. *et al.* Infection of mice with a human influenza A/H3N2 virus induces protective immunity against lethal infection with influenza A/H5N1 virus. *Vaccine* **27**, 4983-4989 (2009).

172. Jubel, J.M., Barbati, Z.R., Burger, C., Wirtz, D.C. & Schildberg, F.A. The Role of PD-1 in Acute and Chronic Infection. *Front Immunol* **11**, 487 (2020).

173. Messenheimer, D.J. *et al.* Timing of PD-1 Blockade Is Critical to Effective Combination Immunotherapy with Anti-OX40. *Clin Cancer Res* **23**, 6165-6177 (2017).